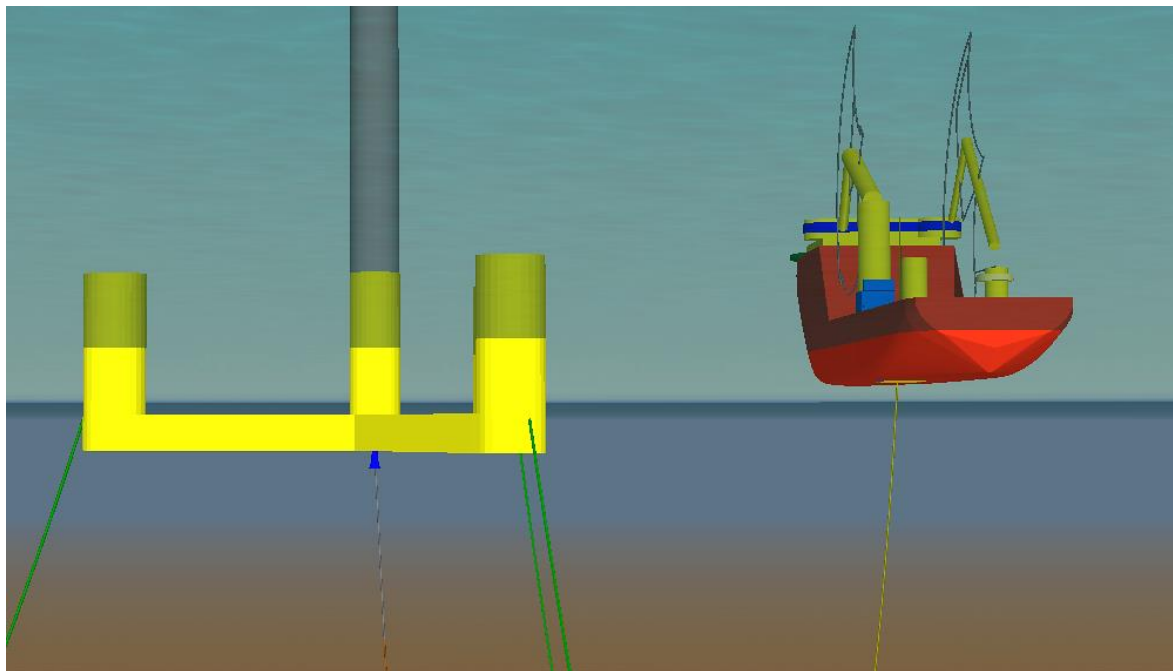




Universitetet
i Stavanger

DEEPOCEAN

Utsira Nord Floating Wind farm – Optimisation of marine operations related to inter-array cable installation.



Master thesis carried out at the University of Stavanger

Field of study: Mechanical engineer

Subject code: MKOMAS

Due date: 15.06.2023

By: Theodor D. Hansen



Universitetet
i Stavanger

Faculty of Science and Technology

MASTER'S THESIS

Study program/ Specialization: Structural and Mechanical Engineering	Spring semester, 2023 Open
Writer: Theodor Didriksen Hansen	
Faculty supervisor: Ove Mikkelsen	
External supervisor: André Ødegård Eilertsen	
Thesis title: Utsira Nord Floating Wind farm – Optimisation of marine operations related to inter-array cable installation.	
Credits (ECTS): 30	
Key words: <ul style="list-style-type: none">• Wind energy• Floating offshore wind farm• Inter Array Cable Installation• Utsira Nord• Environmental conditions• Orcaflex	Pages: 101 + enclosure/ Appendix: 5 Stavanger, 15.06.2023

Preface

The final semester of the master's programme in mechanical and structural engineering at the University of Stavanger features a main project in the course MKOMAS Master's thesis. This 30-credit assignment must address a particular problem related to one or more of the topic areas in the master programme.

I worked as a summer intern at DeepOcean in Haugesund in the summer of 2022, where the focus was logistics for assembly and transport of Norway's first offshore floating wind farm located at Utsira Nord. This was my first encounter with the offshore wind industry and as a mechanical engineering student, I was very impressed by the enormous dimensions of the wind turbines and the new technology involved. During this period I gained invaluable insights into the initiation and early stages of a project, fuelling my curiosity about the offshore wind industry and the Utsira Nord project. I then decided that this was a topic I wanted to learn more about and thereby it triggered the theme for my master's thesis.

I must express my gratitude to a number of persons for their assistance with the thesis writing process. I want to start by thanking my faculty Supervisor, Associate Professor Ove Mikkelsen. I appreciate your helpful comments when I had questions as well as your advice on the structure and content on how to build a good report.

I also like to thank Andre Eilertsen, Technical Manager for Offshore Renewables at DeepOcean, for being available for guidance when I needed it, making valuable objections and for offering an office space for me at DeepOcean in Haugesund. In addition, I want to thank everyone working at DeepOcean Haugesund for giving of their time, wisdom, and thoughts.

Place & date:

Haugesund, 15.06.2023

Theodor Didriksen Hansen



Abstract

The offshore wind industry is experiencing significant growth, with wind farms expanding in size, capacity, and moving to more challenging locations. However, cable faults remain a major concern, particularly during the installation of inter-array and export cables. This thesis aims to research and analyse the installation steps of inter-array cables at the Utsira Nord offshore wind farm. It further seeks to enhance the installation process by identifying functional sea states through a combination of previous work and new data.

The research focuses on answering key questions related to the installation of inter-array cables. This includes identifying the main steps, defining critical phases, and analysing the typical loads that impact cable installation to determine the parameters affecting the process. Additionally, the thesis seeks to determine the optimal environmental conditions for cable installation. The methodology employed in this thesis includes literature studies, experience from employees at DeepOcean regarding offshore operations, and the use of Orcaflex and Excel.

The analysis, primarily conducted using Orcaflex, concentrates on the installation of 1st and 2nd end dynamic section. The floating windmill is treated as a fixed structure in the Orcaflex model, neglecting its movement due to the ongoing development of the foundation concept and limited comprehensive information on weather and environmental factors. The study primarily focuses on tension and curvature acting on the cable during installation, disregarding boat and floating structure considerations that are not directly relevant to the research objectives.

From the knowledge gained in the literature review, an analysis was carried out to investigate crucial parameters in the cable laying process and a conclusion for when it is optimal to do inter-array cable installation operations at Utsira Nord was given. The focus was on tension loads, minimum bending radius, and potential clashes with the Moonpool. This was conducted with both Gumbel and Rayleigh analysis with irregular vessel motions. The result of the analysis illustrated the extent of impact the various environmental wave conditions had on the system.

Throughout the study, certain wave conditions were found to be more favourable than others. Wave directions ranging from 90-135° and 225-270°, simulated with a current velocity of 0.3 m/s, offered the most optimal conditions for cable installation. In contrast, the analysis showed that sea states with wave directions of 0° and 180°, as well as current at 1.0 m/s, presented a higher risk of cable damage.

To enhance the findings of this master's thesis, further analysis of different current velocities is recommended to identify operable sea states under higher currents. Additionally, analysing the system with a moving floating wind turbine, given that sufficient data is available.

Table of contents

Preface	i
Abstract	ii
List of figures	v
List of tables	viii
Abbreviations	ix
1 Introduction.....	10
1.1 Background	10
1.2 Objective	11
1.3 Limitations.....	12
1.4 Methodology	12
1.5 Structure of the study	13
2 Theoretical background.....	14
2.1 DeepOcean	14
2.2 Utsira Nord.....	15
2.2.1 Wind.....	15
2.2.2 Waves	16
2.2.3 Summary wind and waves.....	17
2.3 Daisy Chain	18
2.3.1 1 st and 2 nd end dynamic sections.....	19
2.4 Offshore wind turbine	20
2.4.1 Components.....	20
2.5 Cable installation.....	22
2.5.1 Cable installation parameters	22
2.5.2 Installation methods.....	23
2.5.3 Cable lay vessel – Edda Freya.....	24
2.5.4 Cable structure & Layers.....	26
2.5.5 Subsea power cables.....	28
3 Methodology	30
3.1 Literature study.....	30
3.2 DeepOcean	31
3.3 Orcaflex.....	31
3.4 Excel.....	32
4 Modelling of Analysis.....	32

4.1	Environment	32
4.1.1	Key parameters	32
4.1.2	JONSWAP and wave spectrum.....	34
4.1.3	Current.....	36
4.1.4	Water Characteristics.....	36
4.2	FWT, vessel and deployment method	36
4.2.1	Floating wind turbine	36
4.2.2	Vessel	39
4.2.3	Moonpool J-lay.....	40
4.3	Cable line configuration	40
4.3.1	IAC accessories	42
4.4	Acceptable cable laying criteria	46
4.4.1	Other criteria used in the analysis	47
4.5	Simulation settings	48
4.5.1	Time integration method	48
4.5.2	Simulation period	49
4.5.3	Coordinate system	49
5	Installation steps.....	50
5.1	Main steps.....	50
5.1.1	Phase 1 - Installation of 1st end dynamic section.....	52
5.1.2	Phase 2 - Installation of 2nd end dynamic section	56
5.2	Critical steps	60
6	Sensitivity test	62
6.1.1	Case 2	63
6.1.2	Case 3	66
7	Dynamic analysis	69
7.1	Methods applied	69
7.2	Case 1 - Results	70
7.3	Case 2 - Results	77
7.4	Case 3 - Results	83
8	Discussion	90
8.1	Study approach and corresponding process	90
8.2	The effect of environmental parameters and study results	91
9	Conclusion	93

10	Further work	94
	References	95
	Appendix A	100

List of figures

Figure 1: ROV [5]	14
Figure 2: Utsira Nord Wind Farm [6]	15
Figure 3: Windspeed at Utsira Nord 2021-2022 [8]	16
Figure 4: Historical significant wave height graph for Utsira Nord in 2021-2022 [8].....	17
Figure 5: Utsira Nord drawing of infield cable routes between WTGs at the Utsira Nord field highlighted in purple. Yellow triangle: WTG, Black line: mooring system, Red dot: suction anchor, Purple line: inter-array cable,.....	18
Figure 6: First and end and second end dynamic section, this basically means that the first end of the cable goes to the FWT1, and the second end of the cable goes to the FWT2 [7].	19
Figure 7: components of an offshore wind turbine [12]	20
Figure 8: During the installation of IAC	22
Figure 9: The cable laying process is subject to several parameters [19]	23
Figure 10: S-lay & J-lay [20]	24
Figure 11: Edda Freya [22].....	25
Figure 12: Conductor design [18]	27
Figure 13: Inter-array cable layers [28]	29
Figure 14: Export cable layers [29]	29
Figure 15: DeepOcean office in Haugesund [31].....	31
Figure 16: Environmental load heading definition, created in Bricscad	33
Figure 17: Foundation designed for 15MW FWT	37
Figure 18: Final configuration of FWT model	37
Figure 19: I-tube placement on FWT	38
Figure 20: Illustration of DMA and buoyancy modules on IAC	39
Figure 21: Moonpool J-lay	40
Figure 22: Nodes and segments in a line model [42]	41
Figure 23: Pull-in Head [44]	43
Figure 24: Bend stiffener [45].....	44
Figure 25: Buoyancy modules [46]	45
Figure 26: Dead man anchor is the blue cylinder	46
Figure 27: The yellow circle indicates the location of the lower tensioner on Edda Freya's VLS tower [22]	48
Figure 28: Time and simulation stages [53]	49
Figure 29: Coordinate systems [54].....	50
Figure 30: (1) IAC, (2) Pull-in head, (3) Pull-in wire, (4) I-tube, (5) mooring line. The pull-in head (2) is here deployed and used to pull the IAC from the vessel's moonpool to the I-tube (4) on the wind turbine. Throughout this process, the IAC may experience tension caused by sudden movements.	

However, the presence of a bend stiffener, positioned at the end of the pull-in head helps to mitigate this issue. 52

Figure 31: (1) Buoyancy modules, (2) DMA, (3) IAC, (4) Pull-in head, (5) Pull-in wire. Deployment of IAC attachments. While the pull-in head (4) is being hauled towards the I-tube, the DMA (2) and the buoyancy modules (1) attached to the cable (3) are simultaneously deployed. 53

Figure 32: (1) Buoyancy modules, (2) DMA, (3) IAC, (4) Pull-in head, (5) I-tube. It can be observed that the pull-in head (4) has established a temporarily hang off and is positioned directly under the I-tube (5). The DMA (2) and Buoyancy modules (1) have been hauled out to their desired position, and it is now ready for step 4 and 5. 53

Figure 33: (1) Buoyancy modules, (2) DMA, (3) Pull-in head. The pull-in head (3) remains in its position even after the release of the first DMA. It is observed that the cable has now transitioned into a shape with tighter angles compared to before. 54

Figure 34: (1) Buoyancy modules, (2) DMA. The last DMA (2) has been released, and the IAC is transitioning towards the desired shape known as the lazy wave. 55

Figure 35: (1) IAC, (2) Buoyancy modules, (3) Pull-in head, (4) I-tube. The pull-in head (3) remains in the same position under the I-tube (4), while the IAC (1) is being guided towards the seabed for cable touchdown and is then ready to be fed out along the desired cable route. 55

Figure 36: (1) Buoyancy modules, (2) IAC, (3) I-tube. The final pull-in is now done, the IAC (1) is connected to the I-tube (3), and the installation of the first end cable is complete. The CLV can now continue paying out the cable towards the second end. 56

Figure 37: (1) Buoyancy modules, (2) IAC. Deployment of all buoyancy modules (1) and temporary DMA. The CLV will continue to move in same direction while paying out on cable (2) and monitoring TDP and layback length. 57

Figure 38: (1) DMA, (2) Buoyancy modules, (3) Pull-in wire. The cable is connected to the wire (3) and is ready to haul in the pull-in head. The pull-in will start after step 3 and 4. 57

Figure 39: (1) DMA, (2) Buoyancy modules, (3) IAC. Release of first DMA, it is observed that the cable has now transitioned into a shape with tighter angles compared to before. However, the release of the last DMA in step 4 will assist in rectifying this. 58

Figure 40: (1) DMA, (2) Buoyancy modules, (3) IAC, (4) Pull-in head, (5) I-tube. The last DMA (1) has been released, and the IAC is transitioning towards the desired shape known as lazy wave configuration. The pull-in head (4) remains in the same position until step 5. 59

Figure 41: (1) IAC, (2) Buoyancy modules, (3) I-tube. Final WTG pull-in of DIAC 2nd end. The IAC (1) has now been connected to the I-tube (3), and the installation of the second end cable is complete. The CLV can now proceed to the next operation. 59

Figure 42: The highlighted area indicates the critical region for step 1, specifically showcasing the abrupt motions that occur during the deployment of the pull-in head. This aspect will be analysed in greater detail later in the thesis. 60

Figure 43: The highlighted indicates the critical region for step 2, focusing on the moonpool in case of clashing during the deployment of the temporary DMA and buoyancy modules. This will be further analysed later in the thesis. 61

Figure 44: The circled area indicates the critical region for step 4, again focusing on the IAC motions. This is after the release of the temporary DMA. This aspect will be further analysed later in the thesis. 62

Figure 45: The numbers 1 and 2 indicate the locations where the cable was measured for the sensitivity test to obtain the results for case 2. 63

Figure 46: Case 2 - Maximum tension on cable during different time periods, arc length 140 – 210 m	64
Figure 47: Case 2 - Minimum tension on cable during different time periods, arc length 140 – 210 m	64
Figure 48: Case 2 – MBR during different time periods, arc length 140 – 210 m	65
Figure 49: The numbers 1 and 2 indicate the locations where the cable was measured for the sensitivity test to obtain the results for case 3.	66
Figure 50: Case 3 - Maximum tension on cable during different time periods, arc length 80 - 270 m	67
Figure 51: Case 3 - Minimum tension on cable during different time periods, arc length 80 - 270 m .	67
Figure 52: Case 2 – MBR during different time periods, arc length 80 - 270 m.....	68
Figure 53: Case 1 - deployment of Pull-in head	71
Figure 54: MBR results with no current, note critical MBR is 3.07 m	75
Figure 55: MBR results with current: 0.3 m/s, note critical MBR is 3.07 m	76
Figure 56: MBR results with current: 1.0 m/s, note critical MBR is 3.07 m	76
Figure 57: Case 2 - Deployment of DMA and buoyancy modules through the moonpool in progress.	77
Figure 58: Visual representation of moonpool with dimensions 7.2 m x 7.2 m, made in Bricscad	77
Figure 59: Minimum tension results with no current, note critical compression is below 0 kN	81
Figure 60: Minimum tension results with current: 0.3 m/s, note critical compression is below 0 kN .	82
Figure 61: Minimum tension results with current: 1.0 m/s, note critical compression is below 0 kN .	82
Figure 62: Case 3 - release of DMA	83
Figure 63: MBR results with no current, note critical MBR is 3.07 m	84
Figure 64: MBR results with current: 0.3 m/s, note critical MBR is 3.07 m	84
Figure 65: MBR results with current: 1.0 m/s, note critical MBR is 3.07 m	85
Figure 66: Maximum tension results with no current, note critical limit is 336 kN	86
Figure 67: Minimum tension results with no current, note critical compression is below 0 kN	86
Figure 68: Maximum tension results with current: 0.3 m/s, note critical limit is 336 kN.....	87
Figure 69: Minimum tension results with current: 0.3 m/s, note critical compression is below 0 kN .	88
Figure 70: Maximum tension results, current: 1.0 m/s, note critical limit is 336 kN.....	88
Figure 71: Minimum tension results with current: 1.0 m/s, note critical compression is below 0 kN .	89

List of tables

Table 1: List of abbreviations	ix
Table 2: Thesis structure	13
Table 3: Edda Freya specifications [22]	25
Table 4: Vertical lay system – Key features for cable installation [22]	25
Table 5: Typical IAC [27]	28
Table 6: Typical Export cable [29].....	29
Table 7: Key parameters matrix for simulations	33
Table 8: Water characteristics.....	36
Table 9: Main dimensions FWT [40].....	38
Table 10: Vessel specifications [22].....	39
Table 11: cable specifications [43]	42
Table 12: Pull-in head properties	43
Table 13: Bend stiffener properties	44
Table 14: Buoyancy module properties	45
Table 15: DMA properties	45
Table 16: Acceptable cable lay criteria [43]	46
Table 17: Smallest bending radius recorded.....	65
Table 18: Smallest bending radius recorded	68
Table 19: Maximum cable tension at lower tensioner, minimum tension on cable results and maximum tension on pull-in winch, current: no current	72
Table 20: Maximum cable tension at lower tensioner, minimum tension on cable results and maximum tension on pull-in winch, current: current: 0.3 m/s.....	73
Table 21: Maximum cable tension at lower tensioner, minimum tension on cable results and maximum tension on pull-in winch, current: 1.0 m/s.....	74
Table 22: Moonpool clearance results, no current	78
Table 23: Moonpool clearance results, current: 0.3 m/s	79
Table 24: Moonpool clearance results, current: 1.0 m/s.....	80

Abbreviations

Table 1: List of abbreviations

Abbreviation	Abbreviation meaning
AC	Alternating Current
AHC	Active Heave Compensated cranes
BM	Buoyancy Module
CLV	Cable Lay Vessel
DC	Direct Current
DO	DeepOcean
DMA	Dead Man Anchor
EPR	Ethylene Propylene Rubber
FO	Fibre Optic
FWT	Floating Wind Turbine
HVAC	High Voltage Alternative Current
HVDC	High Voltage Direct Current
IAC	Inter-Array Cable
JDR	JDR cable systems
LOA	Length Overall
MBR	Minimum Bend Radius
OD	Outer Diameter
PP	Polypropylene
RAO	Response Amplitude Operator
TDP	Touch Down Point
VLS	Vertical Lay system
(W)ROV	(Work) Remotely Operated Vehicle
WTG	Wind Turbine Generator
XLPE	Cross-linked polyethylene

1 Introduction

The objective of this chapter is to introduce the research questions. It is also a basis for giving the reader background information on offshore energy and stating the methods that has been employed to deal with these issues.

1.1 Background

Wind energy and offshore wind parks are growing areas of the energy industry. It is assumed the technological development and methodology of installation for offshore wind will make an outburst in the next few decades. Power produced by offshore wind farms has increased a lot during the last years in Europe, from approximately 2 GW in 2008 to approximately 28.5 GW in 2022 [1]. Yet the onshore technology continues to dominate wind capacity growth, the offshore technology is anticipated to increase its share in the next years even more. The European Commission has set a goal for reducing emissions of producing at least 27 % of Europe's total energy consumption from renewable sources by 2030. According to Wind Europe, through 2030, over 28 % of installed capacity will be placed offshore. According to the European Wind Energy Association, 66 GW of installed offshore capacity might be reached in Europe by 2030 [2].

The failure rates of the subsea power cables are a current topic of study and a big issue within the offshore wind sector. Failure of these cables might have severe consequences. In terms of money, identifying and replacing a damaged subsea cable section can cost anything between 0.6-1.2 £ million [3]. Failure in the cables could also harm the offshore Wind turbines as well, and depending on the power distribution system, they could put the entire wind farm out of commission while repairs are made. There are numerous elements present that threaten the cable throughout the installation phase. It is therefore essential to identify the different risks and hazards that are present during these procedures in order to ensure that the installation phase is safe and done right. Understanding the main steps and critical phases of the installation of the cable is also crucial.

In order to fulfil the mechanical qualities of the cable and prevent any complications, it is important to understand the installation methods. One might learn how to complete the installation phase without harming the cable by analysing the important characteristics and steps that cause the cable to be under extreme tension. To prevent less than ideal operating conditions, the cable tension force must be estimated and analysed beforehand and during laying [4].

1.2 Objective

In the installation sequence of an offshore floating wind farm, the final step involves the cable installation process. These cables are specifically engineered to withstand dynamic loads from harsh offshore environmental conditions. The output power of the wind farm turbines is routed through array cables to an offshore substation. The high-voltage power produced by the offshore wind farm is then sent to the onshore substation through export cables, where it is then connected to the local electrical grid. A subsea cable installation may not be as straightforward as it first appears. To successfully install the subsea cable on the seabed, a demanding process must be followed, where many factors must be taken into account, be properly calculated, and monitored. The failure rates of the subsea power cables are a current topic of study and a significant issue within the offshore wind sector. Failure of these cables might have severe consequences. It is therefore essential to identify the different risks and hazards that are present during these procedures in order to ensure that the installation phase is safe and done right.

In this thesis there will be done research and analysis of the steps involving installation of inter-array cable (IAC) between the wind turbine generators (WTG) at the Utsira Nord offshore wind farm, based on the knowledge from earlier work and new data related to this topic. Since the entire installation of a wind farm comprises a wide range of different tasks and operations, this paper tries to enhance some essential parts of the installation process of the inter-array cable. The end product aims to optimize the operation and find essential sea states in order to improve the installation's quality, allowing the operation to function smoothly.

The thesis is based on answering the following research questions related to the problem:

- What are the main steps of the installation of inter-array cables, define the critical phases and analyse typical loads acting on the cables to discover the parameters that affect the installation.
- Analysis of the critical steps, to determine the optimal environmental conditions for cable installation.

1.3 Limitations

To ensure the completion of the project with a time perspective, a series of limitations and simplifications have been implemented. Taken together, these limitations and simplifications are necessary in order to provide a feasible and useful study. The analysis related to Orcaflex has primarily focused on the installation of 1st and 2nd end dynamic section, as these phases have been identified as important stages for cable laying, based on literature study. The model used for this study is not a stationary model, as in stationary models, nothing moves. However, in this case, a crucial part of the operation is locked. In the Orcaflex model, the floating wind turbine (FWT) has been considered as fixed structure, with not taken into account its movement. This decision was made because the foundation concept for the wind turbine has not yet been finalized, and due to lack of comprehensive information on weather, wind, and currents. Further, the study has primarily concentrated on the tension and curvature acting on the cable during the installation process, and not on the boat or floating structures, as they are not directly relevant to the study's objectives.

1.4 Methodology

The research questions described in chapter 1.2 have been addressed using a variety of approaches. Chapter 3 offers a more thorough explanation of the methods employed. However, the following techniques have been used:

- Literature studies
- Discussing with the employees at DO that have experience from offshore operations
- Orcaflex
- Excel

1.5 Structure of the study

Table 2: Thesis structure

Chapter 1	
Introduction	Thesis
Chapter 1 provides an introduction of this thesis's background, which deals with a brief introduction to the floating wind market and cable work. It will also go through the purpose, methodology, structure and limitations.	

Chapter 2	
Theoretical background	Useful information related to the subject
This chapter concerning the theoretical background of this study, including a presentation of DeepOcean. In conjunction with this, an overview of the Utsira Nord project is presented along with general information about wind and waves. An overview of the daisy chain distribution system and the components of wind turbines will also be conducted. Additionally, relevant details to the cable installation phase, cable structure, and the methods involved are given.	

Chapter 3	
Methodology	Data & methods
Provides a further explanation of the methods used for conducting the research and writing this thesis.	

Chapter 4	
Modelling	Scenarios
Chapter 4 gives a closer look at the modelling of the cable installation phase scenarios.	

Chapter 5, 6 & 7	
Study	Analysis and results
Chapter 5, 6 and 7 aims to find the optimal environmental conditions for cable installation, specified for Utsira Nord, of marine operations related to inter-array cable installation, through an analysis.	

Chapter 8, 9 & 10	
Drooling	Discussion, conclusion & further work
The findings and insights generated through this analysis will be discussed in chapter 8. Chapter 9 will present the overall conclusions and summary of the research results, while chapter 10 will provide recommendations for further work in this area.	

2 Theoretical background

2.1 DeepOcean

DeepOcean is an independent, technology-driven solution provider in the ocean industry. In figure 1, one of many assets for DeepOcean is shown. They provide a comprehensive variety of services, ranging from surveys, engineering, project management, and installation, to maintenance and recycling, to businesses in the oil and gas, offshore renewables, deep sea minerals, and other non-energy segments. The Company DeepOcean group which is a world-leading supplier of ocean services, was established in 1999, and has its head office in Oslo, Norway, in addition to major operational hubs in the United States, Mexico, the United Kingdom, and Norway [5]. DeepOcean has a GO GREEN mindset and is constantly working to reduce costs and carbon footprint in order to improve the sustainability of their clients' operations. In relation to this they co-founded the Windstaller Alliance in 2021, which aspires to offer the offshore wind and other offshore renewables segments the most comprehensive, cost-effective product supply, fabrication, and marine services offering available in the world [5].

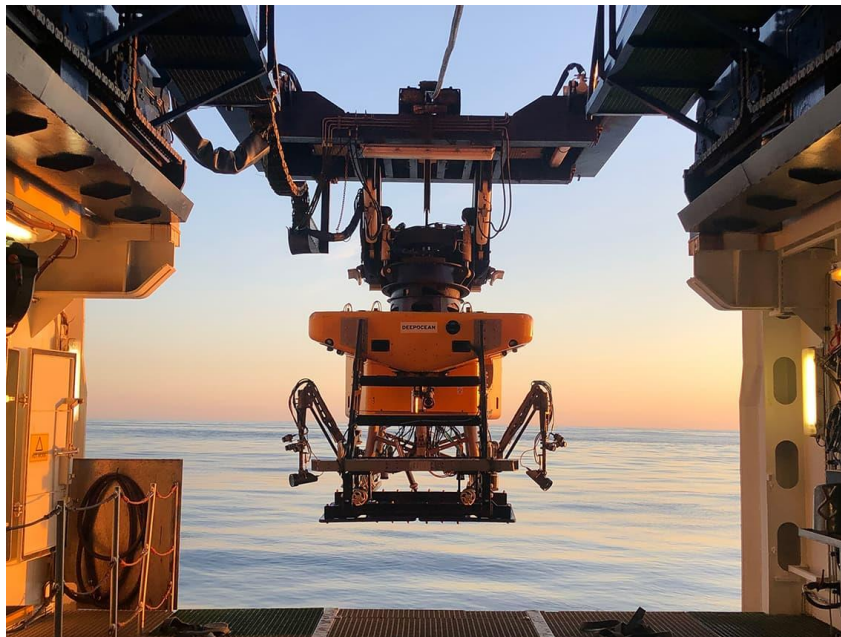


Figure 1: ROV [5]

2.2 Utsira Nord

The Utsira Nord windmill park is located about 12 km west from the island Utsira in Rogaland, Norway. The park spans approximately 42 km in length and 23 km in width. Figure 2 provides a visual representation of the Utsira Nord site. The area comprises three concessions, each containing approximately 30-35 WTGs, resulting in a total of 100 WTGs across the site [6]. The turbines will be spaced at an approximate distance of 2 km from each other. The depth of the sea at this location is 260-270 m, and surveys of the area indicate that the seabed most likely will consist of sand and clay. The deep water requires floating windmills, and not fixed installations. Utsira Nord will have a capacity of 1.5 GW with 100 wind turbines, where each wind turbine is estimated to contribute with 15 MW. Furthermore, the park is estimated to produce 6 TWh yearly meaning that this park alone will produce electricity for approximately 375.000 households in Norway. In other words, the park in Utsira Nord will contribute with 16% off all the electricity to households in Norway, from internal report [7].

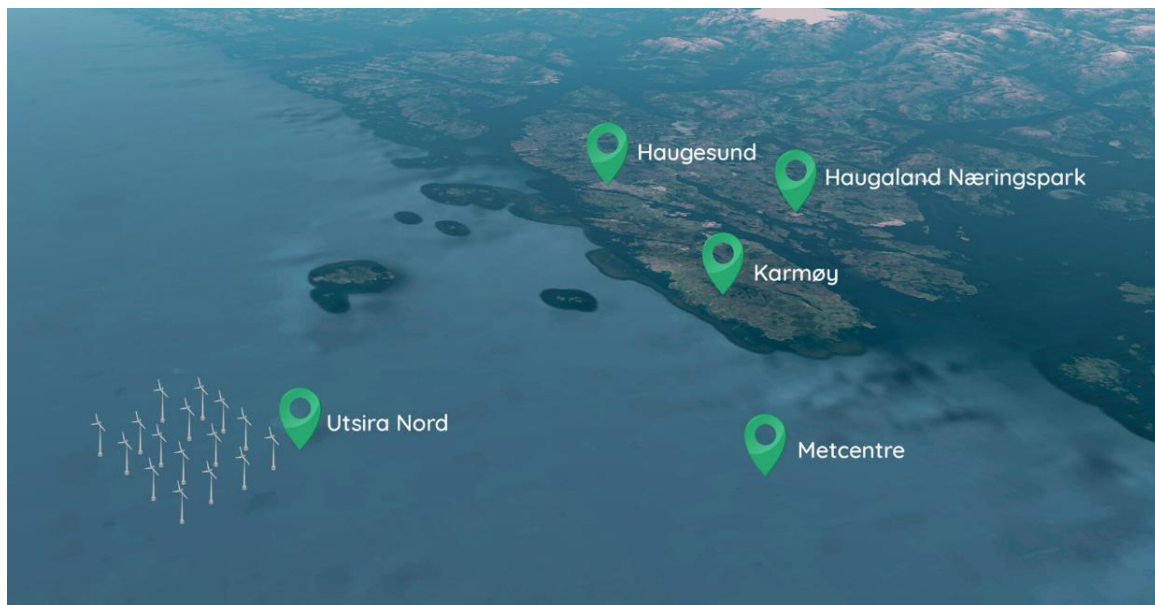


Figure 2: Utsira Nord Wind Farm [6]

2.2.1 Wind

In the years 2021 and 2022, the average wind speed at Utsira was recorded to be 10 m/s. Analysis of historical data from Spinerjie.com indicates that the highest wind flow speeds occur between September and March. Figure 3 provides visual representation of these findings, depicting wind flow speeds that may reach up to 21-25 m/s during these months [8]. The high wind speeds in this region offer significant benefits for offshore wind turbines, as they can facilitate the deployment of larger and more efficient turbines, resulting in increased power generation capacity. Additionally, the consistent and high wind speeds can help to improve the stability and reliability of wind turbine operations, thereby improve the overall performance of the offshore wind farms.

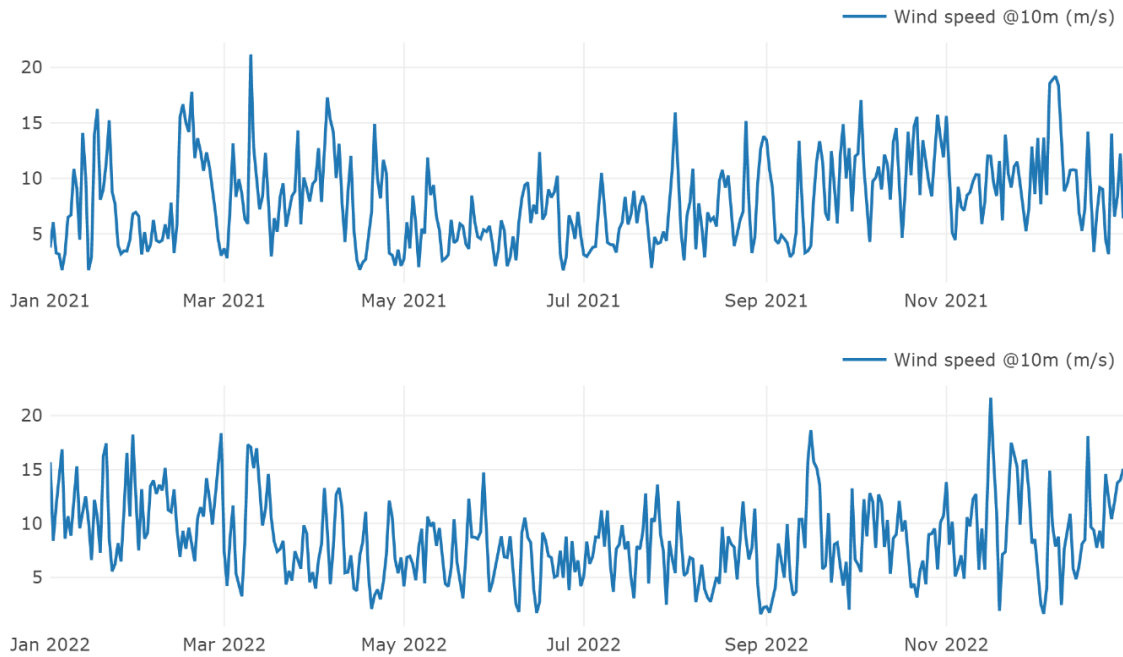


Figure 3: Windspeed at Utsira Nord 2021-2022 [8]

2.2.2 Waves

The offshore wind farm site located at Utsira Nord has been observed to exhibit an average significant wave height of approximately 2.1 meters, with maximum wave heights reaching approximately 8 meters over the period spanning January 1, 2021, through December 31, 2022. Figure 4 provides a visual representation of the significant wave height data collected during this period. Notably, the highest significant wave height recorded within this timeframe was 8.4 meters, corresponding to a maximum wave height of approximately 17 meters. Out in the field, one can experience rough sea conditions, and due to the weather conditions in that area, the waves can vary in terms of their directions [8]. It is important to note that modern WTGs are designed to withstand these conditions, and as such, the waves observed at Utsira Nord are unlikely to have a significant impact on the structural integrity of the turbines. However, it is worth noting that such large waves can still result in reduced efficiency and power production, as well as increased fatigue loading and maintenance requirements. A thorough understanding of the wave characteristics is therefore critical for the planning and operation of offshore wind energy systems.

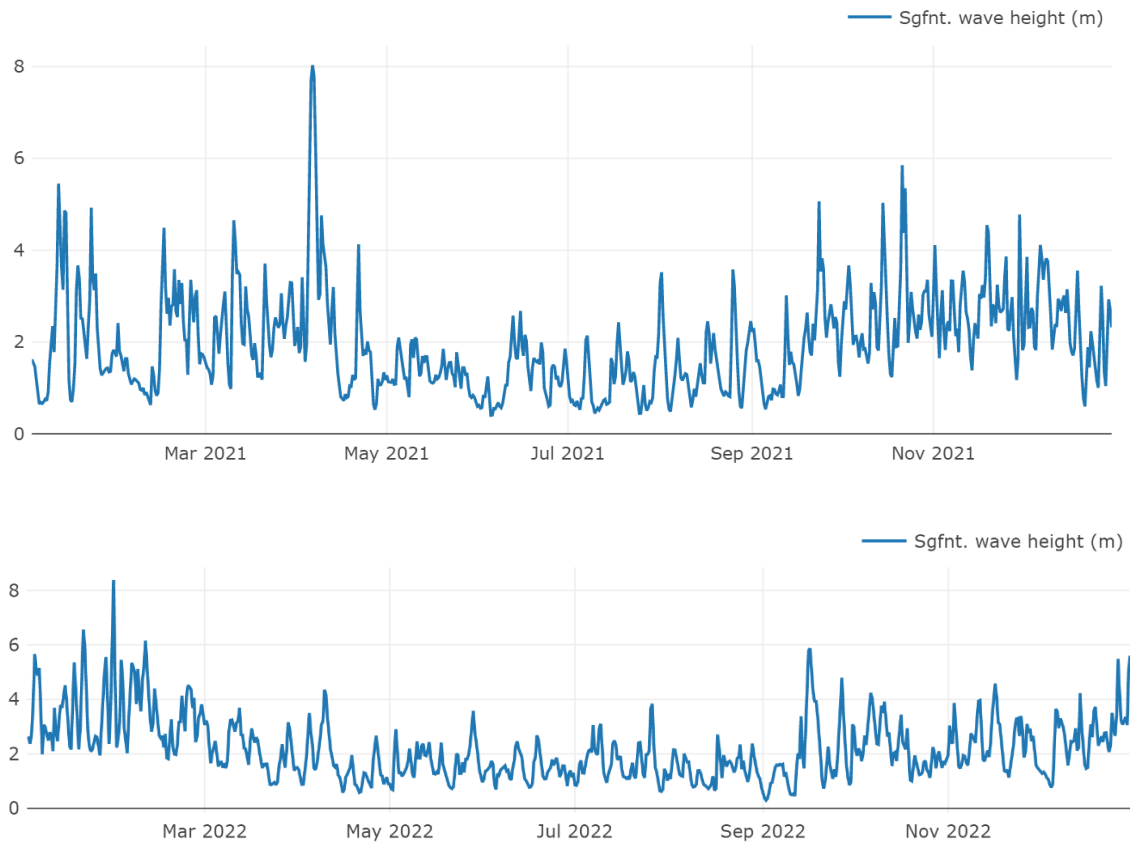


Figure 4: Historical significant wave height graph for Utsira Nord in 2021-2022 [8]

2.2.3 Summary wind and waves

The utilization of weather and wave conditions is a crucial factor in determining the appropriate time for the installation, transportation, and maintenance of offshore wind turbines. The deployment of wind turbines typically desires low wind speeds and minimal wave heights for safe and efficient installation. Based on the wind flow speed graph depicted in figure 3, the months between mid-May and the end of July exhibit the lowest wind speeds, making them the most optimal time frame for wind turbine installation.

In addition to wind speed, wave height is also a critical factor to consider when installing and maintaining wind turbines. As indicated in the wave statistic in figure 4, the wave heights in 2021-2022 are notably lower from early May to mid-October. These observations further support the suitability of the mid-May to the end of July time frame for wind turbine installation and transportation, although the deployment can be considered in September/October if the wave height is sufficiently low.

2.3 Daisy Chain

In the context of offshore wind energy, a "daisy chain" refers to the interconnected arrangement of multiple wind turbines within an offshore floating wind farm. A visual representation of how the system would look at Utsira Nord with 30 WTGs is shown in figure 5. An aspect of this project is that the substation, which is typically located on the seabed, is now planned to be situated onshore at Utsira, as depicted in the figure below. This means that electricity is initially transported to a transformer station located at Utsira, before it is transmitted to the mainland [7]. This cable system layout is the predominant approach for this thesis. In a daisy chain configuration, the wind turbines are connected through a series of IAC, forming a chain that ultimately connects to an offshore substation or directly to the onshore grid. It allows for a sequential connection where the output of one turbine is connected to the input of the next turbine. The installation phase of a daisy chain presents certain challenges due to the interdependence of the turbines and their reliance on one another's arrangement [9].

Once a WTG is assembled, in theory the WTG should be transported out to the designated wind farm site, in this case the Utsira Nord wind farm, for connection to the power system and start generating electricity. However, as the system consists of a series of interconnected turbines, generating electrical power cannot start until all WTGs within a specific series are fully connected. It is then important to note that prolonged periods without voltage can impact the performance and health of the WTG [10].

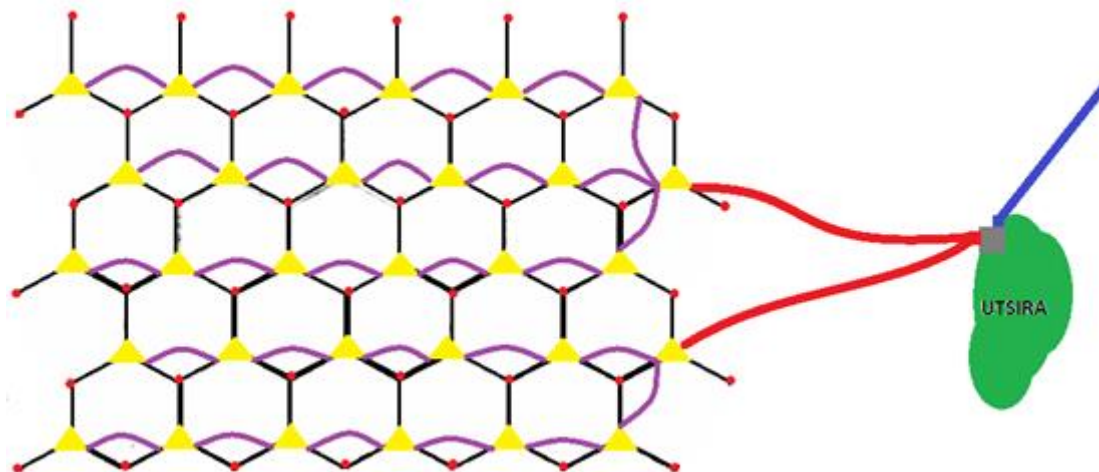


Figure 5: Utsira Nord drawing of infield cable routes between WTGs at the Utsira Nord field highlighted in purple.
Yellow triangle: WTG, Black line: mooring system, Red dot: suction anchor, Purple line: inter-array cable,
Red and Blue line: Export cables, Grey square: Onshore power station.

2.3.1 1st and 2nd end dynamic sections

The installation of dynamic power cables can be divided into two distinct parts, which occur sequentially but not necessarily in a predetermined order. The terms "first end" and "second end" are used to distinguish between two sides of the IAC. Each end is installed and connected to a different FWT, illustrated in figure 6. It can be observed that the same cable is utilized for both ends. Using these terms clarifies that the cable is connected to and spans between two separate FWTs. In this context, the first end of the cable is attached to FWT1, while the second end is connected to FWT2 [11].

The installation process begins by completing the connection at the 1st end and then progresses towards the 2nd end to finalize the installation. This approach is used for the daisy chain distribution system installation, which will be employed in the analysis conducted in this study.

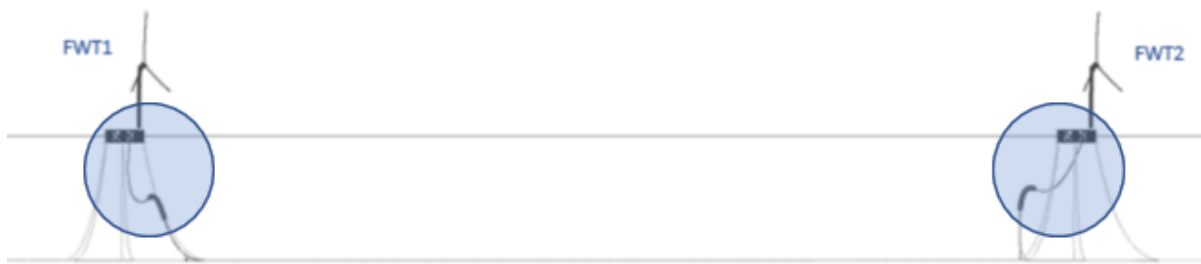


Figure 6: First and end and second end dynamic section, this basically means that the first end of the cable goes to the FWT1, and the second end of the cable goes to the FWT2 [7].

2.4 Offshore wind turbine

This chapter seeks to explain the theory behind an offshore wind turbine, highlighting the key components and how a wind turbine operates. This would hopefully improve the understanding of a wind turbine, which is beneficial given that the offshore wind farm Utsira Nord is the focus of this thesis. The components that will be given the most attention are foundation, tower, nacelle, and rotor, see the components in Figure 7.

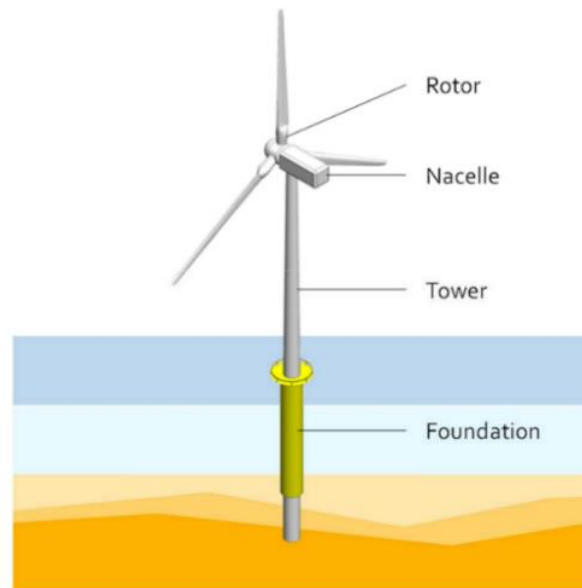


Figure 7: components of an offshore wind turbine [12]

2.4.1 Components

Rotor

A wind turbine rotor consists of the supporting hub and blades. From the aspect of both performance and overall cost, these are considered as the turbine's most crucial parts [13]. Although it is typical for a turbine to have three blades, this is not a requirement. However, the three-blade rotor provides benefits like optimum efficiency. The blades are hollow and composed of a material that is lightweight and durable. The blades are made bigger, more robust and lighter to increase the power production. The blades are designed like an air foil for better aerodynamics. The blade's axis can rotate up to 90° , this motion is known as pitch. The purpose of the hub is to support the blades and allow them to rotate [14].

Foundation

Depending on the water depth, wind turbines in offshore wind farms are raised above the surface of the ocean using various types of foundations. A suitable foundation is essential for ensuring the stability of wind turbines. For instance, monopiles, which are fairly simple constructions made of a

thick steel cylinder that is attached directly to the seabed, are utilised in installations at depths below 15 m. For offshore turbines in deeper water, the foundation floats, but it has the appropriate capacity to hold the weight of the turbine and any forces applied to it. There are three types of floaters that are currently being developed: ballast-stabilized, mooring-line-stabilized, and buoyancy-stabilized foundations [15].

A structure's design seeks to determine the component sizes and foundation type that are appropriate and safe for the site's loading and environmental circumstances. Any structure's likelihood of failing depends on the design's consideration of the load and the strength of the material. As the depth of the sea increases from shallow waters to deep waters, the cost of offshore wind turbine foundations increases simultaneously [16].

Nacelle

The nacelle of a wind turbine is a complex electromechanical system with several components. Significant turbine parts are the generator and the turbine shaft that transfers the harvested power from wind to the generator through a gearbox, which is an essential part of the wind turbine [13]. A yaw orientation system is required to keep the rotor shaft properly aligned with the wind. This mechanism is controlled by an automatic yaw control system with its wind direction sensor usually mounted on the nacelle of the wind turbine [14].

Tower

The three main types of tower designs currently in use are concrete towers, lattice towers, and free-standing towers made of steel tubes. A turbine tower should, as a general rule, be the same height as the circle's circumference. The turbine becomes more susceptible to strong winds as its height increases, as wind speed generally escalates with greater distance from the ground [14]. The site's characteristics have a major influence on the tower selection. Due to the potential for coupled vibrations between the rotor and tower, the stiffness of the tower plays a significant role in the dynamics of wind turbine systems [13].

2.5 Cable installation

Cable installation is the last step of an offshore floating wind farm installation, in figure 8 the installation is in progress. Notably, for an offshore bottom-fixed wind farm, the cables are installed before the WTGs. These cables are specifically engineered to withstand dynamic loads from harsh offshore environmental conditions. The output power of the wind farm turbines is routed through array cables to an offshore substation. The high-voltage power produced by the offshore wind farm is then sent to the onshore substation through export cables, which is further connected to the local electrical grid. A maximum wind speed of 15 m/s and a wave height of 1.5 m are typically the limits for cable installation, whereas a maximum wind speed of 12 m/s and a wave height of 3 m are the limits for cable burial. But a variety of factors can cause these values to change. Depending on the environmental requirements, IEC standards, and DNV guidelines, the array cables should be buried either 1 or 2 m beneath the seafloor in the area between the turbines. This task is done using a trenching ROV operated from a cable lay vessel (CLV) or an onshore location. Export cables are installed similarly to array cables, with the exception that larger equipment is required and that the cables close to the shore should be buried deeper than those farther away [17].

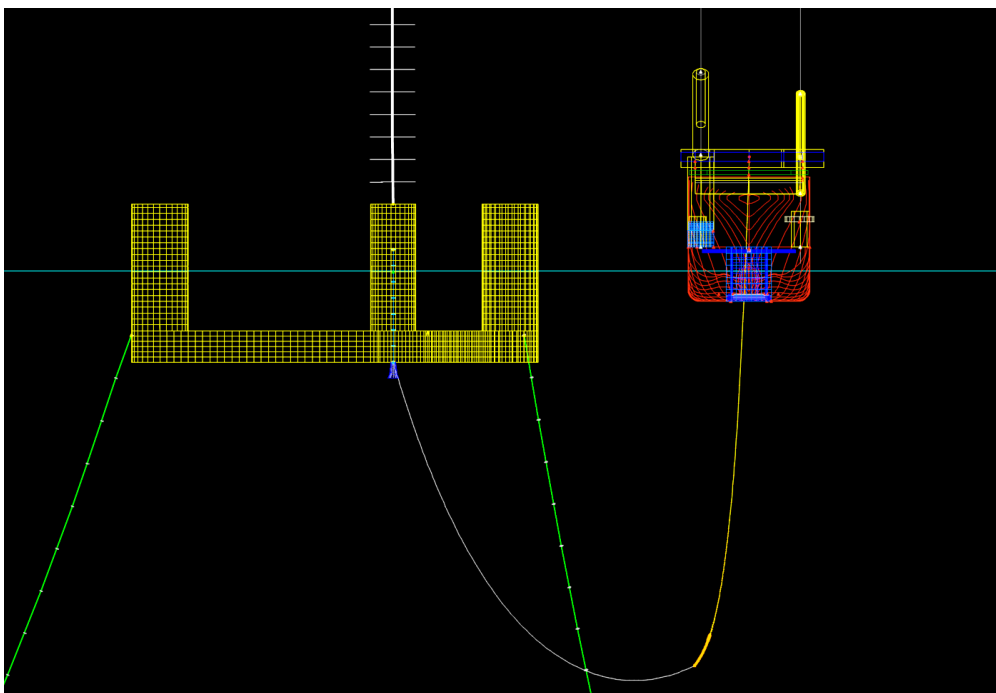


Figure 8: During the installation of IAC

2.5.1 Cable installation parameters

A subsea cable installation may not be as straightforward as it first appears. To successfully install the subsea cable on the seabed, a detailed planned process must be followed, as many factors must be considered, properly calculated, and monitored. As seen in figure 9, a variety of variables affect the laying procedure. Monitoring all these variables will assist in controlling the tension. [18]. Controlling the tension involves monitoring several variables, including bend radius, cable tension, tension on the

WTG winch, tension at the tensioner on the vessel, and moonpool clearance. These variables are affected by several parameters, including water depth, wave forces, current forces acting on the cable, and the motion of the vessel in waves and currents.

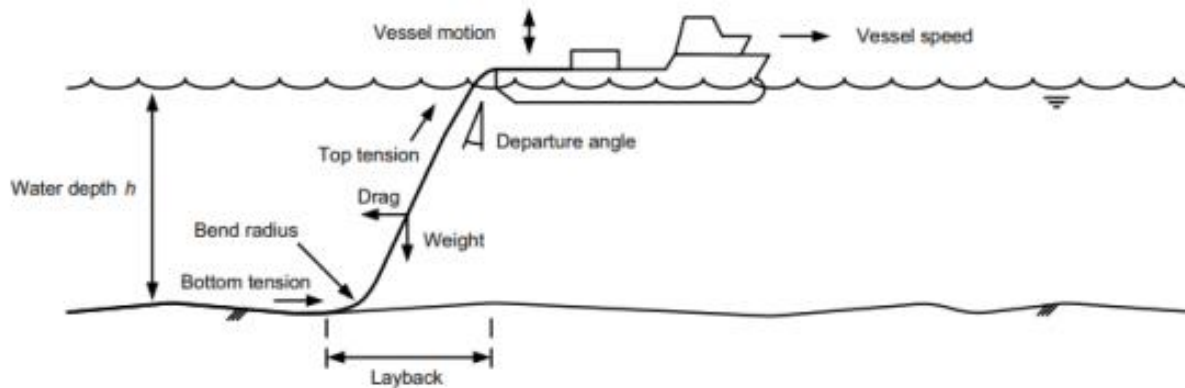


Figure 9: The cable laying process is subject to several parameters [19]

The largest concern during the operation is to maintain a balanced tension in the cable. As mentioned, numerous variables influence the cable tension, which puts demands on the cable's cover layer. In order to produce the correct tension in the cable, the vessel's speed and the tensioner's pay-out speed must be synchronised. The purpose of the cable tensioner aboard the laying vessel is to slow down and regulate the speed of the laying operation. If the cable's axial tension is too high, it will inevitably be damaged or break if the design limit is reached. However, low tension could also lead to disaster [18].

To get even better control on the laying operation, a ROV can be used to monitor the cable. The crew onboard or onshore can keep track of the cable's position with respect to the vessel, the layback distance, and the curvature of the cable's catenary thanks to the ROV's cameras and positioning equipment.

2.5.2 Installation methods

As previously established, laying cables offshore is a challenging task. The requirements and needs of the project will therefore determine which cable-laying platform is best, and the CLV are typically equipped with various deck layouts to handle each particular operation. The capacity for loading, deck area, handling equipment, and manoeuvrability features are some of the most important characteristics for choosing such a platform. To avoid unwanted dynamics on the cable and achieve successful cable lay operations, good manoeuvrability is extra essential [18].

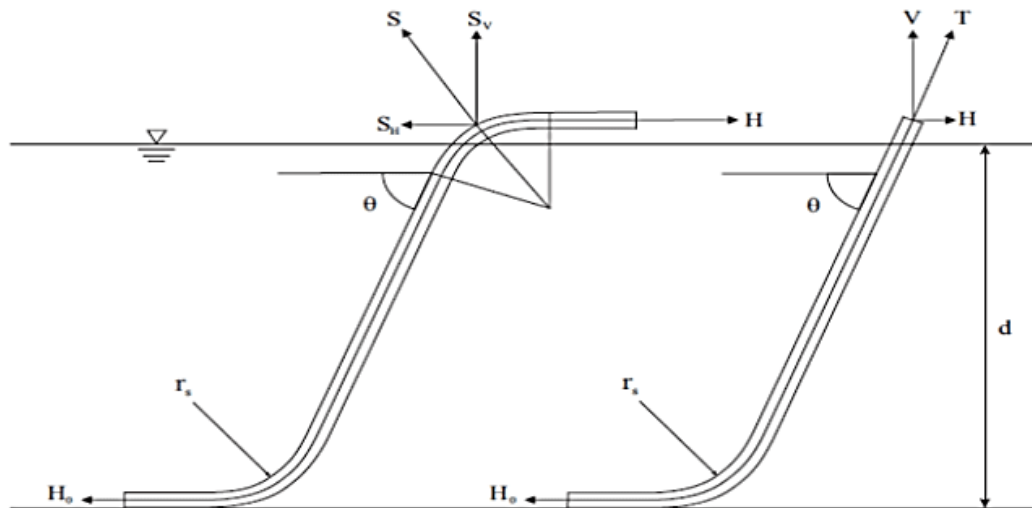


Figure 10: S-lay & J-lay [20]

The two major techniques for deploying a subsea cable are the J-lay over the side of the ship or via a moonpool and the S-lay with a chute/stinger, in figure 10 both methods are shown. The S-lay technique, where the cable is deployed over a chute, is the most preferred one. The chute has a radius that is equivalent to or larger than the minimum bend radius (MBR) of the cable and is made as a rounded part of the vessel's stern. The J-lay method allows for shorter layback lengths because the cable is deployed nearly vertically to the seafloor. The biggest difference between these deployment methods is how the cable bends as it is deployed, from where the tensioner is placed to the seafloor. While the J-lay method will only bend at the touch down point (TDP) and not at the top following the tensioner, the S-lay will be bent over the chute and at TDP [21].

2.5.3 Cable lay vessel – Edda Freya

Edda Freya, a cable vessel in DeepOcean's fleet, is used as basis for the analysis in this thesis as it reflects a possible realistic scenario. The Edda Freya shown in figure 11, is a top-of-the-line DP3 subsea construction and installation vessel, well-suited for a wide range of operations across the globe. Notably, it features an environmentally conscious diesel electric hybrid propulsion system, which maximizes fuel efficiency. The vessel is specifically designed to excel in flexible flowline, risers, and umbilical laying operations, offshore construction, inspection, maintenance, and repair operations.

The Edda Freya boasts an impressive 2300 m² of deck space, as well as a robust 400 t AHC offshore crane capable of lifting 600 t in double-fall mode. Additionally, a 70 t AHC offshore crane is bolted, and easily manoeuvrable to a secondary position. The vessel also features a Huisman 150 t dual tensioner vertical lay system (VLS) used for cable installation, located over the main moonpool, as well as a system for quick mobilization of reels and reel drive systems. An integrated skidding system for modules, two moonpool launch and recovery systems for WROV, and a 3000 t carousel located below deck further contribute to the vessel's exceptional capabilities [22]. More specification is given in table 3 and key VLS features is given in table 4.



Figure 11: Edda Freya [22]

Table 3: Edda Freya specifications [22]

Detail	Description
LOA	149.8 m
Beam	27.9 m
Draft, Min/Design/Max	6.1 m / 7.2 m / 8.5 m
Gross Tonnage	17078 GT
WROV	2 x 220 Hp Kystdesign constructor
Moonpool	7.2 x 7.2 m

Table 4: Vertical lay system – Key features for cable installation [22]

Item	Description
1	2 x 75 t tensioner
2	Electric driven retractable tensioners
3	185 t below deck A&R winch
4	Service crane 18 t, 8 m
5	2 x 10 t Hoisting beams
6	2 x 5 t Moonpool tugger winches
7	2 x 2 t Product handling winches

2.5.4 Cable structure & Layers

Submarine power cables are cables for electrical power running through the sea, below the surface. The significance of submarine power cables has steadily increased in recent decades. With the development of offshore renewable energy, cables are needed to transport the energy from wind, wave, and tidal installations to land. The structure of a subsea power cable depends on whether it is alternating current or direct current which is to be transported [23]. Here, DC cables typically incorporate a single conductor, while AC cables usually consist of three conductors that transport current in three phases. AC cables are designed as three-phase cables, which can be laid either bundled together in a three-core formation or as three separate cables. HVDC cables require less material as they only need a single power line to transport electricity, whereas an HVAC link requires three power lines to carry the same power [24].

A cable is basically an assembly consisting of one or more power cores. Commonly, the inter-array transmission systems of offshore wind farms are based on three-phase AC technology. The conductors are electrically insulated, and water sealed by a sheath. Mechanical protection is provided by an armour of twisted steel wires. The armouring also greatly influences the dynamic behaviour of the umbilical. The design of the cable depends on the conditions of the renewable energy project being developed. Most high voltage cables are individually designed for each single project [25].

The marine environment is of utmost importance, and the subsea cable sector strives to minimize its impact on the environment. Any disturbance to the seabed occurs solely during installation or repair activities and is limited to a narrow section [23].

Conductor

The conductors of offshore power cables are either made of copper or aluminium. Since copper allows for a lower cross section, the outer layers, like lead and steel wires, require less material. Aluminium, though, can be a preferable choice in some circumstances. As costs differ greatly and the metal market is unstable, there is no one ideal option. However, joining these two conductor types will result in a lighter cable. As shown in figure 12, the conductor can take on a variety of forms. The power consumption, the environment, and the cable's length all influence the type and shape of conductor that should be used [18].

- Round conductor (single strand)
 - Oval conductor (single strand)
 - Hollow conductor (single strand)
 - Stranded round conductor
 - Profile wire conductor
 - Profile wire hollow conductor
 - Segmental conductor
 - Segmental hollow conductor
- [18]

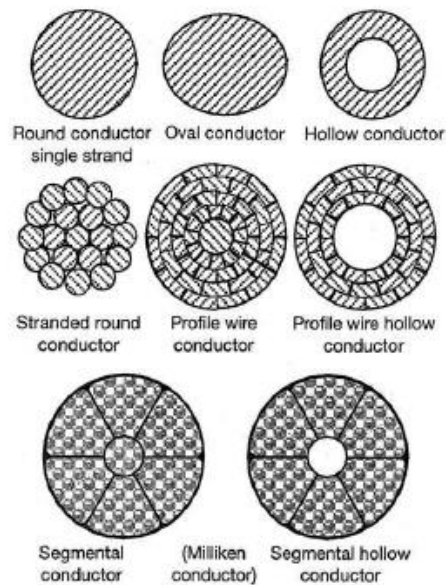


Figure 12: Conductor design [18]

Insulation System

The purpose of the insulation of a cable is to protect the conductors from outside contact, hence it must be durable mechanically and temperature- and aging-resistant. The insulation materials used for underwater cables are the same as those used for onshore cables. Production and application conditions, however, might differ. Mass-Impregnated paper and Cross-Linked Polyethylene are the two insulating types that are most frequently used [18].

Water-Blocking Sheath

Outside the insulation there is a layer of metallic sheath, the majority of high-voltage underwater cables are covered in a metallic sheath, which protects them from moisture and water intrusion. Metals in a variety of shapes, including aluminium, lead, copper, and others, can be used for this purpose. With lead alloy sheaths being the most common, which is subject to the fatigue processes [18].

Armouring

The most prominent component of submarine cable construction is armouring, which is necessary for cables to withstand the installation's tension, protect the cable, and offer the required on-bottom stability. The requirements of the project for which the cable is to be installed, determine how this layer is being put together. Every subsea cable project should consider the tension stability, external threat pattern, and protection needs for each sector of the intended cable route while designing the armouring. The layer's structure and stiffness characteristics have a significant impact on the cable's tensional strength, it is therefore possible to choose between single layer or double layer where each of them has their own distinctive characteristics for strength and flexibility. Typically, galvanised steel

wire is used for the armour layer. The galvanization enables the armour wires to be in direct contact with the seawater without a problem if the outer jacket is not seriously damaged [18].

Usually, single armoured cables are used in conjunction with cable burying, which will protect the cable. Another layer of wire can be added to increase strength while decreasing the torsional stress on the cable. The two layers can avoid the incursion of sharp edges from anchor flukes, cable ploughs, rocks, etc. when they have different lay directions. Double armoured cables are frequently employed in situations where extra protection against the marine environment is required, such as in places where there is a significant risk of crush damage and aggressive seabed incursions. Even though a double layer protects significantly better than a single layer, Double armoured cables are more difficult to instal since they are much heavier and less flexible [18].

Outer serving

To avoid scratches that can weaken the anti-corrosion effect of bitumen and zinc layers, an outer sheath must be placed over cables in order to provide overall protection, secure the armouring during handling and installation, and help distribute forces brought on by such activities. The purpose of the cable's outer sheath is to protect the underlying armouring against abrasion and corrosion [18].

For modern subsea power cables, the main types of servings are extruded polymeric outer servings and servings made from wound yarn layers [18]. The outer layer of yarns or extruded polymers is applied on top of the outer armour layer, in part to make it easier to identify and make visible cables using colour [26].

2.5.5 Subsea power cables

Example of how typical layers of an IAC and Export cable can look like, is shown in table 5 and 6.

Table 5: Typical IAC [27]

66kV cable designed for offshore wind	
Conductor	Cu or Al conductors longitudinally water blocked
Conductor screen	Extruded semi conductive compound
Insulation	EPR
Insulation screen	Extruded semi conductive compound
Screen	Individual Cu-tape screen on each phase
Fibre optic unit	Up to 3 FO units with metal tube
Lay up	Three power cores laid up with extruded fillers
Armor bending	Polypropylene
Outer protection	Polypropylene yarns in customizable colours
Armouring	One layer of galvanized steel wires, flushed with bitumen

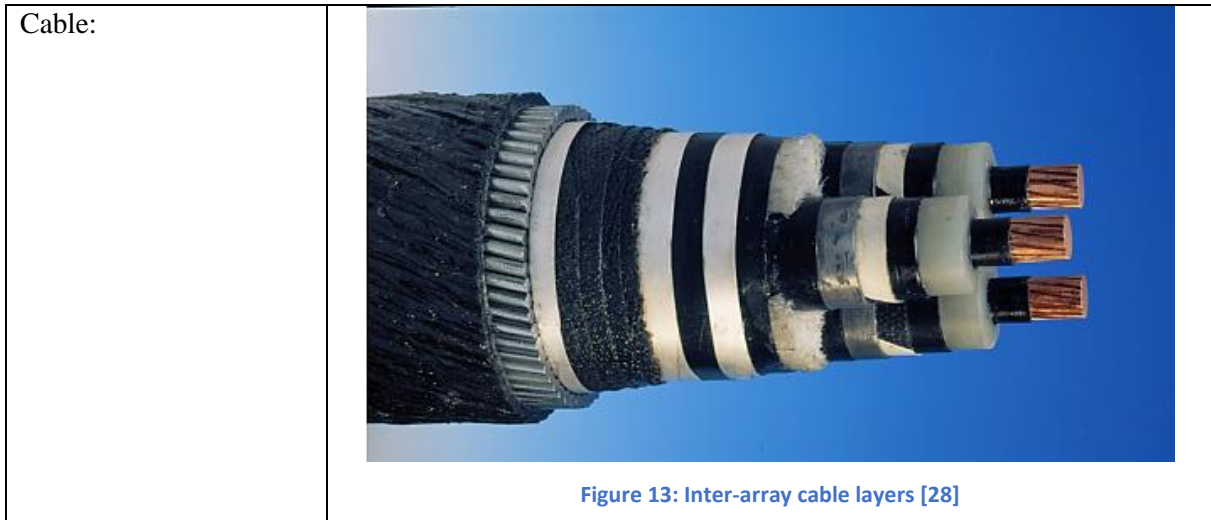



Table 6: Typical Export cable [29]

Typical 400 kV export cable design for offshore wind	
1.	Conductor (Al or Cu)
2.	Inner semi conducting layer
3.	XLPE insulation
4.	Outer semi-conducting layer
5.	Swellable tape
6.	Lead sheath
7.	PE over sheath
8.	Fibre optic cable
9.	Filer profiles
10.	Bedding (PP)
11.	Armouring
12.	Outer serving (PP)
Cable:	 <p data-bbox="692 1879 1032 1908">Figure 14: Export cable layers [29]</p>

3 Methodology

The methods and data that were used to address the research topics of this work will be further explained in this chapter. In order to provide results that accurately reflect the realities of the offshore industry, a variety of methods have been used, as previously mentioned in chapter 1.4. In this thesis, a variety of literature have been studied, and feedback from DO personnel has been gathered. Their knowledge and viewpoints have been helpful in developing this thesis.

3.1 Literature study

In the initial phase an essential part of my master thesis was the preparation work, getting familiarized with the offshore wind industry, IAC installations and other relevant information regarding this matter. This was followed by collecting as much data as possible on various aspects of wind energy, with specific focus on the different steps involved in cable installation and what that might entail. Books, compendiums, previous master's theses, scientific articles and subject-specific reports served as the main sources for the literature study.

There was a lot of useful data available on the subject, but it has been essential to use caution when obtaining it. Therefore, evaluating the validity of the data was a key step in locating and assessing literature. To assess the quality and relevance of the information, four criteria from SNL were employed as points of reference [30]:

- Credibility: Is the source to be trusted?
- Objectivity: Is the source neutral?
- Accuracy: Do you find traces of cheating or sloppiness?
- Suitability: Do you find the answers you need?

Numerous services have been explored to locate comprehensive and trusted information on each topic. Through the literature study, reliable data has been collected from a number of sources bearing in mind the four points from SNL. Examples are internal Utsira Nord project documentation, Google Scholar, online databases like Scopus, and websites like Offshore Technology and Wind Europe.

3.2 DeepOcean

DeepOcean is a leading provider of subsea services that has been involved in a number of offshore operations, such as installation of structures, flexible risers and pipelines. Being able to sit at DeepOcean's office in Haugesund, shown in figure 15, a company with so much competence, gave the opportunity to receive information and get help from people with extensive knowledge of the industry and who work on projects where they actually do the planning and the execution. Having the opportunity to ask DO personnel if there was anything I wondered about, has been of great help to this task, as they are people with long experience and high competence within their area. Input was achieved through discussions, guidance with different data programmes for analysis and information regarding offshore cable installation.



Figure 15: DeepOcean office in Haugesund [31]

3.3 Orcaflex

To analyse and resolve technical issues, Orcaflex is primarily utilised by naval architects, engineers, consultants and designers. Orcaflex is a highly regarded and industry-leading programme for the static and dynamic analysis of offshore marine systems. In terms of power, performance, and capability Orcaflex is considered a step ahead other packages when it comes to dynamic analysis software [32].

A model was first created, which consisted of the system components, geometries, and boundary conditions. The marine environment was then defined by providing relevant data, such as water characteristics and wave motions, to simulate the real-world scenario. General simulation settings were then specified to dictate the accuracy and precision of the results. Next, both static and dynamic analyses were performed, where the relevant results were extracted.

Orcaflex has the capability to model a wide range of objects, including [11]:

- Vessels
- Winches
- Subsea structures
- Turbines
- Lines

3.4 Excel

Once the data was collected, it was then plotted in Microsoft Excel, which is a program based on spreadsheets that allows for calculations, information analysis, and processing of lists and numerical data [33]. This provided a clear view of the variables and made it easier to compare the different sea states and wave conditions.

4 Modelling of Analysis

In this chapter, the modelling of the cable installation scenarios will be described.

4.1 Environment

4.1.1 Key parameters

The accuracy of simulations is highly dependent on how the simulations are performed and the parameters chosen. The range of parameters chosen for the analysis can result in a significant number of simulations. Therefore, it is essential to carefully consider the parameters that have an impact on the variables.

A matrix was created to handle the complexity, containing the key parameters needed for the simulation. The matrix for the simulations is established below in table 7. The environmental headings are visualized in figure 16 to provide a clearer understanding of the matrices. The combination of these parameters provides valuable information on the necessary number of simulations and the computational resources necessary to accomplish them.

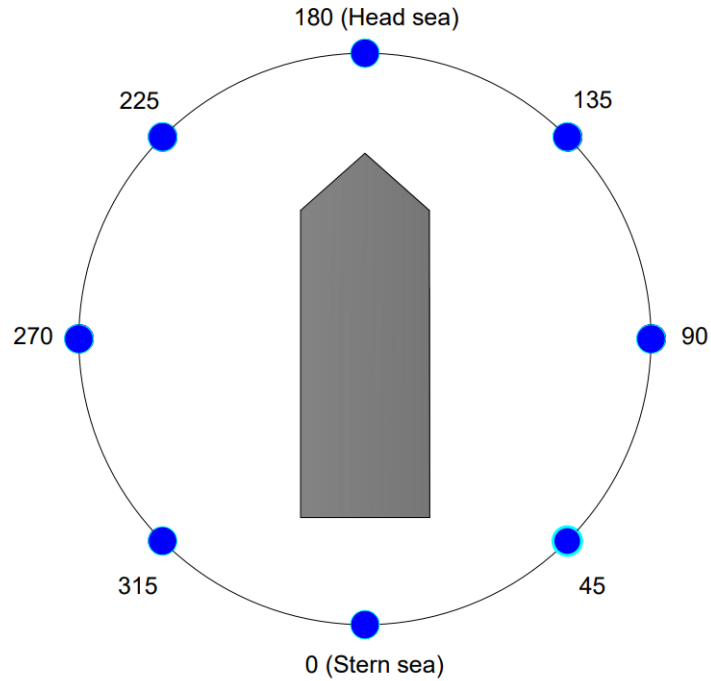


Figure 16: Environmental load heading definition, created in Bricscad

Table 7: Key parameters matrix for simulations

Key Parameters								
Vessel	(head sea)	(beam sea)			(stern sea)	(beam sea)		
- Heading	180	135	90	45	0	315	270	225
Cable								
-Configuration	JDR 3 x 800 mm ² 66kv							
-Deployment speed [m/s]	0							
-Deployment position	Moonpool							
Environment								
- Collinear surface current speed [m/s]	0, 0.3, 1.0							
- H _s [m]	2, 3, 4							
- T _p [s]	8							
- Water depth [m]	260							
- Seabed friction coefficient [-]	0.5							

4.1.2 JONSWAP and wave spectrum

Wave spectrum refers to the distribution of energy over the range of frequencies that make up a particular wave field. The JONSWAP spectrum is based on the assumption that wave energy is transferred from wind to water through a nonlinear process. The spectrum is used to estimate the expected wave height and period in a given sea state, and it is often used in the design of offshore structures, ships, and other marine systems. The JONSWAP spectrum is a modified version of the Pierson-Moskowitz spectrum, which was developed earlier to describe the ocean wave spectrum. The JONSWAP spectrum is more accurate for describing sea states with higher wind speeds. The dynamic simulations were conducted using an analysis that directly incorporates irregular waves, using the JONSWAP spectrum to generate realistic ocean wave conditions [34].

Irregular waves, which are waves that have different wave heights and wave periods, unlike regular waves that have a constant wave height and wave period. Irregular waves can be represented by a wave spectrum, which describes the distribution of wave energy over different frequencies [35].

Significant wave height is an important parameter used to describe the sea state, which is the state of the ocean surface. It is defined as the average height of the highest one-third of waves, measured over a period of 20 minutes. The higher the significant wave height, the more energy is present in the wave field, and the more severe the sea state can be. It is a key factor in determining the loads and forces that structures will experience in different sea states [36].

The wave spectrum is defined as [37]:

$$S(f) = \frac{5}{16} H_s^2 f_p^4 f^{-5} \exp \left[-\frac{5}{4} \left(\frac{f}{f_p} \right) \right] \quad (\text{Eq.1})$$

- H_s: Significant wave height
- f_p: Peak frequency [rad/s] = 2π/T_P
- F: Frequency [rad/s]

The wave spectrum is modified to create the JONSWAP wave spectrum and is defined as [38]:

$$S_J(f) = A_\gamma S(f) \gamma^{\exp \left(-0,5 \left(\frac{f-f_p}{\sigma f_p} \right)^2 \right)} \quad (\text{Eq.2})$$

- σ : Spectral Width parameter
 σ_1 for $f \leq f_p$
 σ_2 for $f > f_p$
(average: $\sigma_1 = 0.07$, $\sigma_2 = 0.09$)
- γ : Non-dimensional peak shape parameter
(average: $\gamma = 1$)
- A_γ : $1 - 0.287 \ln(\gamma)$, a normalising factor

The peak shape factors γ can be found by [38]:

$$\begin{array}{lll} \gamma = 5 & \text{for} & \frac{T_P}{\sqrt{H_S}} \leq 3,6 \\ \gamma = e^{(5,75 - 1,15 \frac{T_P}{\sqrt{H_S}})} & \text{for} & 3,6 < \frac{T_P}{\sqrt{H_S}} < 5 \\ \gamma = 1 & \text{for} & 5 \leq \frac{T_P}{\sqrt{H_S}} \end{array}$$

One can find different combinations of significant wave height and wave period within the given framework [38]:

$$3,6 < \frac{T_P}{\sqrt{H_S}} < 5$$

A 3-hour operable sea state is the default duration for sea state in Orcaflex but simulating that kind of magnitude requires significant computational effort. It is therefore possible to change the duration depending on the user's requirements. The critical factor is to determine the maximum safe sea state for the operation. Although the operation may take many hours or even days, critical steps like landing equipment on the seabed may take only a few minutes. Therefore, using a 3-hour storm for such short operations would be too conservative [39].

In order to reduce simulation time, a 1-hour storm has been utilized in the simulations. This duration was chosen due to its relatively short time span and the option to abort if needed. For cases 2 and 3, as is presented in chapter 5.2, a one-hour operable sea state was established, and a sample of this duration was obtained through sensitivity testing. The results of this testing can be found in chapter 6.

However, if there are a number of short operations that cannot be interrupted nearby, it may be necessary to conduct a 3-hour storm analysis regardless. The objective is to save time during simulations without compromising accuracy. For case 1, presented in chapter 5.2, this approach is not used, and the Gumbel distribution method is applied instead. A more detailed explanation of this approach will be provided in chapter 7.1.

4.1.3 Current

For all the scenarios simulated in Orcaflex, current is included. These scenarios are more exposed and therefore more sensitive to the effects. Additionally, it is advisable to include multiple current rates for each scenario, as it is common in studies to vary a parameter with at least three values for comparative reasons. The flow profile remains linear across the entire water depth, and an assumption is made that the flow direction aligns with the wave direction.

4.1.4 Water Characteristics

In order to analyse various scenarios, Orcaflex offers a variety of settings for modelling the seafloor. The steps being analysed make use of the water characteristics presented in table 8.

Table 8: Water characteristics

Property	Value
Water depth range [m]	260
Density [kg/m ³]	1025
Kinematic viscosity [m ² /s]	1.35 x 10 ⁻⁶
Temperature [°C]	10
Friction coefficient [-]	0.5

4.2 FWT, vessel and deployment method

4.2.1 Floating wind turbine

The FWT considered is based on a final configuration of a 15 MW wind turbine design and serves as the initial reference point for this study. This model originates from DeepOcean and has been employed to further refine the model specifically for this study. The base model, which can be observed in figure 17, provides a visual representation of the FWT configuration.

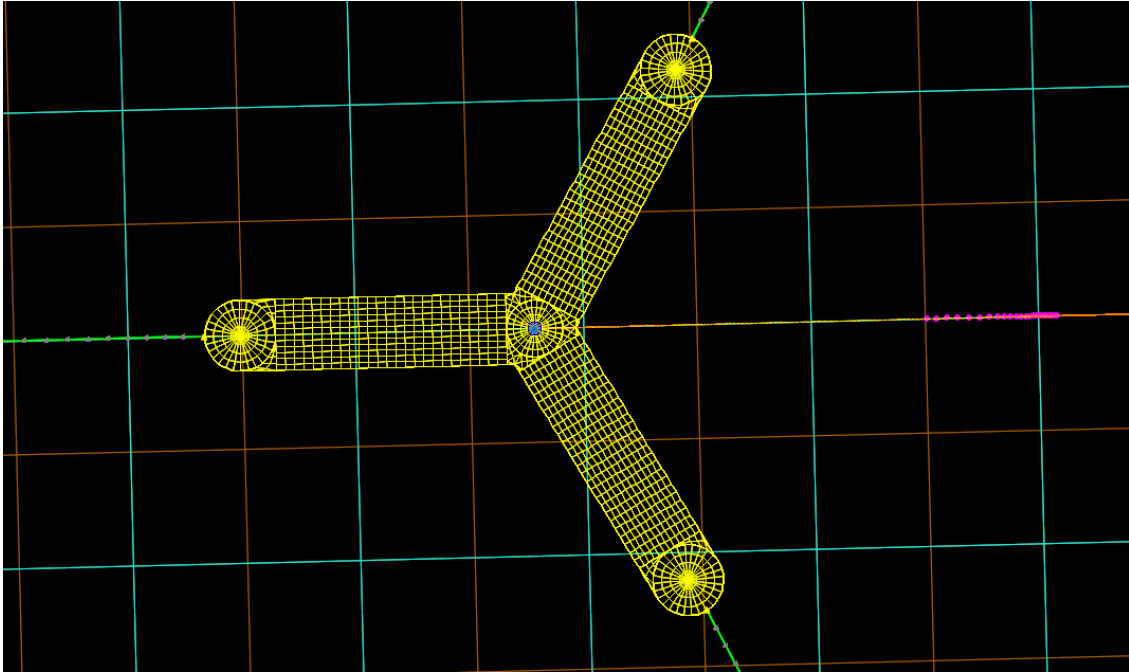


Figure 17: Foundation designed for 15MW FWT

The FWT features three outer columns along with a central column housing the wind turbine, as illustrated in figure 18. Detailed dimensions of the FWT model can be found in table 9 below, which also all outlined steps in chapter 5.1 are based on.

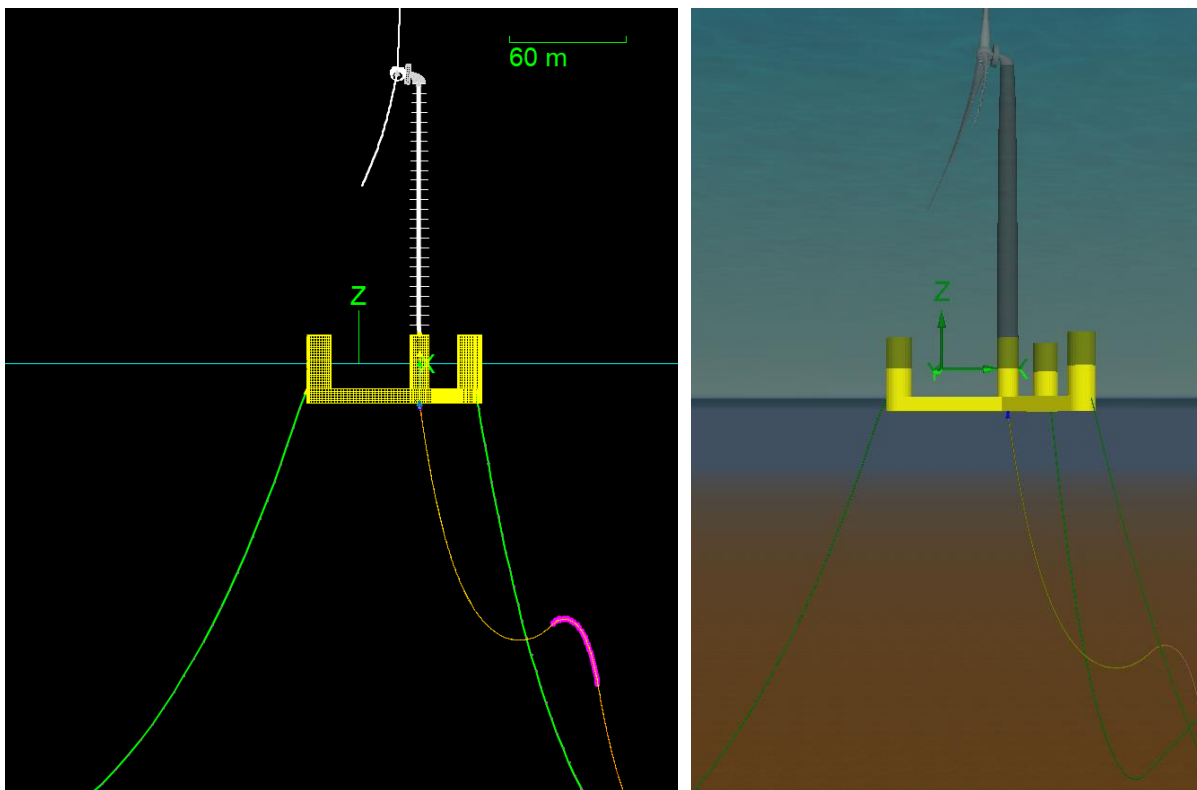


Figure 18: Final configuration of FWT model

Table 9: Main dimensions FWT [40]

Dimension	Value
OD Outer Columns [mm]	12500
OD Inner Column [mm]	10000
Height Columns (with foundation) [mm]	28000 (35000)
Distance Outer Column to Inner Column [mm]	51700
Distance Outer Column to Outer Column [mm]	89700
Tower Height [mm]	1294950
OD Tower [mm]	10000
Blade Length [mm]	1164140
Total Turbine Height [mm]	2459090

The I-tube is strategically positioned in the central region of the FWT structure, as illustrated in figure 19. The positioning of the I-tube optimizes the operational flexibility and facilitates the cable installation operations.

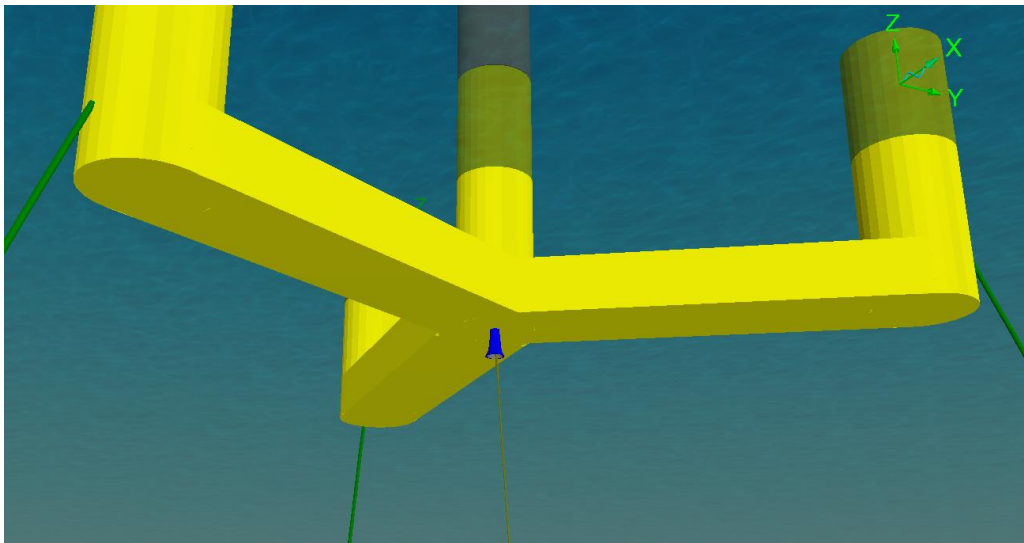


Figure 19: I-tube placement on FWT

24 buoyancy modules have been included in the analysis, each module having a uniform weight of 350 kg. These buoyancy modules are positioned along the cable, spanning the arc length ranging from 160 m to 206.5 m, a visualisation of this is shown in figure 20. In addition to the buoyancy modules, the cable features a dead man anchor (DMA). The DMA comprises two chains, each weighing 3.5 t. It is positioned 4 m ahead of the buoyancy modules, 156 m from the initial point of the cable. The cable itself has been constructed with a total length of 359.5 m. Including these specific details in the analysis allows for a more accurate and thorough evaluation of the cable system's dynamics and behaviour during its deployment and operation.

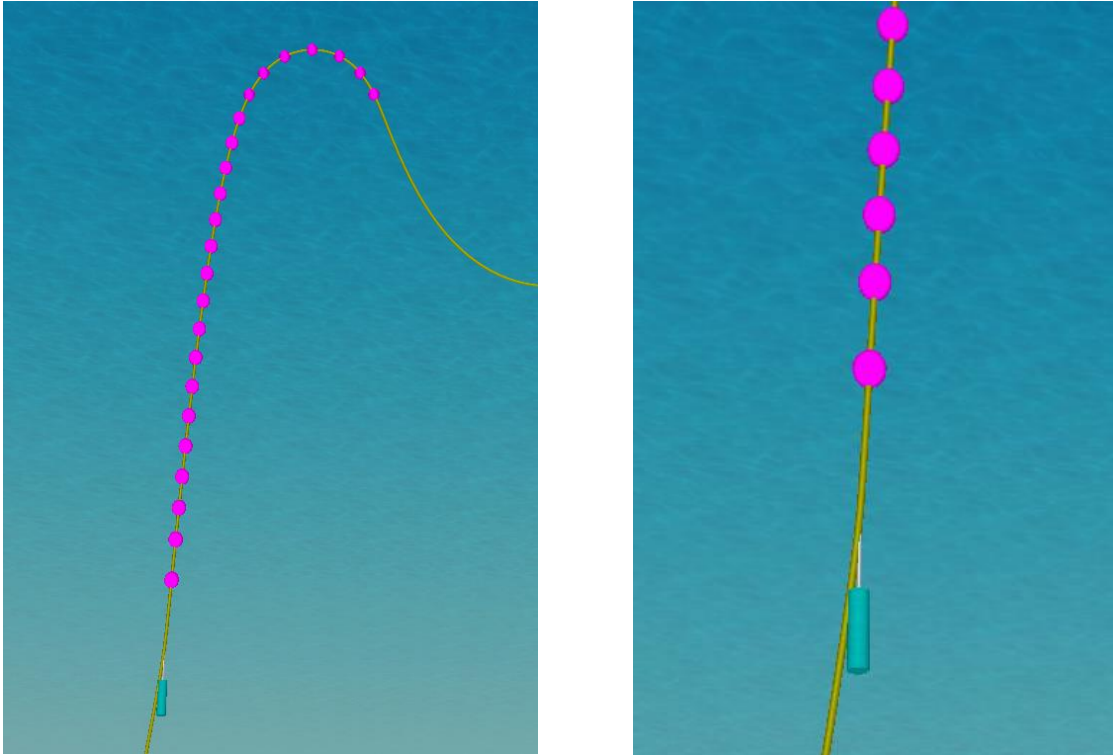


Figure 20: Illustration of DMA and buoyancy modules on IAC

4.2.2 Vessel

The simulations in Orcaflex were conducted using one of DeepOcean's vessels, Edda Freya, as a reference. Detailed specifications of the vessel can be found in table 10 below and table 3 in chapter 2.5.3. Edda Freya has been modelled to possess unrestricted movement in waves, allowing for motion in all degrees of freedom, as determined by the displacement response amplitude operator (RAO).

Table 10: Vessel specifications [22]

CLV: Edda Freya	
Length overall [m]	149,8
Length between perpendiculars [m]	138,8
Deadweight [t]	9018
Breadth [m]	27
Depth [m]	12
Draft [m]	6.72

4.2.3 Moonpool J-lay

When using the J-lay method through a moonpool, the cable deployment takes place at the centre of the vessel, passing through the moonpool, as shown in figure 21. This method allows for a safe deployment of cables while reducing the risk of damage to the cable during installation. As the base vessel for this thesis is Edda Freya, which is equipped with a moonpool, the dimensions of the moonpool have been considered in the design. The moonpool has a size of 7.2 x 7.2 m, providing sufficient space for the cable to pass through while avoiding contact with the sides of the vessel.

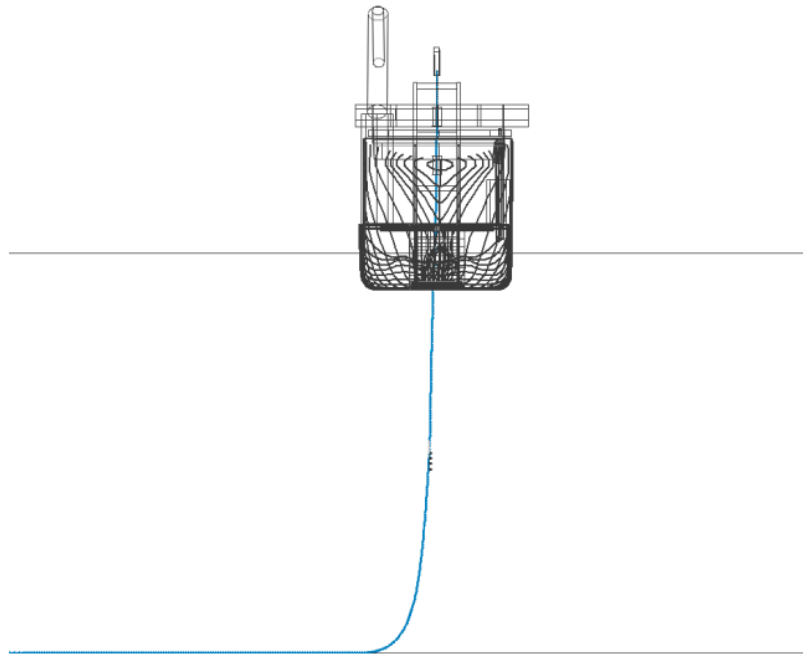


Figure 21: Moonpool J-lay

4.3 Cable line configuration

The array cables used in wind farms are now commonly designed to handle 66 kV, whereas in the past, 630 mm² copper was the largest cable size used for 33 kV wind farms. As new projects are being planned or constructed, larger cables with a rating of 66 kV and a size of 800 mm², made of either copper or aluminium, are becoming more prevalent. The higher voltage rating has been the subject of intense technical development, as it allows for greater capacity to be connected on a single string, thereby reducing the length of cable needed and minimizing the number of switchgear bays required at the substation [41]. In appendix A the IAC 800 mm² 66 kV used for this study can be found.

For all the scenarios the JDR 3 x 800 mm² 66 kV was used. The configurations assume three copper conductors, extruded XLPE isolators, two fibre optic cables, with a single layer of steel armour wires embedded in bitumen. The outer serving of the cable consists of a two-layer PP yarn. The cables

cross-sections, along with full specifications and limits, can be found in appendix A. Main specifications are listed in table 11.

The use of nodes and segments is an essential part of line modeling in Orcaflex. A line is represented by a series of nodes (clump) that are connected by segments, as shown in figure 22. Each node represents the location of a point along the line, while each segment represents the part of the line that connects two nodes. The nodes and segments are then used to define the geometry and properties of the line, and they can be added or removed to adjust the model's accuracy. In order to analyze the integrity of a cable, the lumped mass method is used to calculate the dynamic equilibrium for each node in the cable, resulting in a set of discrete equations of motion. Finite difference methods are used to solve these equations in the time domain and indicate the displacement, stress, and tension of the node [42].

The discretization of elements has a significant impact on a model's accuracy in finite element methods. In the context of cable analysis, an assumption is made regarding the line segment lengths of the cable that were deemed significant for the analyses. A segment length of 0.5m for the mid-span is considered relevant for the analysis.

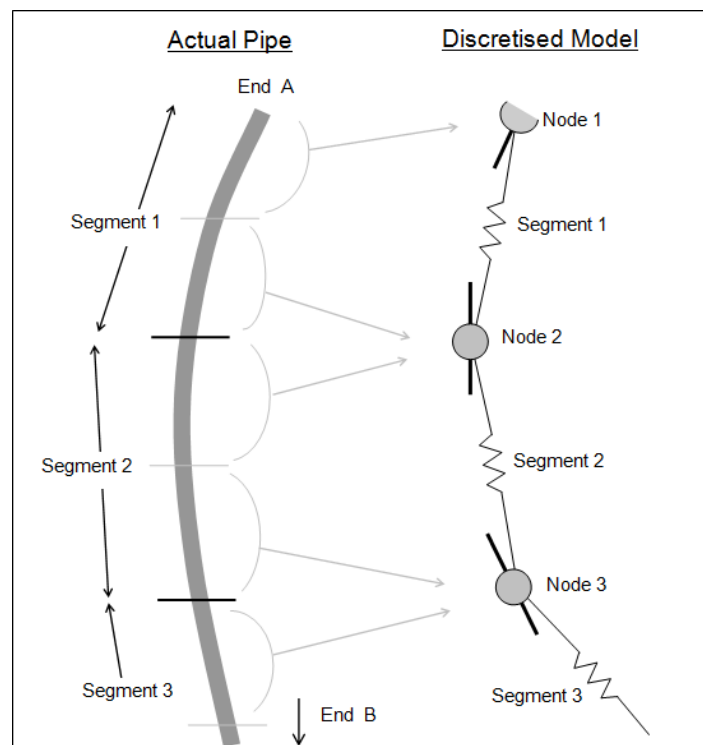


Figure 22: Nodes and segments in a line model [42]

Table 11: cable specifications [43]

Property	3 x 800 mm ² 66kV
Overall diameter [mm]	190
Weight in air [kg/m]	72,8
Weight in seawater [kg/m]	46,1
Axial stiffness [MN]	845
Bending stiffness [kNm ²]	21,2
Torsion stiffness [kNm ²]	6,6

4.3.1 IAC accessories

Inter-array cable installation in offshore floating wind farms is a demanding operation that needs the employment of some accessories to ensure a smooth and effective completion of the process and have therefore been included in the model. These accessories are necessary to address challenges that may arise during installation, including underwater obstacles, and cable routing challenges.

The DIAC accessories needed for the cable installation:

- Pull-in Head Assembly
- Bend Stiffener Assembly
- Buoyancy Modules
- Dead man anchor

Pull-in head

A pull-in head, also known as a J-tube pull-in head, is a specialized tool designed to facilitate the connection of the subsea power cable to the wind turbine. An example of how a pull-in head can look is shown in figure 23, and the properties used for the simulations are presented in table 12. It is typically mounted on the WTG foundation and is used to guide the cable into the J-tube or cable protection system that runs from the WTG to the seabed [44].

Proper installation and use of the pull-in head are critical to the successful installation of subsea power cables for offshore wind farms. The pull-in head must be properly aligned with the J-tube, and the tension on the cable must be carefully controlled to prevent damage to the cable or the pull-in head [44].



Figure 23: Pull-in Head [44]

Table 12: Pull-in head properties

Property	Value	Unit
Weight	1790	kg
Length overall	7.2	m

Bend stiffener

The Dynamic Cable Bend Stiffener is a type of bend stiffener that is designed to protect submarine power cables from damage caused by bending, buckling, and abrasion. It is typically made of moulded polyurethane material and is installed around the cable to maintain a consistent bend radius, reducing the risk of damage. The added stiffness provided by the stiffener ensures that the cable remains stable under high loads, reducing the risk of failure and increasing reliability. This means it will protect the minimum bending radius (MBR) of the cable under defined tension and angle combinations, preventing fatigue damage in the hang-off region by limiting bending stresses and curvature to acceptable levels. Additionally, Dynamic Cable Bend Stiffeners are customizable to suit specific cable configurations and requirements, and are easy to install, offering benefits such as reduced downtime and lower maintenance costs. A typical design of a bend stiffener is shown in figure 24, and the characteristics used in the simulations are shown in table 13 [45].

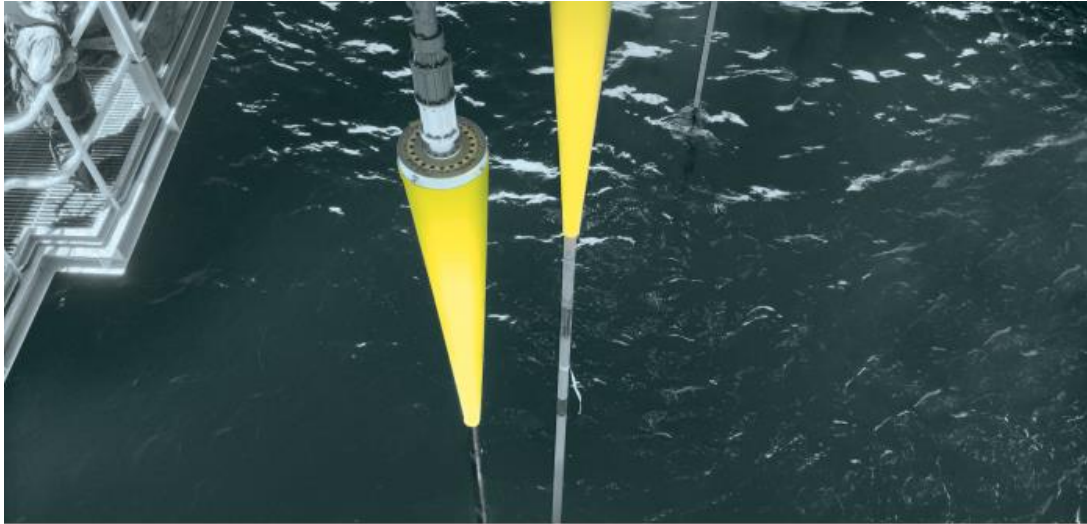


Figure 24: Bend stiffener [45]

Table 13: Bend stiffener properties

Property	Value	Unit
Length, rigid base	0.5	m
Length, flexible cone	4.0	m

Buoyancy modules

Buoyancy modules are essential for subsea operations, helping control the ascent, descent, and positioning of equipment and structures in the water column. The buoyancy characteristics used for this study are shown in table 14. Buoyancy modules are based on a flexible, modular system that can easily be adapted to meet project-specific needs, typically installed between a subsea structure and a surface vessel or platform. By adding buoyancy to subsea components, buoyancy modules reduces weight and drag, making it easier to install and manoeuvre. The modules consist of a series of individual buoyancy blocks made from a high-strength, low-density foam material encased in an abrasion-resistant outer skin [46].

Distributed buoyancy modules consist of two main components: the clamp and buoyancy elements. The clamp axially secures the buoyancy element to the dynamic section of the submarine power cable, ensuring axial capacity is maintained throughout the design life of the system. The density of the buoyancy element is dependent on the intended uplift and service depth. Supplied buoyancy modules are designed for immersion in seawater to the specified water depth for the full design life of the dynamic submarine power cable system. With its modular design and reliable components, buoyancy modules offer a flexible and cost-effective solution for controlling the buoyancy of subsea equipment, providing necessary lift and stability for successful subsea operations. Figure 25 below show an illustration of how buoyancy modules typically are attached to a submarine power cable [46].

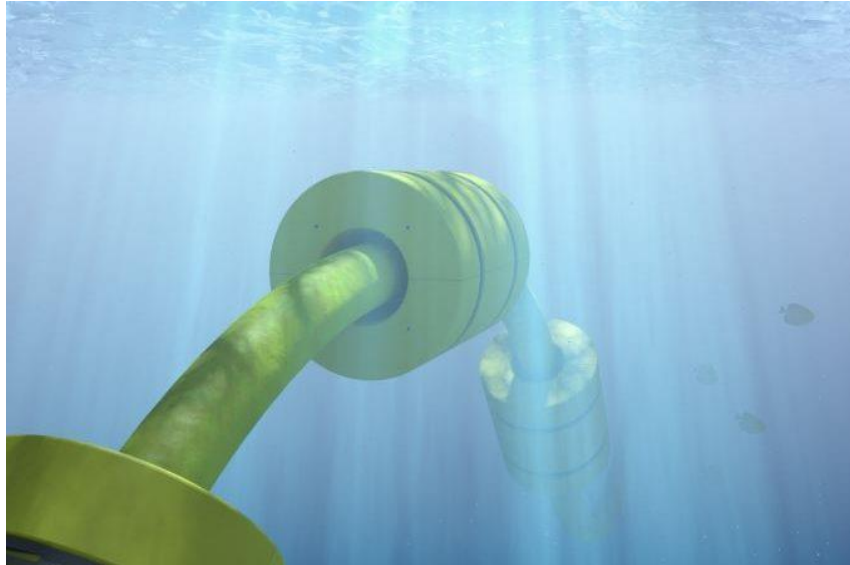


Figure 25: Buoyancy modules [46]

Table 14: Buoyancy module properties

Property	Value	Unit
Length BM	1.0	m
Total weight	350	kg

Dead man anchor

The dead man anchor consists of a heavy object, with sufficient weight to resist the forces exerted by ocean currents and waves. Its fundamental purpose is to provide stability and prevent the cable from floating up to the surface or drifting off course when deploying buoyancy modules. An example of a DMA is visualized in figure 26 and the characteristics used for this study are shown in table 15.

Strategically placed at regular intervals along the cable, the DMA serves multiple indispensable functions. It plays an important role in upholding the desired cable configuration by providing necessary tension and preventing excessive movement. Additionally, it aids in reducing cable bending and fatigue by keeping the cable in a controlled position [47].

Table 15: DMA properties

Property	Value	Unit
Length	4.0	m
Total weight	3.5	t

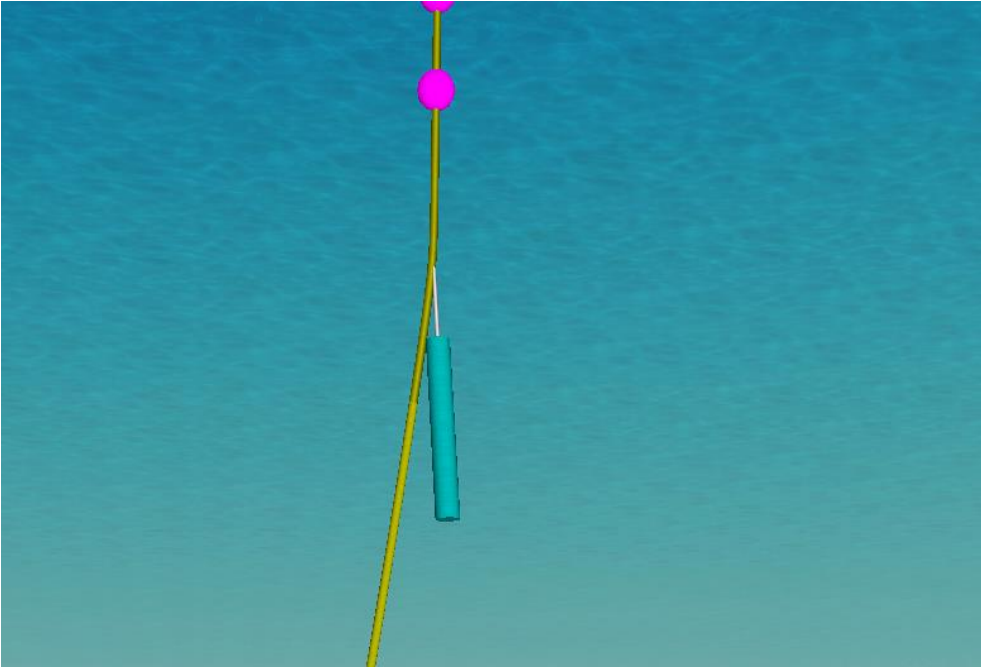


Figure 26: Dead man anchor is the blue cylinder

4.4 Acceptable cable laying criteria

To ensure that a cable can be successfully installed at the seabed without any damage to its integrity, specific criteria must be met. These criteria serve as limitations to the maximum allowable tension on cable and compression, MBR, and sidewall pressure (SWP). A list of cable limitations used for this study can be found in table 16, collected from appendix A. These limitations are crucial to consider during cable installation, as exceeding any of them can cause damage to the cable and affect its performance.

Table 16: Acceptable cable lay criteria [43]

Cable type:	Max. Allowed Tension [kN]	SWP [kN/m]	MBR [m]	Compression [kN]
3 x 800 mm ²	336	50	3.07	Unknown

Maximum Allowable Tension on cable and Compression

When installing a cable at the seabed, it is crucial to ensure that the cable can withstand the maximum allowable tension and compression. Maximum allowable tension is the maximum amount of force that a cable can withstand before it breaks or sustains permanent damage. Similarly, maximum allowable compression is the maximum amount of force that a cable can withstand before it buckles. These values are important to prevent overloading the cable during installation or operation, which can cause significant damage to the cable or even failure [48].

Minimum Bend Radius

The minimum bend radius refers to the smallest radius a cable can be bent without causing damage to the cable. Bending the cable beyond the MBR can cause the cable to kink, flatten, or even break, which can compromise the integrity of the cable. MBR is particularly important during cable installation, where the cable is often subject to high bending stresses as it is routed around seabed obstacles or curved seabed contours [49].

Side Wall Pressure

When installing a cable at the seabed, the cable can experience side wall pressure, which refers to the pressure exerted by the surrounding soil or sediment on the cable. The cable must be designed to withstand this pressure to prevent it from collapsing or buckling, the limit is determined by the manufacturer. The SWP can vary depending on the seabed soil characteristics, such as its stiffness, density, and water content, and the cable's installation depth. Properly accounting for SWP during cable installation and operation is critical to ensuring the cable's long-term integrity and reliability [50].

4.4.1 Other criteria used in the analysis

Minimum tension on cable

The evaluation of minimum tension aims to determine whether slack occurs during the installation process, which can affect the stability. This is done by examining negative values, which indicate the presence of instability. The significance of examining minimum tension on cable is to avoid zero values in the top tension region, where the cable is deployed [51].

Maximum tension on pull-in winch

Represents the highest safe load it can support, must be considered when determining the maximum tension that can be applied to it. This pull-in winch is located on the WTG, and the maximum tension allowed in the analysis is set to be 10 t. The maximum cable tension during installation must not be greater than the winch's rated capacity, in order to prevent any complications or issues throughout the installation process.

Maximum cable tension at lower tensioner

Within the Edda Freya VLS tower, two tensioners are present, and for the purpose of this study, the cable has been positioned on the lower tensioner. Depending on operational requirements, both tensioners may be employed, or alternatively, only one of them. As this study assumes use of the lower tensioner, this is considered the starting point for the cable in the model. The maximum tension allowed on the lower tensioner is 75 t [22]. Figure 27 illustrates the location of the lower tensioner on the vessel, indicated by a yellow circle.



Figure 27: The yellow circle indicates the location of the lower tensioner on Edda Freya's VLS tower [22]

4.5 Simulation settings

4.5.1 Time integration method

The explicit and implicit integration schemes are the two ways of time integration supported by Orcaflex. The explicit solution is based on the central difference method, which computes the response at the next time step using information from the current and previous time steps. The implicit solution is based on the backward differentiation method, which computes the response at the next time step using information from the current time step and a prediction of the future response [52].

The implicit solution is generally considered to be more accurate and stable than the explicit solution. This is because the explicit solution can suffer from numerical instability when the time step is too large, or the system is highly nonlinear. In contrast, the implicit solution can be significantly faster as it allows for larger time steps as well as variable time steps, and more complex systems without numerical instability. Additionally, the implicit solution can provide better accuracy for systems with low damping or large stiffness, where the explicit solution may require very small-time steps for accurate results. In this dynamic simulation, it was assumed that the implicit integration method would be appropriate for the dynamic analyses and reduce time needed for simulation [52].

4.5.2 Simulation period

In Orcaflex, the simulation time is specified by setting the simulation period, which determines the length of the simulation and controls the time step size. Figure 28 shows how the simulation time can be divided into different stages, allowing users to capture specific parts of the simulation or time-shift one aspect of the model in relation to others. Each part of the model has its own user-specified time origins, with the default time origins of all parts being zero and in line with global time [53].

The simulation period is divided into a number of stages, with the durations of each stage specified according to the analysis objectives. Typically, the first stage is the build-up stage, which gradually ramps up the motions of the environment and vessel from zero to their full size before the main simulation stages begin. This allows for a smooth transition from static positions to dynamic motions. Once the build-up stage is complete, the simulation time begins, marking the start of the main simulation stages [53].

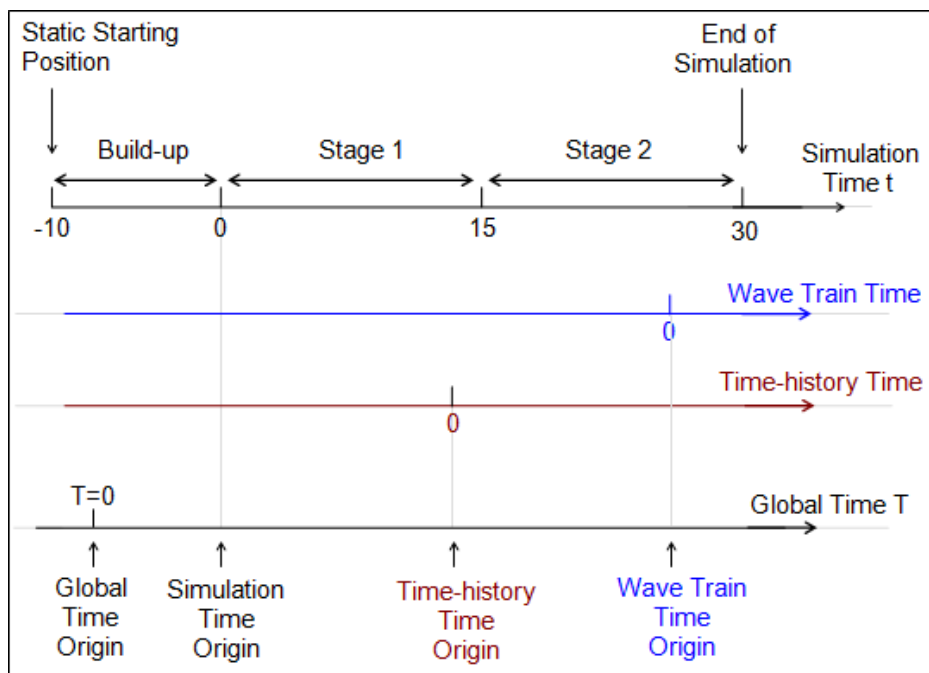


Figure 28: Time and simulation stages [53]

4.5.3 Coordinate system

Creating a model involves taking into account multiple coordinate systems. These include a global frame of reference (GXYZ), local coordinate systems for each object in the model (LXYZ), line end orientations (EXYZ), and a coordinate system specific to a particular vessel (VXYZ), shown in figure 29. All these coordinate systems are right-handed and follow the convention that positive rotations occur clockwise in the direction of the axis of rotation. By considering these various coordinate systems, Orcaflex allows for a comprehensive analysis of the dynamic behaviour of complex systems, accounting for the relative motions and orientations of different components [54].

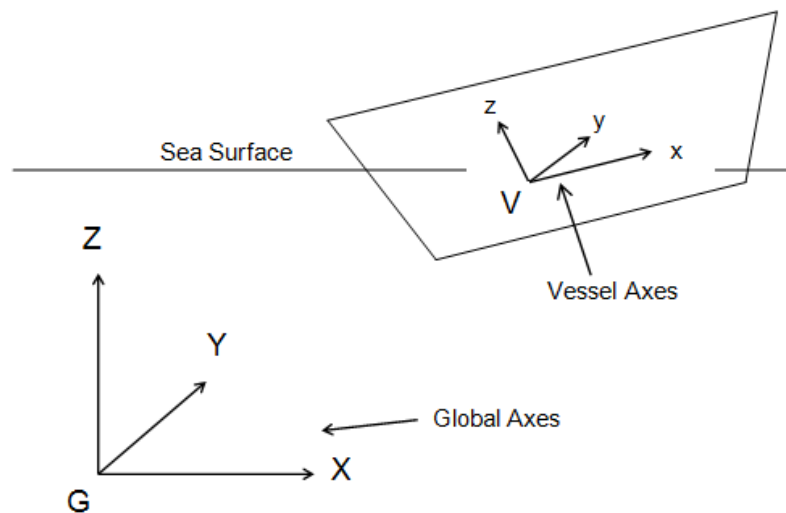


Figure 29: Coordinate systems [54]

5 Installation steps

Analysing the main steps of the dynamic inter-array cable installation phase is important for identifying potential risks, challenges, and opportunities for optimization. By breaking down two main phases, which include the installation of the first end dynamic section, and the second end dynamic section into key phases, one can better understand the sequence of tasks and it also helps identifying the critical dynamic steps that require extra attention to successfully install the cable system. These steps are those that involve movement and changes in tension of the cable which can cause damage to the cable or the installation vessel. This can be further analysed with calculations using Orcaflex to determine minimum and maximum cable tension, bend radius (MBR), tension on pulling winch and potential clashing issues with other components of the system such as neighbouring anchor lines or the moonpool. This information gives valuable input to the development of a detailed plan and to identify any areas where additional resources or modifications may be required.

5.1 Main steps

Installation of dynamic inter-array cables divided in 2 main phases:

1. Phase 1 – Installation of 1st end dynamic section
2. Phase 2 - Installation of 2nd end dynamic section

The analysis focuses on the main steps of phase 1 and phase 2, which are divided into several sub-steps for evaluation under still water conditions. Specifically, the most weather-sensitive steps from each phase are analysed using dynamic properties for wave and current, with a focus on subsea operations. It should be noted that operations on the CLV deck and topside FWT are not included in

the analysis. Overall, the analysis of these critical installation phases and the tension calculations involved will help to identify any potential challenges that may arise during the operation. By using Orcaflex to model the installation process and calculate the tension involved in each step, optimization of the installation process can be done and ensure that the project is completed successfully.

Below is an overview of the main steps involved in phases 1 and 2 made, built upon internal reports [40]. A further analysis of these two phases can be found in chapter 5.1.1 and 5.1.2. In chapter 4.3.1 theory is provided regarding the accessories used in IAC installation, such as the pull-in head, bend stiffener, buoyancy modules, and DMA. Their functions and properties within the model are presented, shedding light on their specific roles in the installation process.

For phase 1- Installation of 1st end dynamic section, the following main tasks have been analysed:

1. Deployment of pull-in head assembly
2. Deployment of DMA and buoyancy section
3. Establish temporary hang off from WTG
4. Release of first DMA chain
5. Release of last DMA chain
6. Cable touchdown & cable lay
7. Final WTG (FWT) pull-in

For phase 2 – Installation of 2nd end dynamic section, the following main tasks have been analysed:

1. Deployment of DMA and buoyancy section
2. Deployment of Pull-in head Assembly
3. Release of first DMA chain
4. Release of last DMA chain
5. Final pull-in of DIAC 2nd end
6. Installation of IAC completed

5.1.1 Phase 1 - Installation of 1st end dynamic section

The following shows the different tasks/steps that have been analysed for phase 1:

Step 1 – Deployment of pull-in head assembly

In the first step of the cable installation, the pull-in head assembly is deployed through the CLV moonpool and connected to the WTG winch wire. In the analysis, this wire is already connected to the pull-in head and the WTG. The cable is paid out while the pull-in winch located inside the WTG hauls in on the wire, while the vessel remains stationary. In other words, the primary objective of this step is to deploy the pull-in head, establish a connection with the winch, and guide it into the I-tube where it is secured.

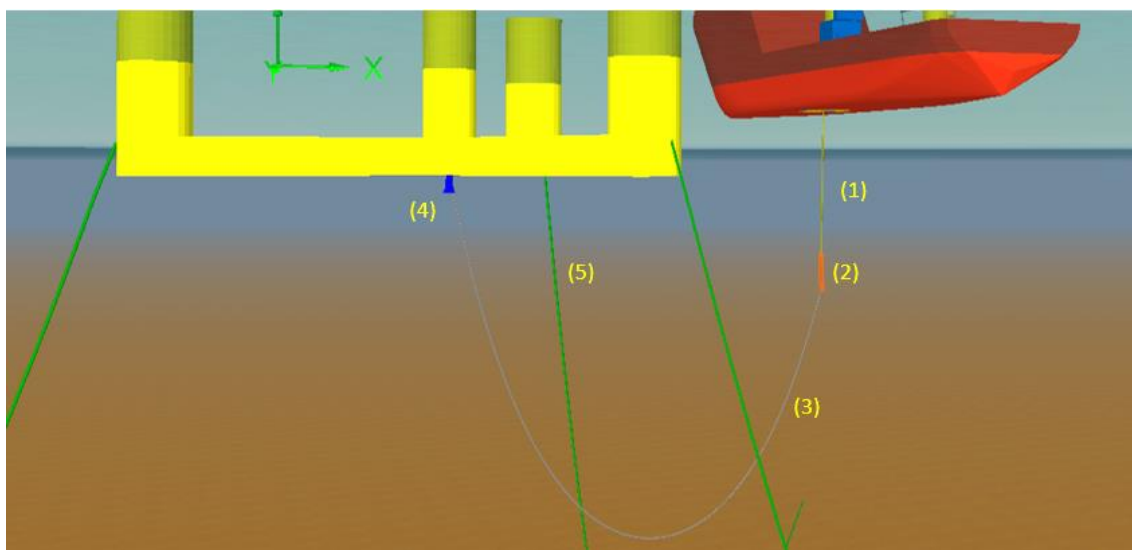


Figure 30: (1) IAC, (2) Pull-in head, (3) Pull-in wire, (4) I-tube, (5) mooring line. The pull-in head (2) is here deployed and used to pull the IAC from the vessel's moonpool to the I-tube (4) on the wind turbine. Throughout this process, the IAC may experience tension caused by sudden movements. However, the presence of a bend stiffener, positioned at the end of the pull-in head helps to mitigate this issue.

Step 2 – Deployment of DMA and buoyancy section (DMA chain, 2 x 3.5 t)

This step involves the deployment of temporary DMAs along with the buoyancy elements. Each DMA consists of two chains weighing 3.5 t each. The WTG winch will haul in the cable while it is being paid out, and the vessel will remain in position. To ensure proper line tension and prevent buoyancy sections from floating to the surface, ballasting weights are attached to the IACs before each buoyancy section. This measure not only maintains sufficient line tension but also minimizes the risk of the IACs making contact with the moonpool doors.

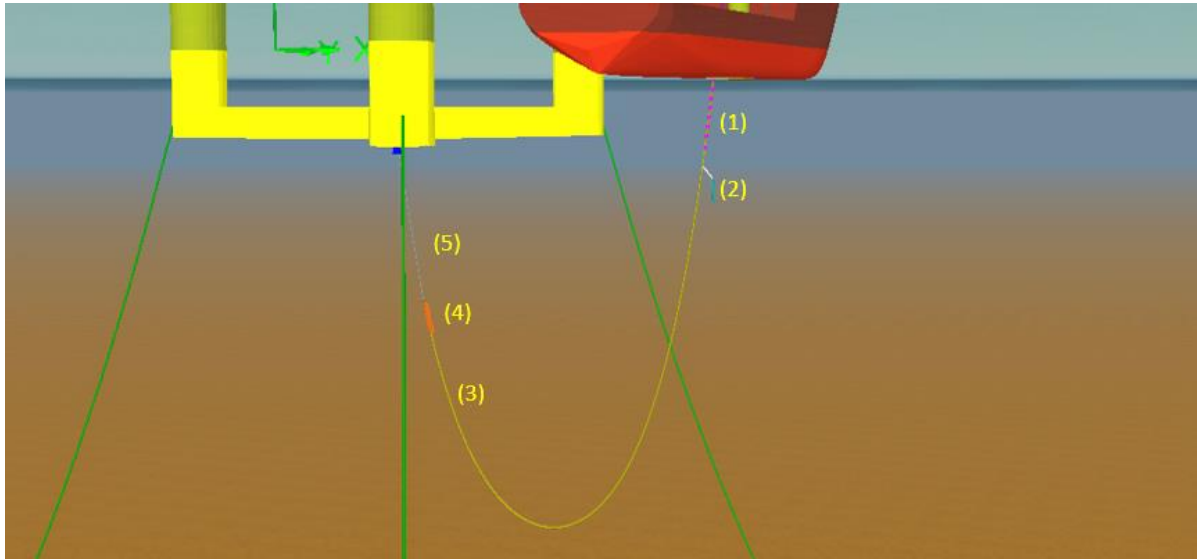


Figure 31: (1) Buoyancy modules, (2) DMA, (3) IAC, (4) Pull-in head, (5) Pull-in wire. Deployment of IAC attachments. While the pull-in head (4) is being hauled towards the I-tube, the DMA (2) and the buoyancy modules (1) attached to the cable (3) are simultaneously deployed.

Step 3 – Establish temporary hang off from WTG

This step involves determining the appropriate depth at which to hold the pull-in head under the I-tube while waiting for steps 4 and 5 to be completed. To determine the appropriate depth is dependent on the method used for this process. In this step, the bending radius of the cable is the critical factor that must be considered when determining the appropriate depth, in order to prevent excessive tension on the cable, which could damage the cable.

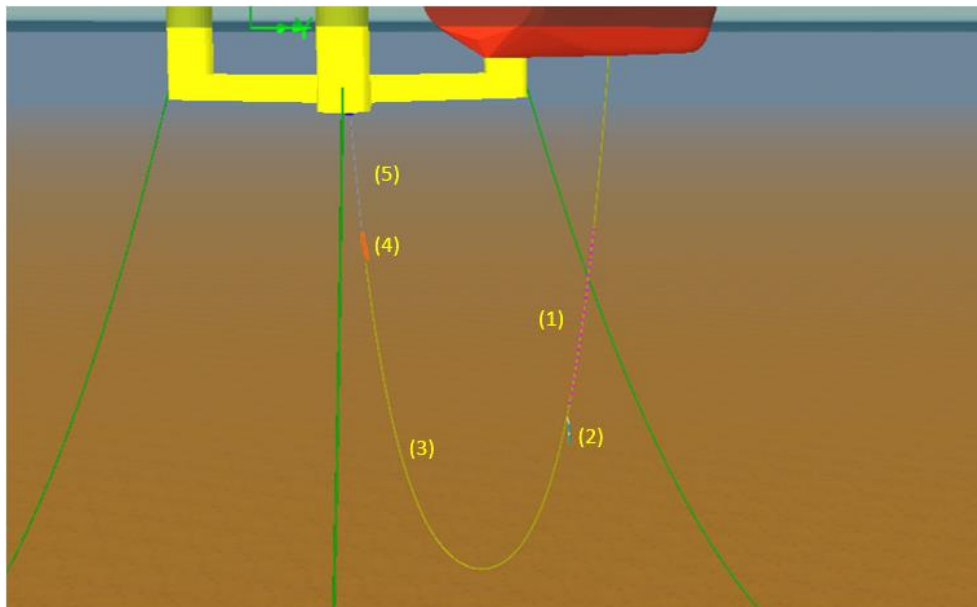


Figure 32: (1) Buoyancy modules, (2) DMA, (3) IAC, (4) Pull-in head, (5) I-tube. It can be observed that the pull-in head (4) has established a temporarily hang off and is positioned directly under the I-tube (5). The DMA (2) and Buoyancy modules (1) have been hauled out to their desired position, and it is now ready for step 4 and 5.

Step 4 – Release of first DMA chain (3.5 t)

In step four, the 1st DMA is to be removed. The temporary DMA is positioned at the predetermined target location, and the vessel continues to pay-out while moving to maintain a pliant wave configuration. After the release of the first DMA, the cable undergoes abrupt motions, as illustrated in figure 33. The IAC transitions from a U-shape to tighter U-shapes, potentially affecting the bending radius values.

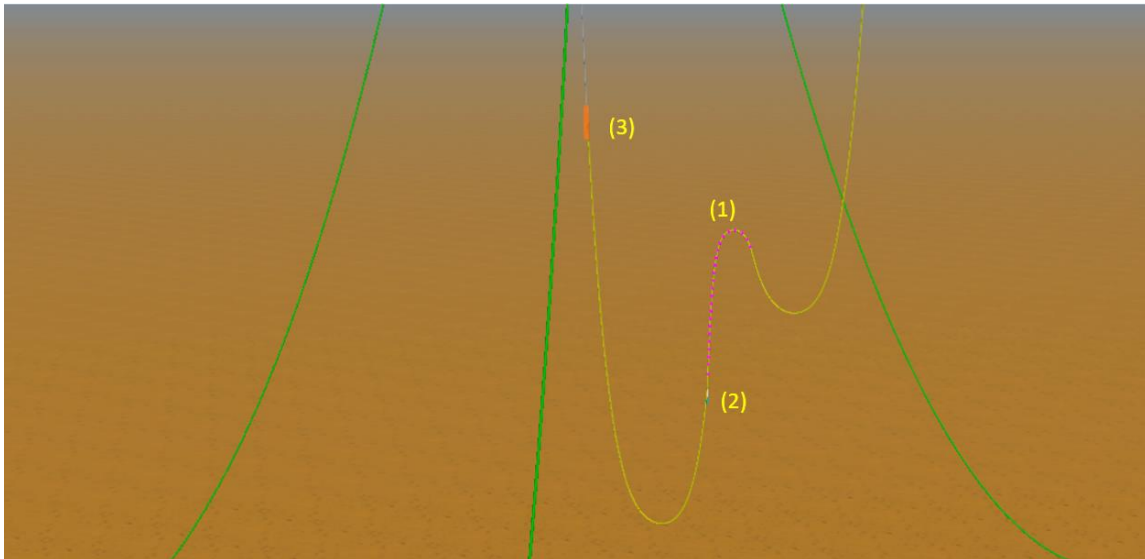


Figure 33: (1) Buoyancy modules, (2) DMA, (3) Pull-in head. The pull-in head (3) remains in its position even after the release of the first DMA. It is observed that the cable has now transitioned into a shape with tighter angles compared to before.

Step 5 – Release of last DMA chain (3.5 t)

After releasing the first DMA, the vessel will continue paying out the cable while moving in the same direction away from the WTG. At that stage the last DMA will be disconnected and released, transitioning the IAC to a smoother shape. Throughout this disconnection process, the CLV will maintain its positioning, and after the release, the last DMA will be recovered using a vessel crane.

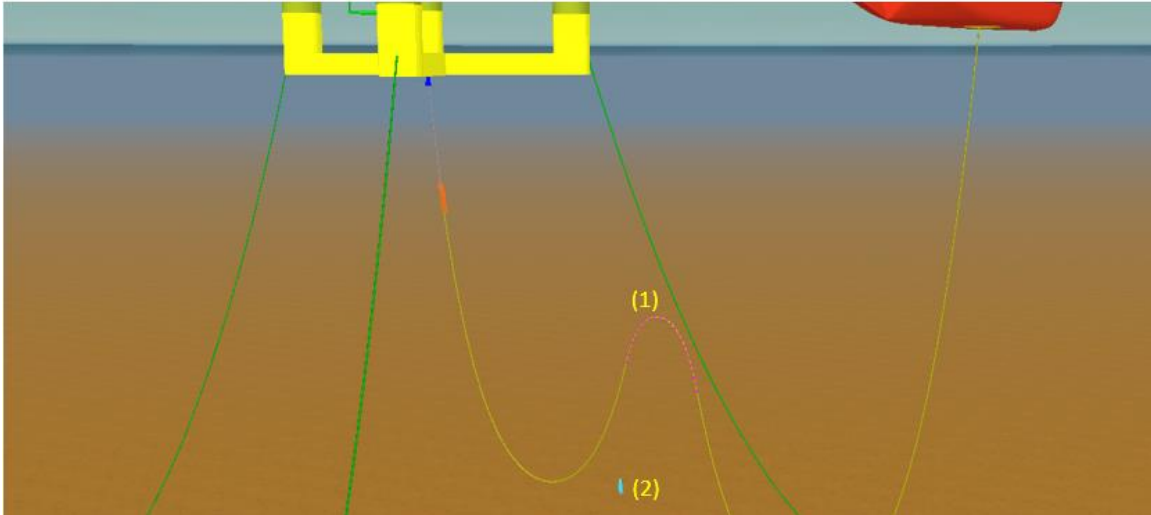


Figure 34: (1) Buoyancy modules, (2) DMA. The last DMA (2) has been released, and the IAC is transitioning towards the desired shape known as the lazy wave.

Step 6 – Cable touchdown & cable lay

This step involves the operation of landing the cable on the seabed and the subsequent laying of the cable along the intended route. The cable is slowly lowered onto the seabed, with the tension and speed of the cable being closely monitored and controlled. Once the cable touches the seabed, the installation process continues with the laying of the cable.

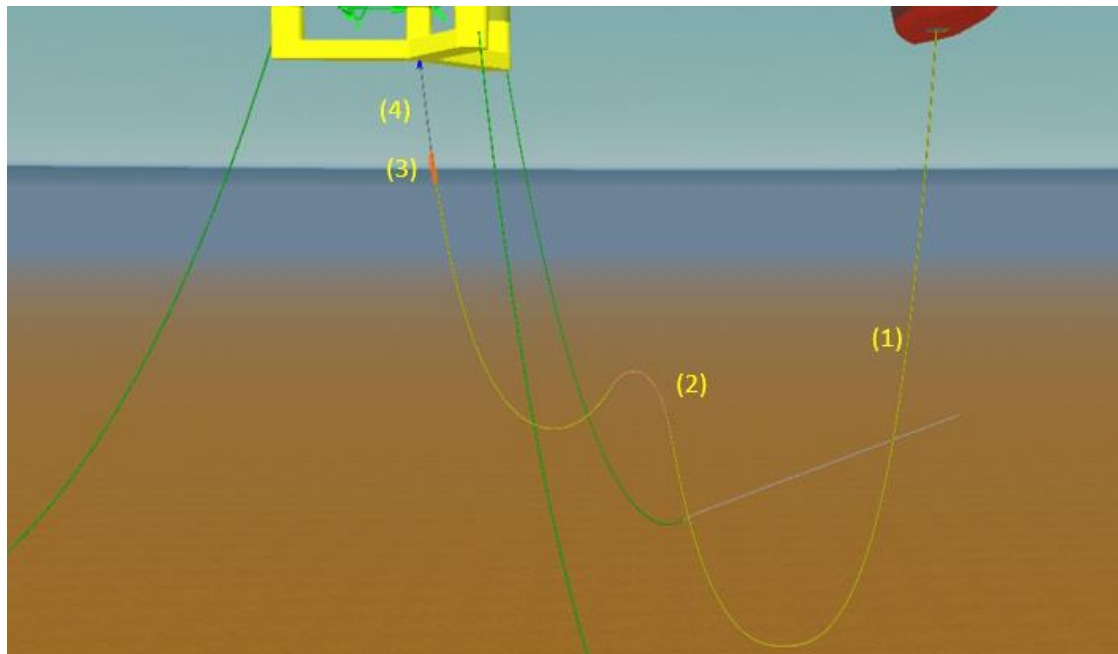


Figure 35: (1) IAC, (2) Buoyancy modules, (3) Pull-in head, (4) I-tube. The pull-in head (3) remains in the same position under the I-tube (4), while the IAC (1) is being guided towards the seabed for cable touchdown and is then ready to be fed out along the desired cable route.

Step 7 – Final WTG pull-in (depending on cable installation method)

In this step the final pull-in of the IAC to the WTG can commence. The pull-in head has now been passed through the I-tube and secures the cable. Once the first IAC end is connected to the WTG, the cable will be further paid out and laid on seabed in designated route while monitoring cable tension, MBR and layback. (Opt1: Final pull-in of 1st end cable to commence before cable touchdown to seabed, Opt2: pull-in to commence after 2nd end pull-in. This may be done by aid of quadrant.)

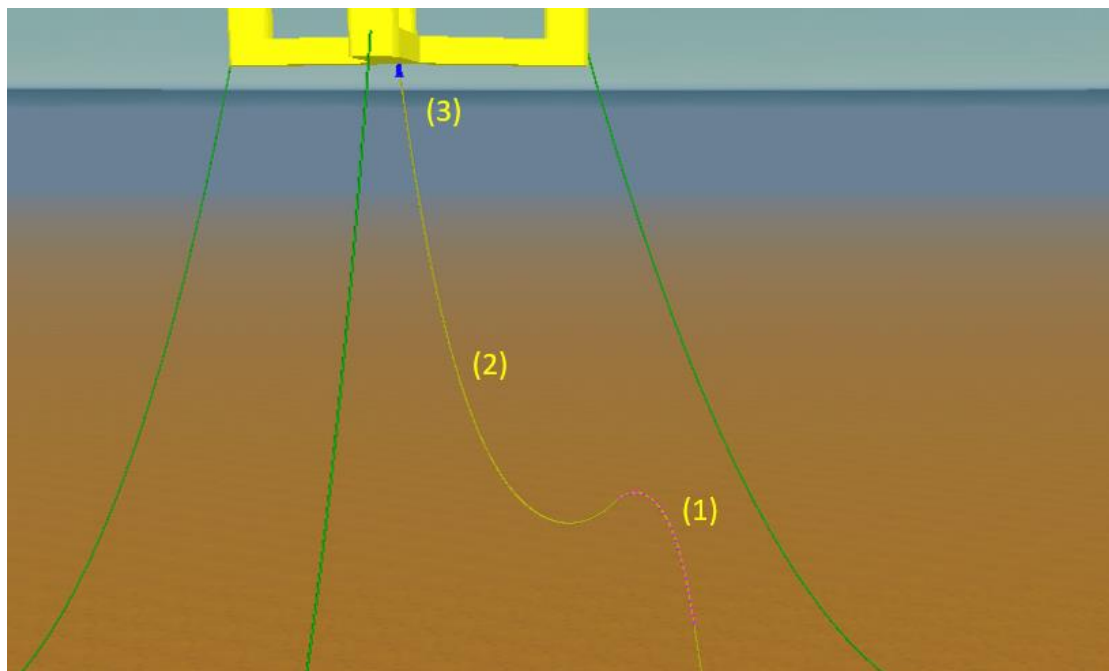


Figure 36: (1) Buoyancy modules, (2) IAC, (3) I-tube. The final pull-in is now done, the IAC (1) is connected to the I-tube (3), and the installation of the first end cable is complete. The CLV can now continue paying out the cable towards the second end.

5.1.2 Phase 2 - Installation of 2nd end dynamic section

The following shows the different tasks/steps that have been analysed for phase 2:

Step 1 - Deployment of DMA and buoyancy section (DMA chain, 2 x 3.5 t)

This step entails deploying temporary DMAs along with buoyancy elements. Each DMA consists of two chains, each weighing 3.5 tons. The chains are attached to the cables 4 m before the first buoyancy module. The DMAs assist pulling the buoyancy elements down through the water column. The vessel, Edda Freya, will move towards the WTG while the cable is being deployed through the moonpool, ensuring that the layback length does not exceed the cable's MBR limit.

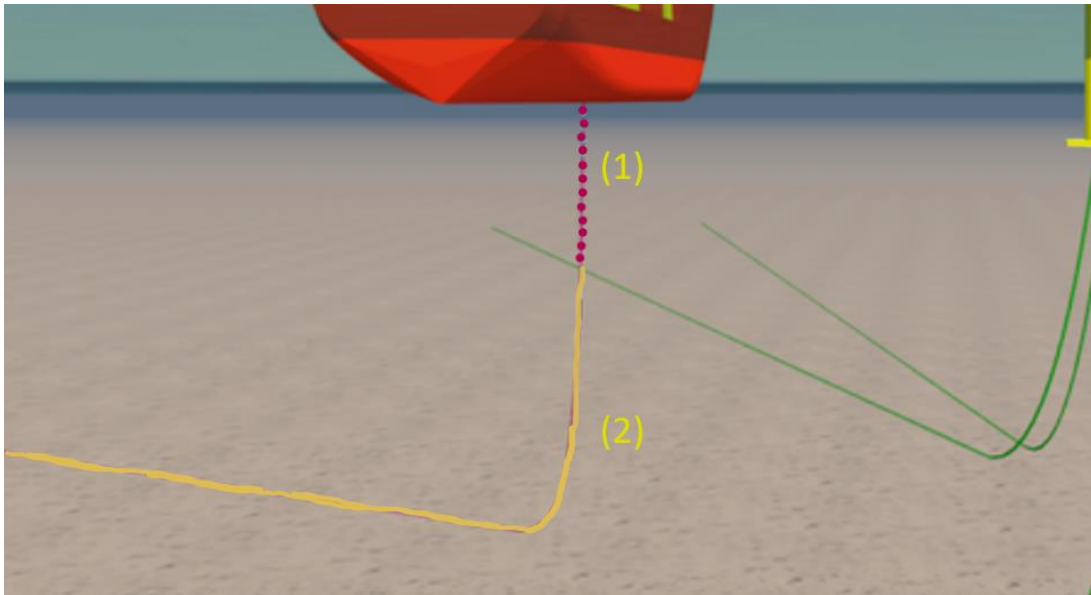


Figure 37: (1) Buoyancy modules, (2) IAC. Deployment of all buoyancy modules (1) and temporary DMA. The CLV will continue to move in same direction while paying out on cable (2) and monitoring TDP and layback length.

Step 2 - Deployment of Pull-in head Assembly

In the second step of phase 2, the pull-in head assembly is deployed through the CLV moonpool and connected to the WTG winch wire. The cable is paid out while the winch hauls in on the WTG wire, while the vessel remains stationary. The primary objective of this step is to deploy the pull-in head, establish a connection with the winch, and guide it into the I-tube where it is secured.

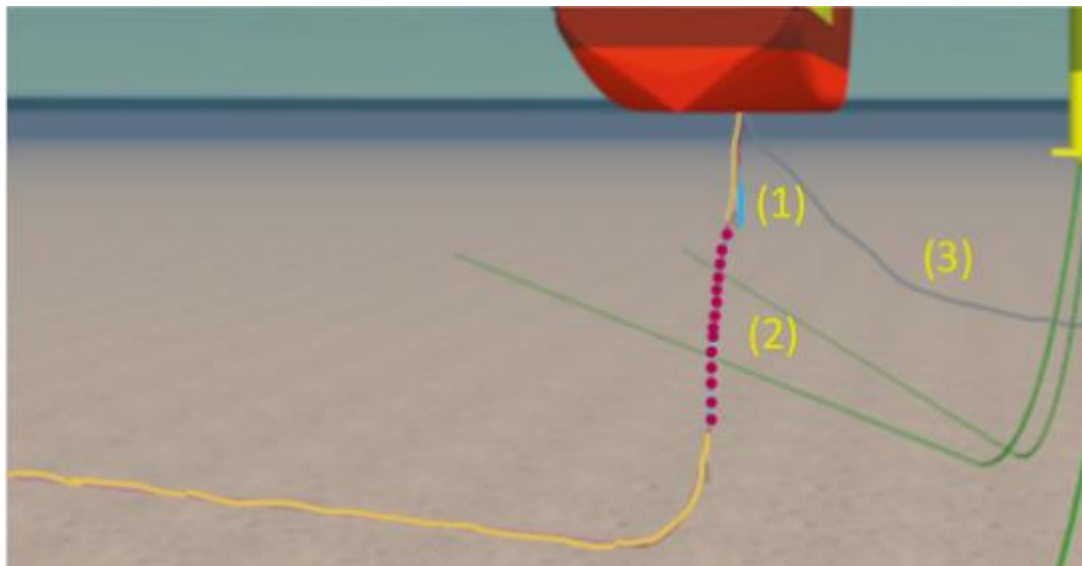


Figure 38: (1) DMA, (2) Buoyancy modules, (3) Pull-in wire. The cable is connected to the wire (3) and is ready to haul in the pull-in head. The pull-in will start after step 3 and 4.

Step 3 - Release of first DMA chain (3.5 t)

In step three, the first DMA is released. At this stage the vessel will remain in its position and no further cable is paid out at this time. After the release of the first DMA, the cable undergoes abrupt motions such as in step 4 in phase 1, visualized in figure 39. The IAC transitions from a smooth shape to small U-shapes, potentially affecting the bending radius.

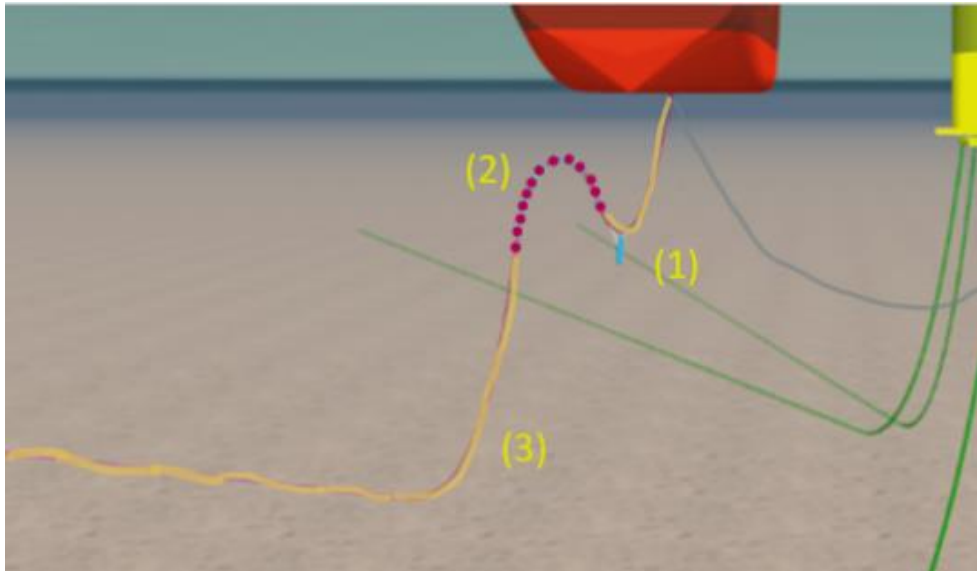


Figure 39: (1) DMA, (2) Buoyancy modules, (3) IAC. Release of first DMA, it is observed that the cable has now transitioned into a shape with tighter angles compared to before. However, the release of the last DMA in step 4 will assist in rectifying this.

Step 4 - Release of last DMA chain (3.5 t)

After releasing the first DMA, the vessel will continue to pay out the cable while moving towards the WTG in the same direction. The last DMA will be disconnected and released. After the release, the IAC will transition to the desired shape for this operation, known as the lazy-wave configuration. Throughout the disconnection process, the CLV will maintain its position. Once the last DMA is released, it will be recovered using a vessel crane.

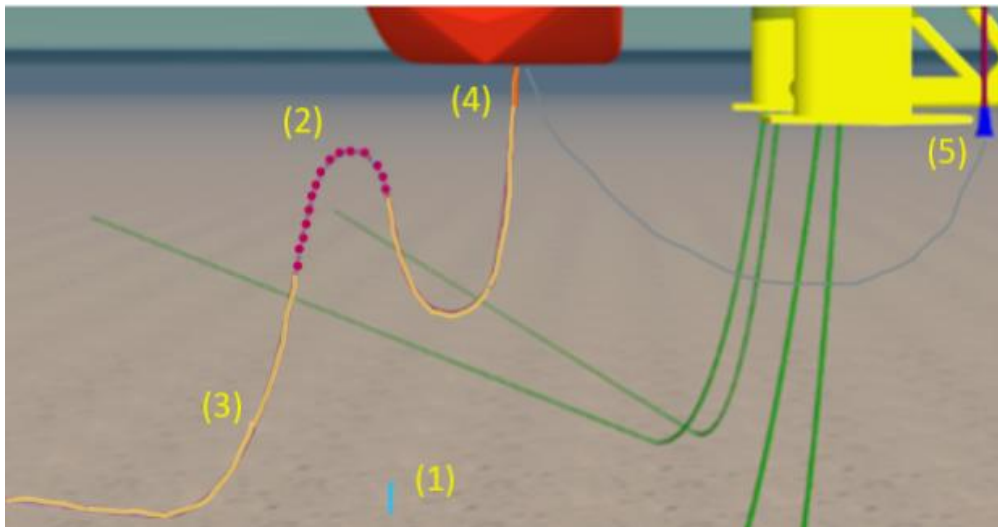


Figure 40: (1) DMA, (2) Buoyancy modules, (3) IAC, (4) Pull-in head, (5) I-tube. The last DMA (1) has been released, and the IAC is transitioning towards the desired shape known as lazy wave configuration. The pull-in head (4) remains in the same position until step 5.

Step 5 - Final WTG pull-in of DIAC 2nd end

When step 4 is completed, the final pull-in to the WTG can begin. The IAC 2nd end pull-in head is pulled into the I-tube on the WTG and the cable is secured. Once the IAC second end is connected to the WTG, the installation of the phase 2 is completed.

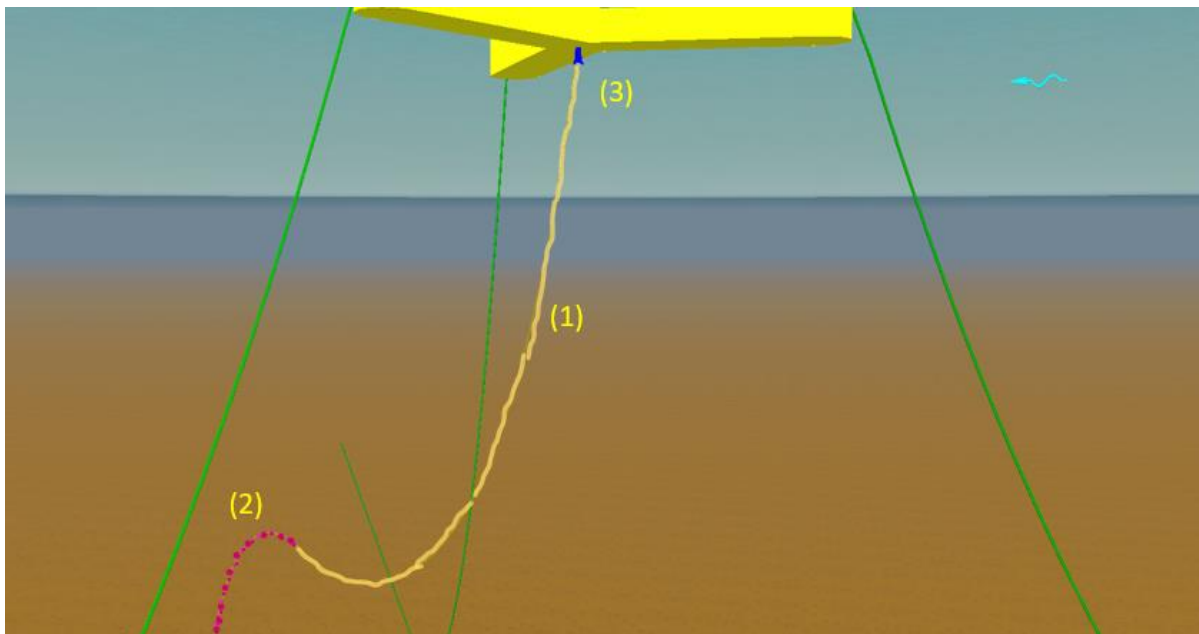


Figure 41: (1) IAC, (2) Buoyancy modules, (3) I-tube. Final WTG pull-in of DIAC 2nd end. The IAC (1) has now been connected to the I-tube (3), and the installation of the second end cable is complete. The CLV can now proceed to the next operation.

5.2 Critical steps

After reviewing the various steps and previous studies, an assessment was conducted to determine which steps should be further pursued. The selected steps were then subjected to dynamic analysis, involving the configuration of multiple dynamic cases to highlight critical stages in terms of tension variables, bending, and the potential for clashes during the installation process. The objective of the dynamic analysis was to highlight possible limitations of the subsea IAC's armour and outer layer, particularly under tension load, and to identify key parameters affecting the tension's fluctuation. The dynamic properties of environmental conditions were also factored in the analysis. The analysis made a good basis for determining the environmental conditions and functional sea state most conducive to the cable installation method.

In chapter 5.1, the main steps of the IAC installation scheme were analysed. It was noted that there was considerable overlap between the steps in phase 1 and phase 2. As a result, only the steps from phase 1 were selected for further analysis, as they were considered representative of the overall process. The analysis examines the IAC installation scheme further broken down into 3 critical scenarios:

Case 1: Step 1 – Deployment of pull-in head assembly (figure 42)

Case 2: Step 2 – Deployment of DMA and buoyancy section (figure 43)

Case 3: Step 4 – Release of first DMA chain (figure 44)

Step 1 is considered critical as the IAC is exposed to low bending radius in the pull-in head area, when the pull-in head is deployed and pulled towards the I-tube on the FWT. This is due to the rapid movement and tight angles involved in the process, as illustrated in figure 42.

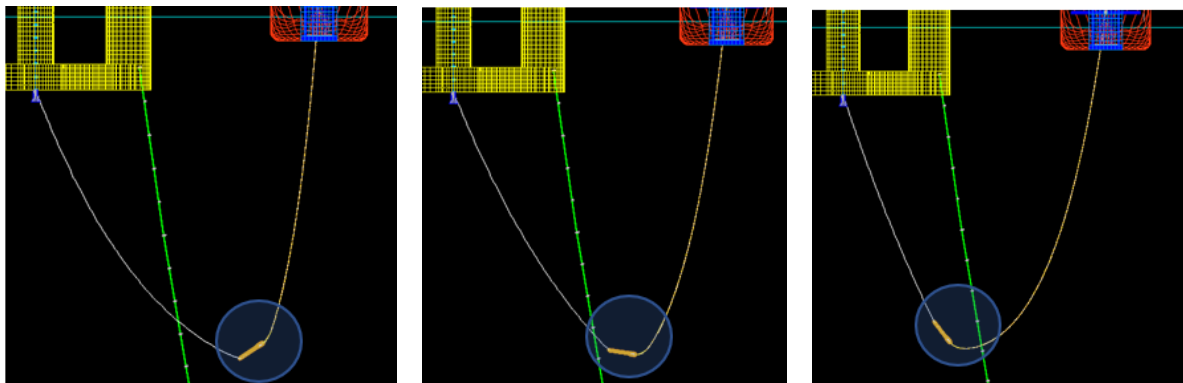


Figure 42: The highlighted area indicates the critical region for step 1, specifically showcasing the abrupt motions that occur during the deployment of the pull-in head. This aspect will be analysed in greater detail later in the thesis.

Step 2 involves the deployment of DMA and buoyancy modules. A visual representation of this scenario is shown in figure 43, which requires a closer examination of the moonpool area. This is because the deployment of these attachments generates a significant upward force that may result in the cable getting too close or even touching the moonpool. Hence, it is crucial to pay attention to the clearance between the cable and the moonpool during this phase to avoid any potential damages or hazards.

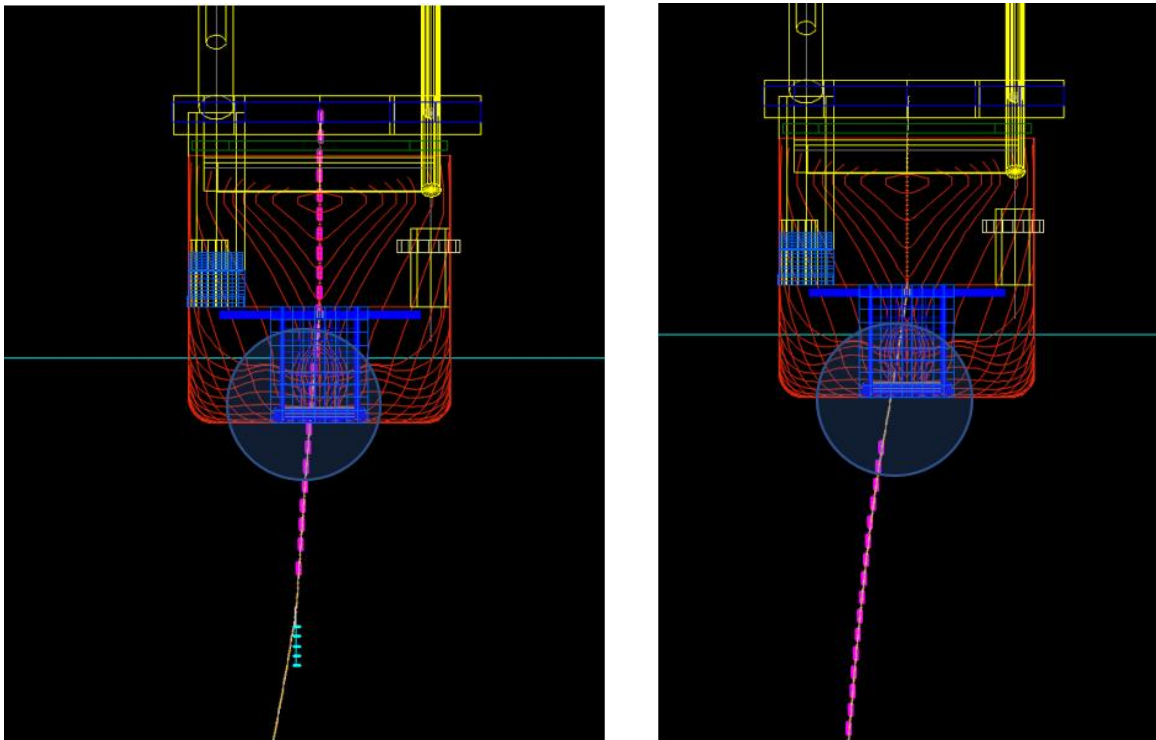


Figure 43: The highlighted indicates the critical region for step 2, focusing on the moonpool in case of clashing during the deployment of the temporary DMA and buoyancy modules. This will be further analysed later in the thesis.

Finally, step 4 involves releasing the first DMA chain, which initiates the upward movement of the cable, thereby forming a wave-like shape. However, it should be noted that the cable does not attain a smooth waveform immediately, as it undergoes a rather abrupt shape initially. The abrupt shape of the release leads to an increased likelihood of generating additional tension on the IAC, and exposes it to low bending radius, as illustrated in figure 44.

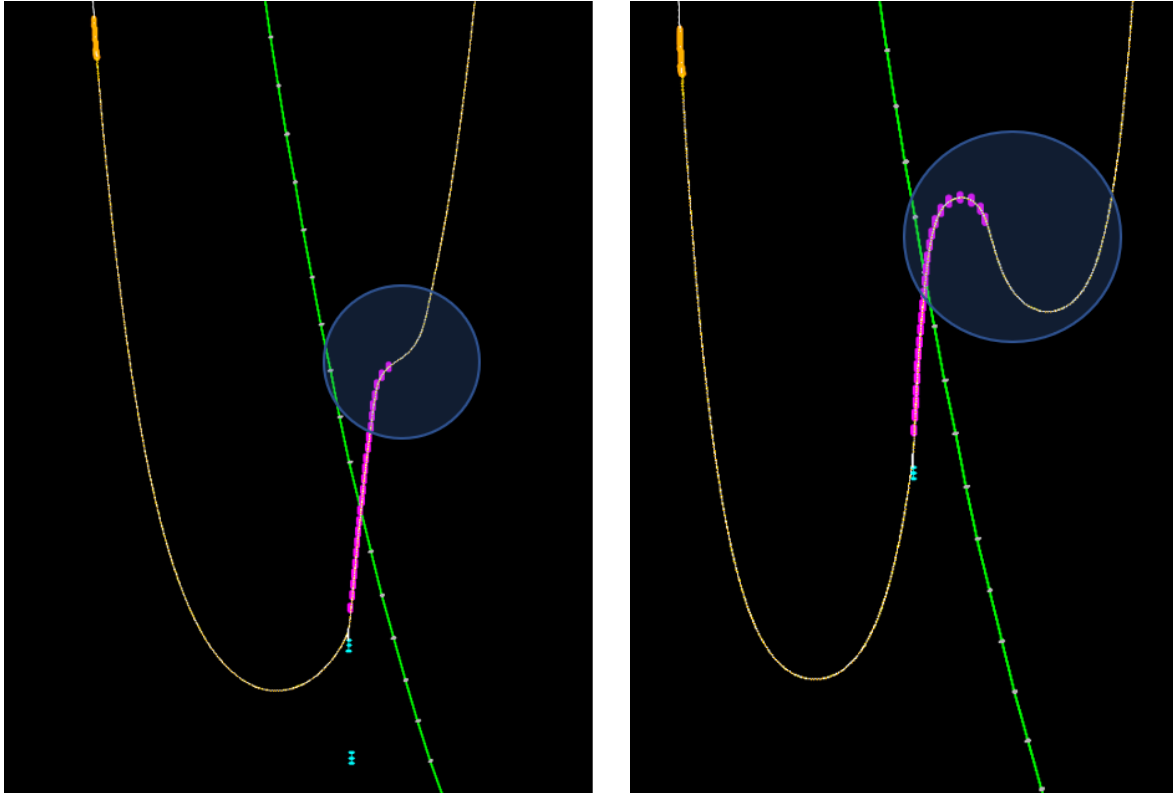


Figure 44: The circled area indicates the critical region for step 4, again focusing on the IAC motions. This is after the release of the temporary DMA. This aspect will be further analysed later in the thesis.

6 Sensitivity test

A simple sensitivity analysis test is performed on the IAC, analysing the effect of different variables such as MBR, maximum and minimum cable tension. The purpose of this test was to assess whether it was feasible to reduce the simulation time period without significantly impacting the accuracy of the results. Such an approach would have the advantage of saving valuable computational resources. For Case 2 and 3, three different simulation periods were investigated, and their outcomes were compared against a 1-hour operable sea state. Figure 45 illustrates the range of where the sensitivity test was conducted on the cable for case 2. Similarly, figure 49 presents the corresponding range for case 3. The examined simulation periods were:

- 30 minutes
- 10 minutes
- 5 minutes

The analysis focused on investigating the bending stiffness and MBR with J-lay method through the moonpool of the cable-laying vessel Edda Freya, which was modelled to be able to move freely in waves in all degrees of freedom based on the displacement (RAO). The simulations were conducted at a water depth of 260 m and 33 m between the vessel and the FWT. By conducting this sensitivity analysis, it was possible to gain insights into the effects of MBR and bending stiffness on cable tension values and optimize the simulation time while still maintaining an acceptable level of accuracy. The simulations conducted in the sensitivity test were compared to the acceptable cable laying criteria outlined in table 16 in chapter 4.4.

6.1.1 Case 2

The effects of different bending stiffness configurations on maximum and minimum tension values were investigated. However, the analysis revealed that the differences in tension across different time periods were relatively small, as shown in figure 46 and 47, making it harder to distinguish the impact of different bending stiffness configurations. Further examination showed that the tension values obtained from 30-minute simulations were with minimal deviations compared to 1-hour. The tension values obtained from 10-minute simulations were not significantly different from those obtained from 1-hour simulations. Therefore, the simulation period of 10-min was a suitable choice, as the deviations in tension values were minimal, and could save time without impacting the accuracy.

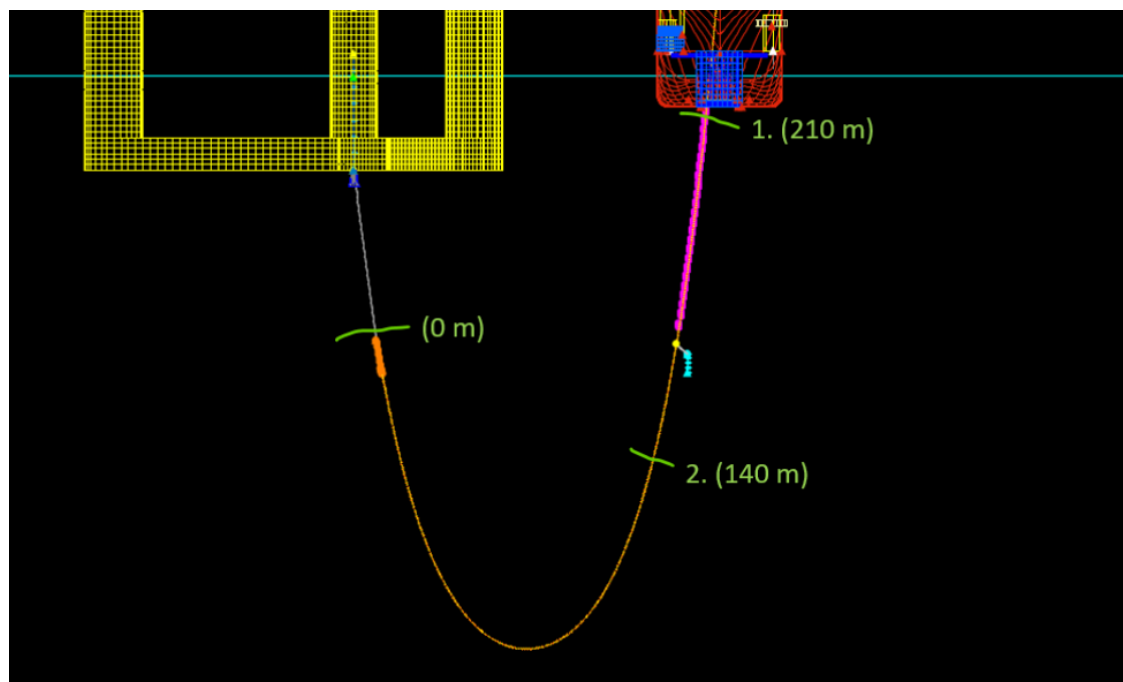


Figure 45: The numbers 1 and 2 indicate the locations where the cable was measured for the sensitivity test to obtain the results for case 2.

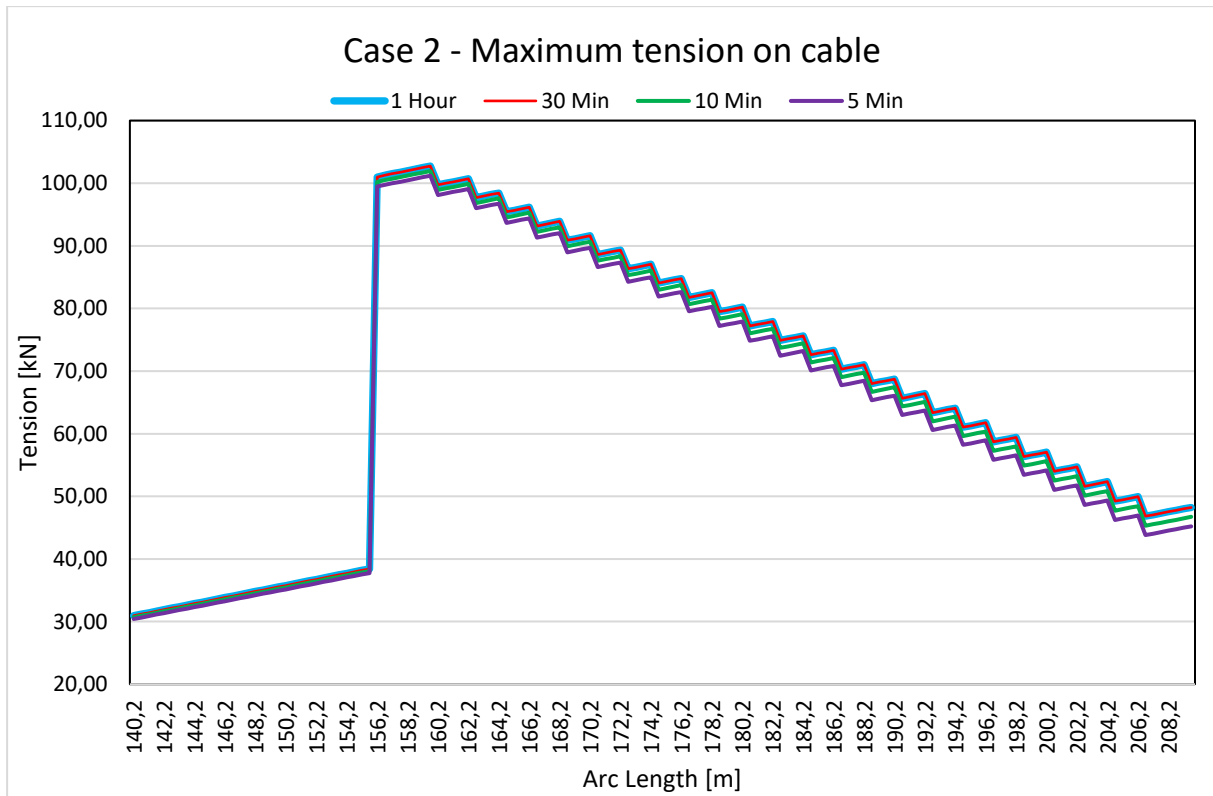


Figure 46: Case 2 - Maximum tension on cable during different time periods, arc length 140 – 210 m

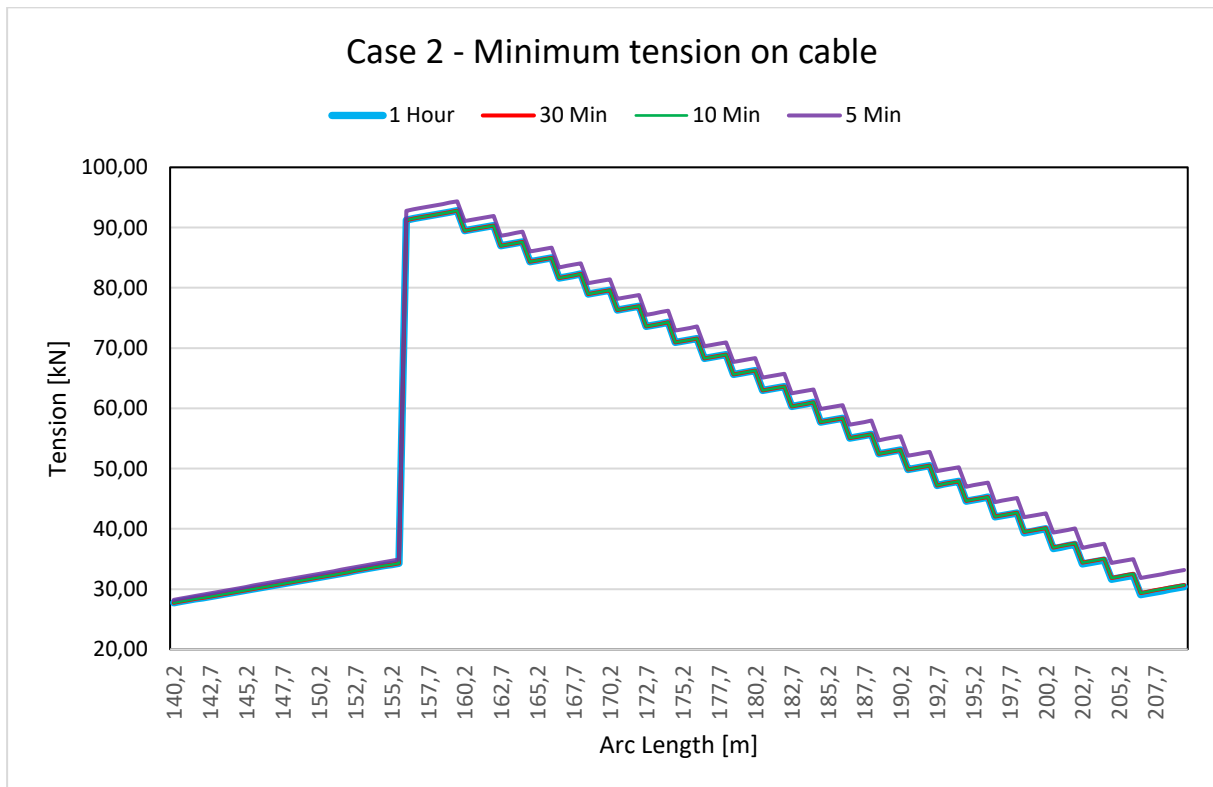


Figure 47: Case 2 - Minimum tension on cable during different time periods, arc length 140 – 210 m

Regarding MBR, the differences observed in this case were not prominent either. The smallest bending radius value recorded was 13.20 m, which was well above 3.07 m which is the minimum value set in this case, as shown in table 17 and figure 48. However, it was observed that the difference in MBR values for the 5-minute simulation period was slightly more significant than for the other two simulation periods. Thus, it follows that the 10-minute simulation period would be a good option for further simulations.

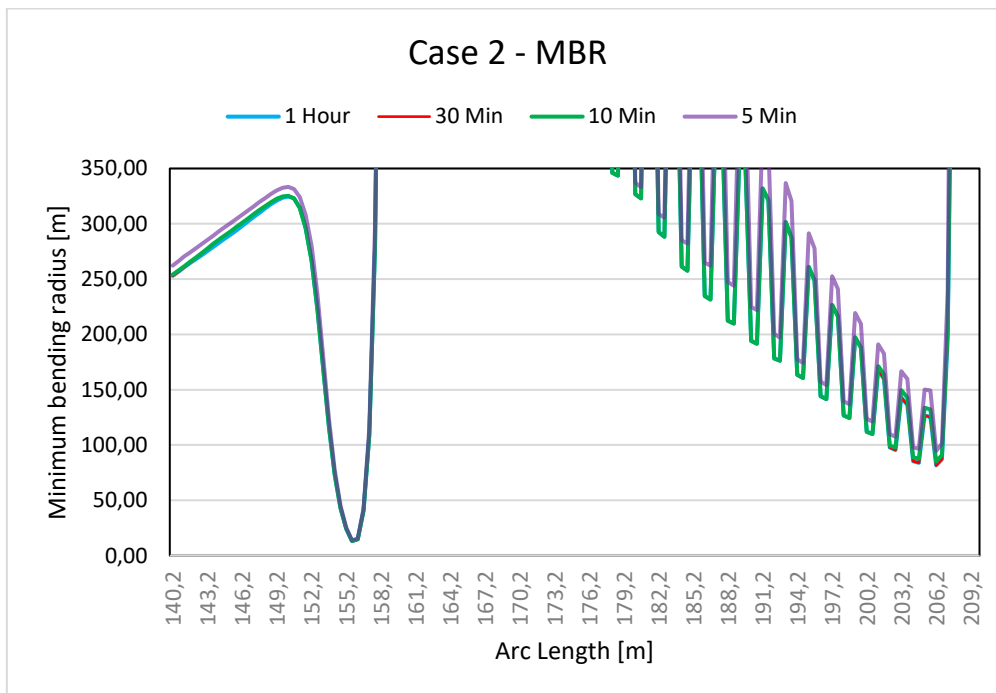


Figure 48: Case 2 – MBR during different time periods, arc length 140 – 210 m

Table 17: Smallest bending radius recorded.

Arc Length [m]	MBR [m]			
	1 hour	30 min	10 min	5 min
154,2	73,23	73,23	73,23	77,65
154,7	43,02	43,02	43,02	45,46
155,2	24,16	24,16	24,16	25,43
155,7	13,20	13,20	13,20	13,83
156,2	14,90	14,90	14,90	15,60
156,7	40,49	40,49	40,49	42,65
157,2	108,49	108,49	108,49	114,97

6.1.2 Case 3

Like case 2, the impact of the different bending stiffness configurations was not prominent, and the deviations observed were even smaller, see figure 50 and 51. The maximum allowable tension on the cable was 336 kN, which was not exceeded in any of the investigated time periods. Since there was minimal variation between the different simulation periods, with only a difference of 0.04 kN between the 1-hour and 5-minute time periods, the conclusion was that the shortest simulation period could be used for further simulations.

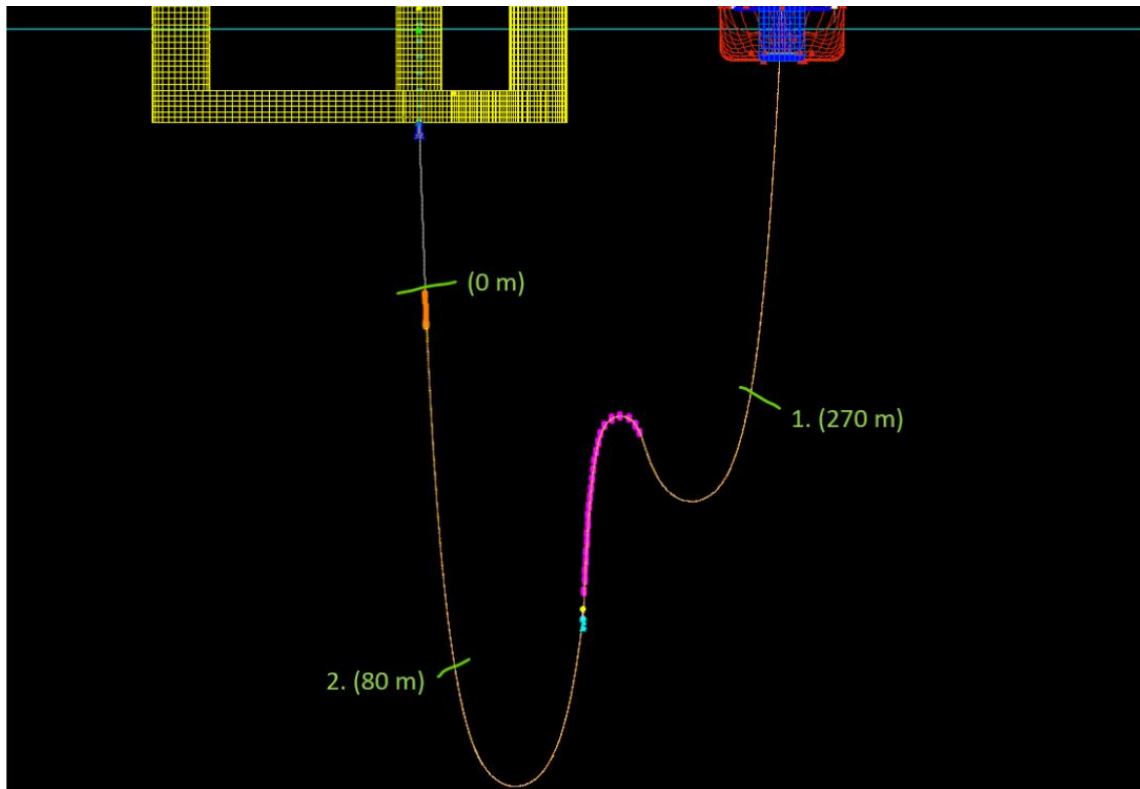


Figure 49: The numbers 1 and 2 indicate the locations where the cable was measured for the sensitivity test to obtain the results for case 3.

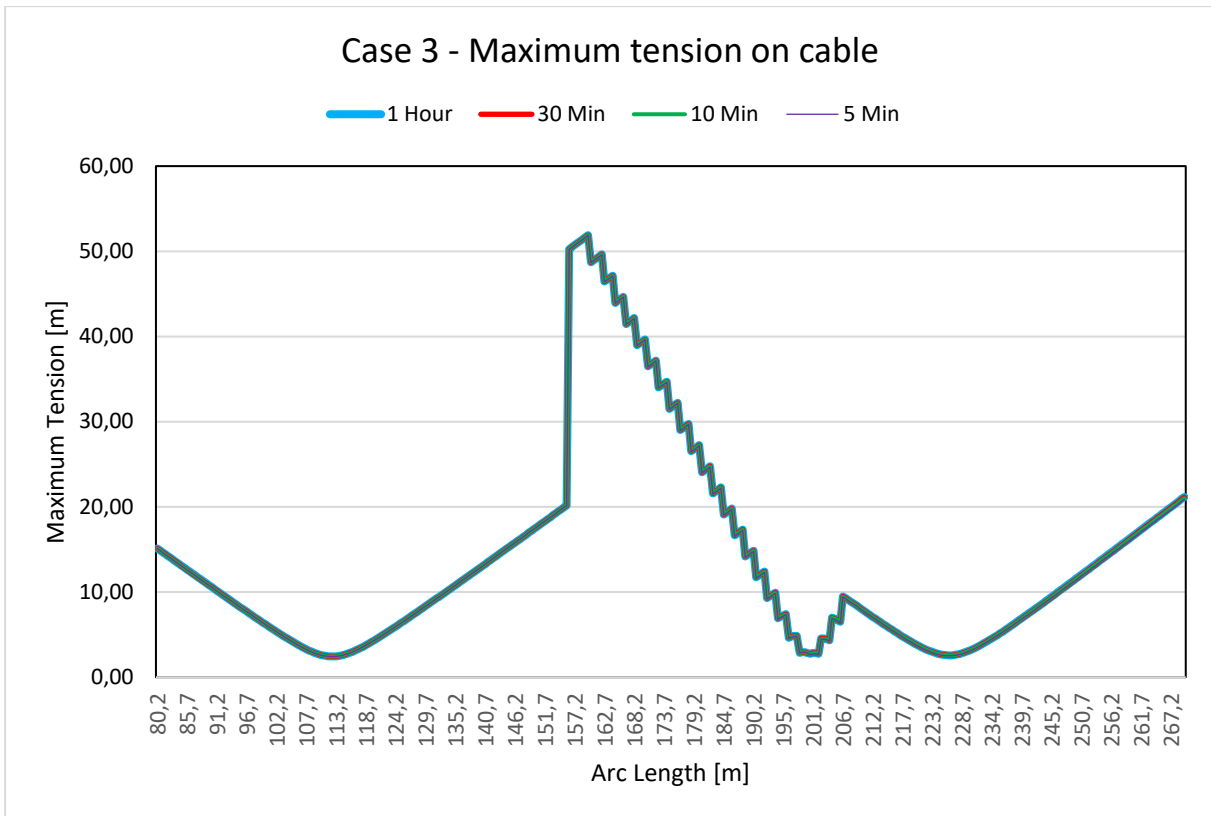


Figure 50: Case 3 - Maximum tension on cable during different time periods, arc length 80 - 270 m

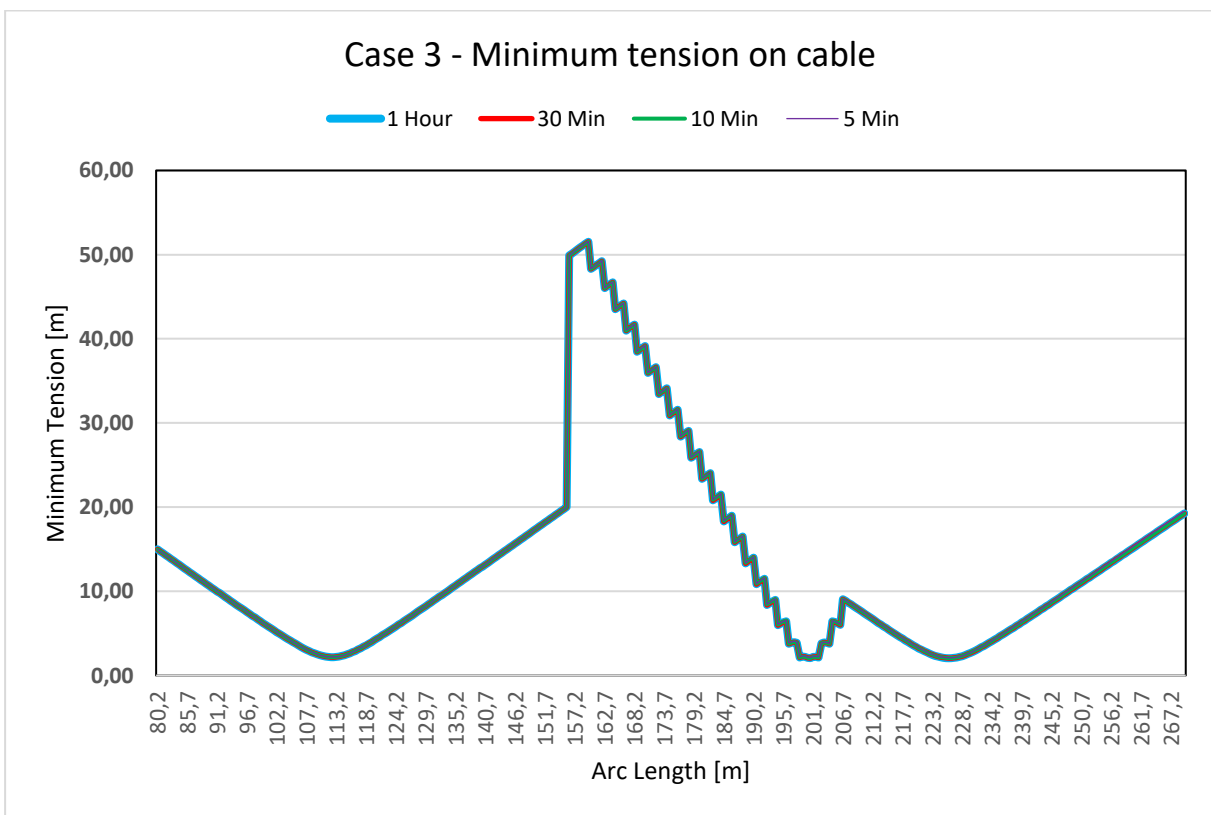


Figure 51: Case 3 - Minimum tension on cable during different time periods, arc length 80 - 270 m

Figure 52 shows that there are three cases where the bending radius is getting closer to the MBR, also indicating no significant differences when comparing the three time periods up against the 1-h simulation period. Examination of table 18, at arc length 199 – 202 m, revealed acceptable values for the contenders in accordance with the MBR. Thus, the results of the bending stiffness and MBR studies were in agreement, and further simulations for Case 3 were conducted using the 5-minute time period.

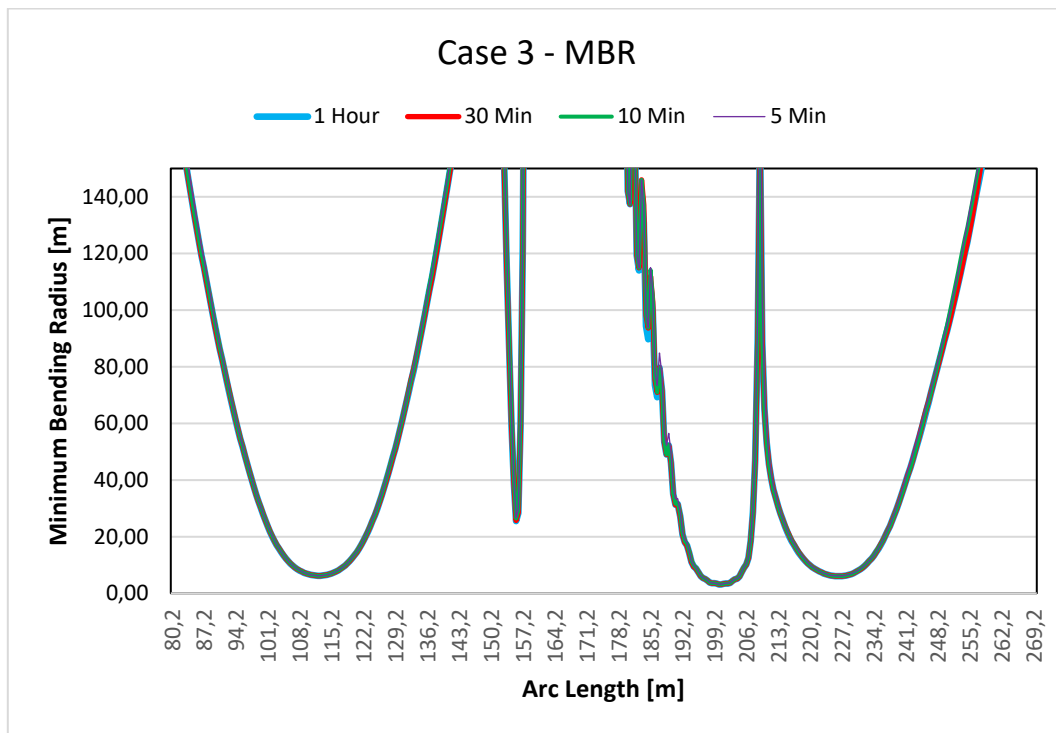


Figure 52: Case 2 – MBR during different time periods, arc length 80 - 270 m

Table 18: Smallest bending radius recorded

MBR [m]				
Arc Length [m]	1 hour	30 min	10 min	5 min
199,2	3,56	3,56	3,56	3,61
199,7	3,41	3,41	3,41	3,45
200,2	3,12	3,12	3,12	3,16
200,7	3,11	3,11	3,11	3,16
201,2	3,36	3,36	3,36	3,42
201,7	3,49	3,49	3,49	3,55
202,2	3,47	3,47	3,48	3,51

7 Dynamic analysis

To pinpoint the independent factors that may have a substantial individual impact on a dependant variable, the dynamic analysis is used. In the context of subsea cable installation, the dependent variable could be the cable's tension or bending stress, while the independent variables could be the environmental conditions, vessel characteristics, cable specifications, among others. By conducting these dynamic analyses, one can determine how changes in these independent variables affect the cable's performance [53].

The dynamic analysis can be valuable when testing the limits of cable specifications under non-operable conditions. These conditions could include extreme environmental loads, vessel motions, and cable installation procedures that are beyond the cable's specified limits. By conducting sensitivity analysis under such conditions, one can identify potential weaknesses in the cable system and design remedial measures to improve its performance and reliability [53].

7.1 Methods applied

Installation analyses incorporate irregular wave spectra to achieve more accurate outcomes, particularly when conducting fatigue analyses. It is essential to account for the irregular sea states and corresponding vessel motions that occur in real-world scenarios. To assess the behaviour of different deployment methods under such irregular motions, several irregular sea states were simulated using a JONSWAP wave spectrum. Time domain simulations were conducted for each dynamic stage of the installation scope, considering various combinations of environmental parameters.

The weather window of operation for the cable laying process, is determined by the sensitivity of the Edda Freya's motions. This sensitivity is commonly addressed in cable installation analyses as an operational constraint. The dynamic forces and motions working on the IAC during the laying process have a substantial impact, directly influencing the design of the cable itself as well as the preferred installation method [55].

As commonly acknowledged, the current model under consideration is non-stationary, implying the absence of fixed positions. However, this particular model involves a fixed component that plays a critical role, while the remaining movements are primarily driven by environmental factors such as waves, currents, and wind.

In the analysis of case 1, the Gumbel method was applied. To account for the unpredictable nature of extreme wave events, the Gumbel distribution is commonly used when dealing with activities like releasing or reeling in the winch/cable or when the vessel is in motion. The reason behind this approach is that it is challenging to accurately determine when the highest waves will occur. In Orcaflex, the Gumbel distribution plays a major role when estimating the design conditions for offshore structures exposed to extreme wave conditions [56]. The utilization of multiple simulations

with varying initial conditions, known as seeds, enables the identification of instances where the highest waves align with the most critical stages of the operation. Precisely timing the waves and determine whether wave troughs or crests present the highest risk, pose significant challenges in this context. 480 seeds are simulated for the currents chosen in this analysis, with necessary input parameters, such as wave height, period, direction, and current, to simulate different wave conditions. Key parameters used can be found in table 7. Orcaflex utilizes these wave seeds to perform time history synthesis, involving generating a series of waves based on the specified wave seeds, making it possible to analyse the dynamic response of offshore structures under different wave conditions [57].

In chapter 6 a sensitivity test was done for case 2 and 3, where the results from that test has been further put into an analysis, a Rayleigh analysis. The Rayleigh distribution is often utilized to model the amplitude of random oscillations or vibrations, and is used in these particular cases to generate random wave amplitudes to simulate realistic wave conditions [58]. By applying this method, it is easier to gain valuable insights of offshore systems behaviour and performance under extreme wave conditions. Setting up the simulations for case 2 and 3 reflected the assumptions made in the key parameter matrix, table 7. The combination of the matrix and the Rayleigh distribution will contribute to the identification of the parameters of interest. This analysis enables makes it possible to draw conclusions regarding the installation of the IAC and the potential occurrence of any issues.

In the simulation of the three cases, the cable lay performance for the JDR cable was evaluated based on predefined criteria shown in table 16 of chapter 4.4 which is outlined from appendix A in the thesis. These criteria serve as standards which the simulation results are compared against. Each case focuses on specific areas of interest determined as critical in chapter 5.2. Different parameters are examined for each case to address the unique concerns associated with these critical factors.

By analysing these parameters and prioritizing the critical areas identified earlier, a comprehensive evaluation of the IAC performance during the installation steps was conducted. This approach helps gain a better understanding of how the cable behaves under different conditions and enables the identification of potential challenges.

7.2 Case 1 - Results

The primary focus here is the MBR of the inter-array cable, which has a limit of minimum radius 3.07 m. The MBR plays a significant role in this case as the cable is subjected to abrupt motions during the deployment of the pull-in head, as discussed in chapter 5.2. Figure 53 illustrates this scenario, where the cable starts to experience higher curvature. Additionally, important variables such as the maximum tension on the cable at the lower tensioner, minimum tension on the cable, and maximum tension on the pull-in winch are considered. These criteria are detailed in Chapter 4.4.

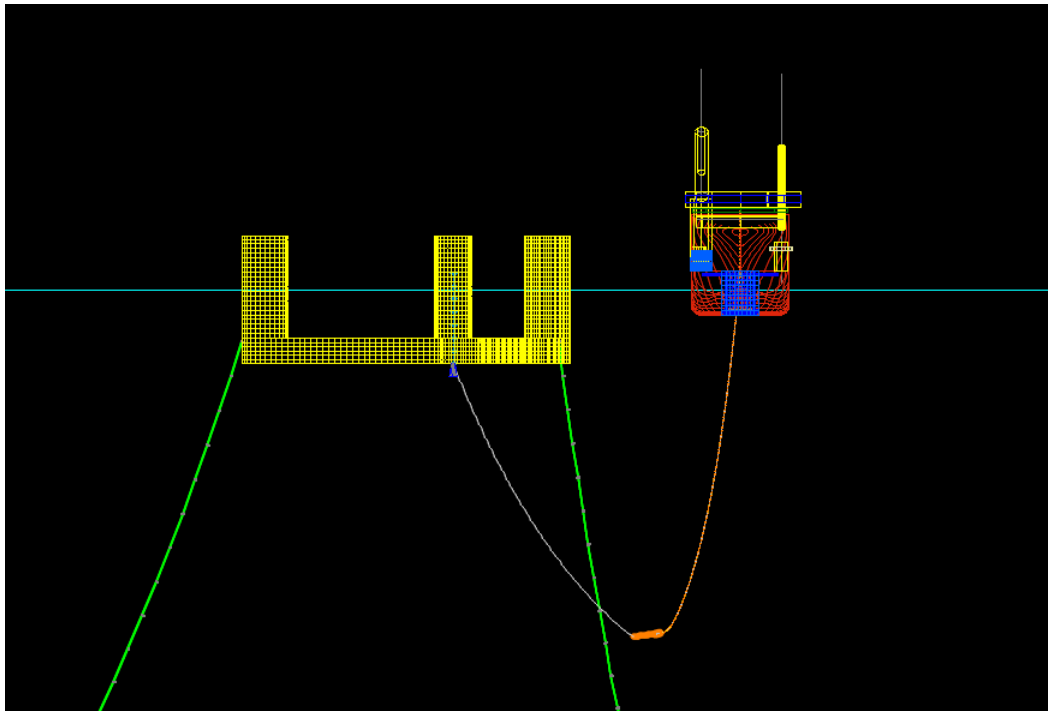


Figure 53: Case 1 - deployment of Pull-in head

At no current

Maximum cable tension at lower tensioner

- Through an examination of the analysis results presented in table 19, it becomes evident that the outcomes are highly promising, as the highest observed value does not exceed 90.74 kN. A potential pattern suggests that wave directions at 0° and 180° have the highest recorded maximum values across all wave heights at no current.

Minimum tension on Cable

- The avoidance of zero tension is crucial as it can lead to slack, which can affect the stability. Fortunately, in this case all the values remain stable between 2.10 – 2.34 kN and the possibility of slack can be disregarded. The same pattern is also valid here.

Maximum tension on pull-in winch

- Upon examining table 19, no indications arise to suggest any challenges or complications associated with the cable installation process in relation to the pull-in winch. Significantly, all observed values remain below 10 t, with no results exceeding 32.69 kN. In essence, it can be concluded that the cable, cable accessories, and parameters exert minimal influence on the pull-in winch.

Table 19: Maximum cable tension at lower tensioner, minimum tension on cable results and maximum tension on pull-in winch, current: no current

No current				
Hs [m]	Wave Dir [°]	MaxTen Cable lower tensioner [kN]	MinTen Cable [kN]	MaxTen pull-in Winch [kN]
2	180	79,49	2,23	31,68
2	225	76,73	2,31	31,50
2	270	75,98	2,31	31,40
2	315	76,71	2,30	31,48
2	0	79,93	2,26	31,77
2	45	75,31	2,30	31,44
2	90	74,26	2,34	31,35
2	135	75,30	2,31	31,42
3	180	83,78	2,23	31,88
3	225	78,65	2,26	31,62
3	270	77,14	2,30	31,58
3	315	78,38	2,24	31,59
3	0	84,47	2,19	31,95
3	45	77,04	2,27	31,52
3	90	75,36	2,31	31,44
3	135	76,67	2,28	31,47
4	180	90,74	2,24	32,44
4	225	79,20	2,23	31,77
4	270	78,28	2,29	31,64
4	315	79,80	2,25	31,79
4	0	90,20	2,10	32,69
4	45	77,71	2,21	31,58
4	90	76,56	2,33	31,52
4	135	77,45	2,27	31,48

At current 0.3 m/s:

Maximum cable tension at lower tensioner:

- The results from the analysis presented in table 20, shows that the highest recorded value is 88.84 kN. Notably, the same pattern found with no current is also found in this instance, indicating that wave directions of 0° and 180° consistently exhibit the highest maximum values across all wave heights. This pattern is also evident in the other parameters within current 0.3 m/s.

Minimum tension on Cable

- All the values consistently stay within the range of 2.17 – 2.36 kN, and there is therefore no need to consider any slack. The observed pattern holds true in this scenario as well.

Max tension on pull-in winch

- Based on the data presented in table 20, no evidence indicates any challenges or complications associated with the cable installation process related to the pull-in winch. Notably, none of the recorded values exceed 32.89 kN.

Table 20: Maximum cable tension at lower tensioner, minimum tension on cable results and maximum tension on pull-in winch, current: 0.3 m/s

Current 0.3 [m/s]				
Hs [m]	Wave Dir [°]	MaxTen Cable lower tensioner [kN]	MinTen Cable [kN]	MaxTen pull-in Winch [kN]
2	180	81,04	2,31	31,58
2	225	76,49	2,36	31,36
2	270	74,82	2,34	31,34
2	315	75,77	2,33	31,47
2	0	79,50	2,29	31,86
2	45	76,10	2,31	31,45
2	90	74,85	2,30	31,37
2	135	75,48	2,33	31,35
3	180	84,62	2,25	31,78
3	225	78,35	2,33	31,51
3	270	76,72	2,35	31,39
3	315	77,93	2,30	31,59
3	0	84,24	2,23	32,18
3	45	76,80	2,28	31,44
3	90	76,02	2,30	31,45
3	135	76,71	2,31	31,42
4	180	88,84	2,25	32,31
4	225	79,25	2,29	31,52
4	270	77,75	2,34	31,57
4	315	79,01	2,28	31,69
4	0	88,64	2,17	32,89
4	45	78,05	2,28	31,59
4	90	76,12	2,30	31,50
4	135	77,87	2,28	31,53

At current 1.0 m/s:

Maximum cable tension at lower tensioner:

- The results from the analysis are presented in table 21, where the highest recorded value is 113.26 kN. At current 1.0 m/s, it is a bit more challenging to discern a clear pattern from the different wave heights since there are less values that stand out. This observation applies to

other parameters associated with this specific current as well. However, it is important to note that these values do not reach critical levels.

Minimum tension on Cable

- In the present case, all the recorded values consistently exhibit stability, with lowest tension value recorded at 2.32 kN, thereby rendering the possibility of slack negligible.

Max tension on pull-in winch

- In table 21, the recorded values consistently remain below 32.60 kN, indicating the absence of any issues pertaining to the cable installation process.

Table 21: Maximum cable tension at lower tensioner, minimum tension on cable results and maximum tension on pull-in winch, current: 1.0 m/s

Current 1.0 [m/s]				
Hs [m]	Wave Dir [°]	MaxTen Cable lower tensioner [kN]	MinTen Cable [kN]	MaxTen pull-in Winch [kN]
2	180	80,10	2,41	31,33
2	225	74,80	2,44	31,11
2	270	74,87	2,39	31,23
2	315	85,41	2,37	31,38
2	0	79,89	2,41	31,80
2	45	74,97	2,38	31,37
2	90	73,51	2,36	31,16
2	135	74,13	2,42	31,07
3	180	83,22	2,35	31,49
3	225	78,33	2,44	31,25
3	270	76,98	2,37	31,26
3	315	91,59	2,32	31,48
3	0	84,97	2,36	32,10
3	45	75,68	2,34	31,49
3	90	74,06	2,37	31,18
3	135	74,81	2,42	31,21
4	180	90,37	2,37	31,82
4	225	79,24	2,38	31,32
4	270	78,35	2,37	31,39
4	315	113,26	9,45	31,89
4	0	88,47	2,35	32,60
4	45	86,89	2,42	31,57
4	90	75,03	2,35	31,21
4	135	76,72	2,39	31,23

MBR

At no current:

The results in figure 54 reveals the impact of abrupt motions on the cable, with three instances demonstrating a bending radius below the critical MBR. All these specific cases reflect wave directions of 180°. Despite the marginal deviation from specified critical MBR, this finding implies that the operation should not be carried out under these circumstances. Upon closer examination of the neighbouring cells in the figure, it becomes evident that these critical values are consistently observed for wave directions of 0° and 180° across the three wave heights and currents.

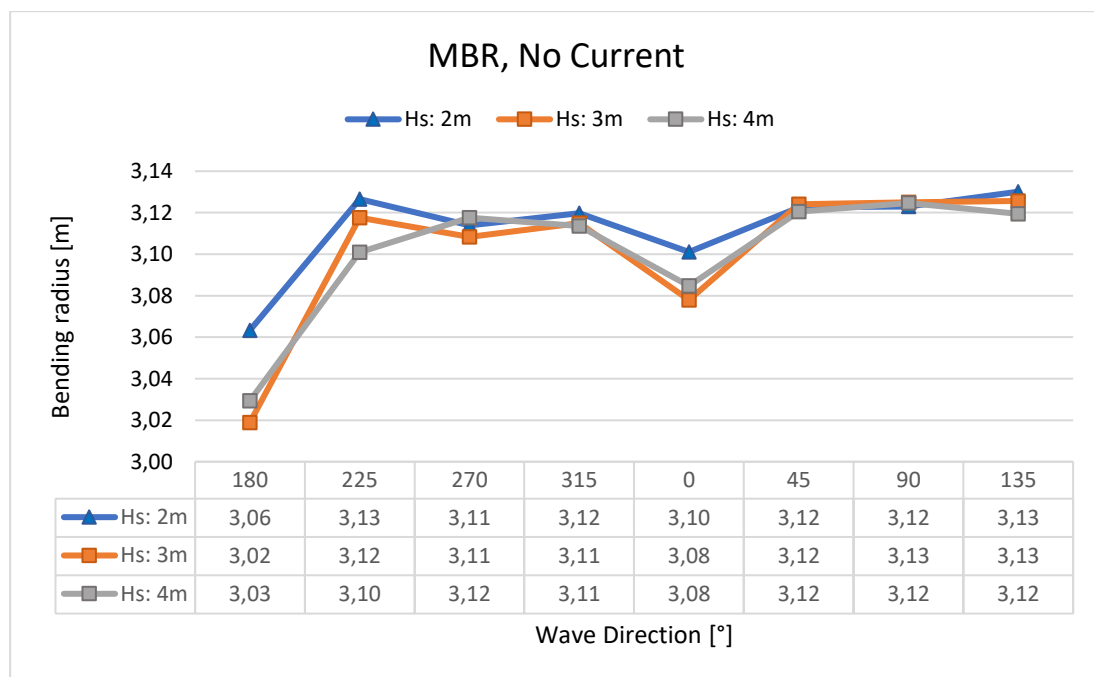


Figure 54: MBR results with no current, note critical MBR is 3.07 m

At current 0.3 m/s:

By analysing the data in figure 55, it becomes evident that the MBR falls below the specified threshold as wave height increases from 2 m to 4 m, and instances of cable damage are likely to occur. The findings indicate that wave directions of 180° and 0° exhibit MBR values four times with current speed at 0.3 m/s.

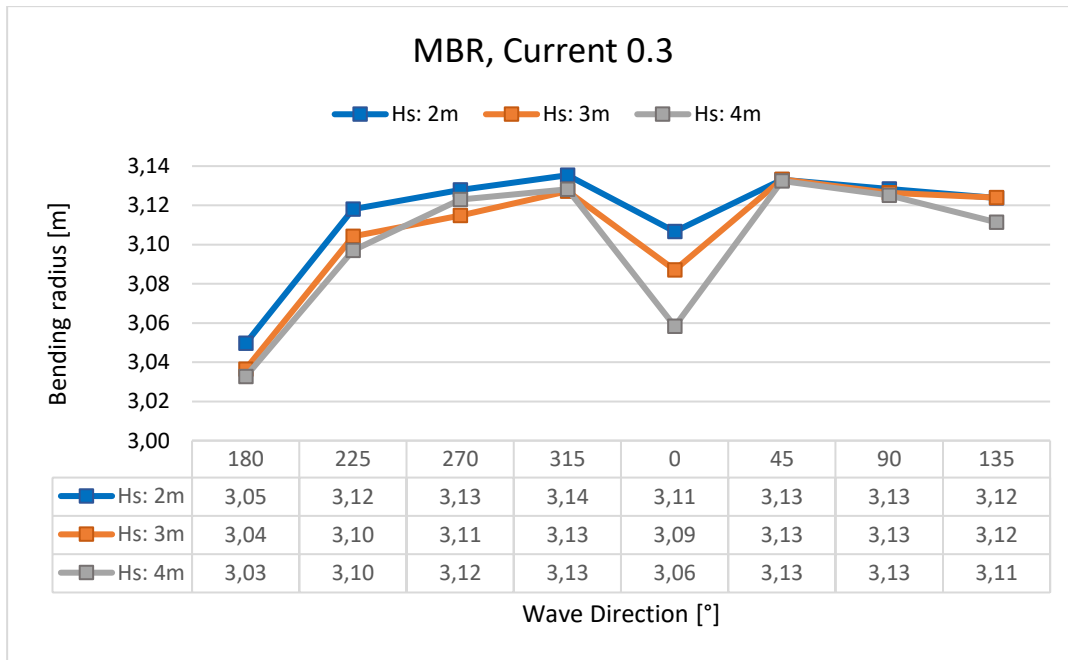


Figure 55: MBR results with current: 0.3 m/s, note critical MBR is 3.07 m

At current 1.0 m/s:

Based on the analysis of figure 56, it is possible to see that the MBR values vary among the different wave directions. The wave directions with bending radius values below the specified critical MBR of 3.07 m appears in the 180° case. What can be observed in this case is that as the wave height increases at a current speed of 1.0 m/s, the bending radius values become more critical, particularly when the wave direction is 180°.

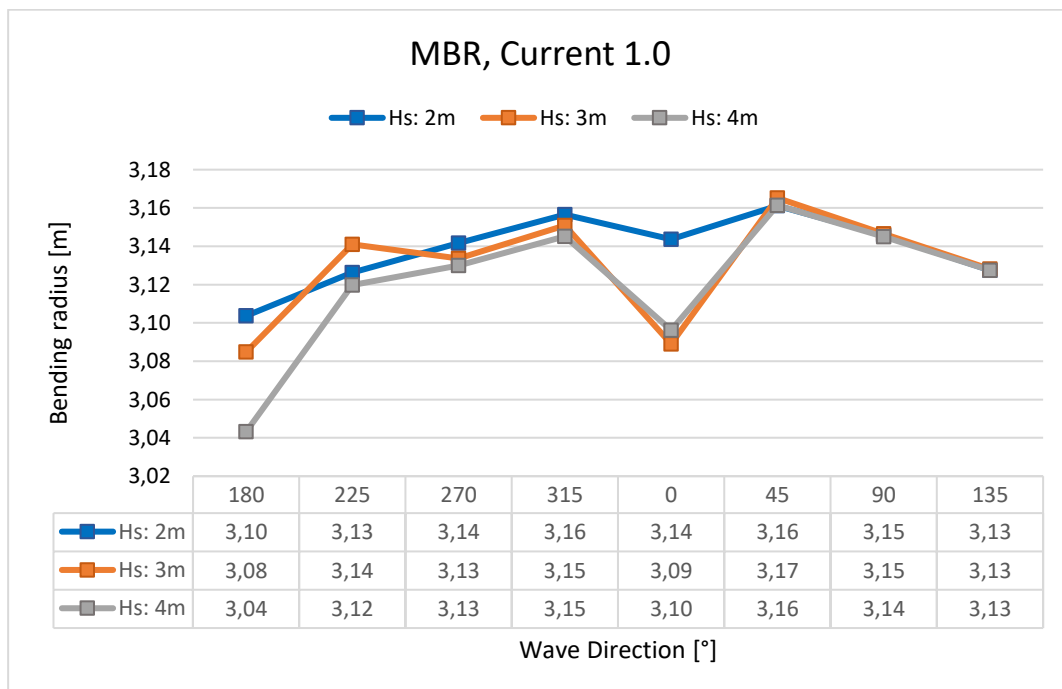


Figure 56: MBR results with current: 1.0 m/s, note critical MBR is 3.07 m

7.3 Case 2 - Results

The primary focus in Case 2 is the moonpool during the deployment of the DMA and Buoyancy modules. Figure 57 illustrates an instance of the deployment procedure. If the recorded values exceed 0 m, it indicates that the IAC has come in contact with the moonpool structure, potentially causing damage to the cable. Figure 58 provides a visual illustration of the moonpool with dimensions of 7.2 m x 7.2 m. Variables such as the minimum tension on the cable are taken into consideration, with a minimum allowed tension of 0 kN, indicating potential slackness or loss of tension. Although the MBR is not the primary focus in this case, it is worth noting that no bending values below 10 m were recorded, indicating that the cable did not experience abrupt motions during deployment.

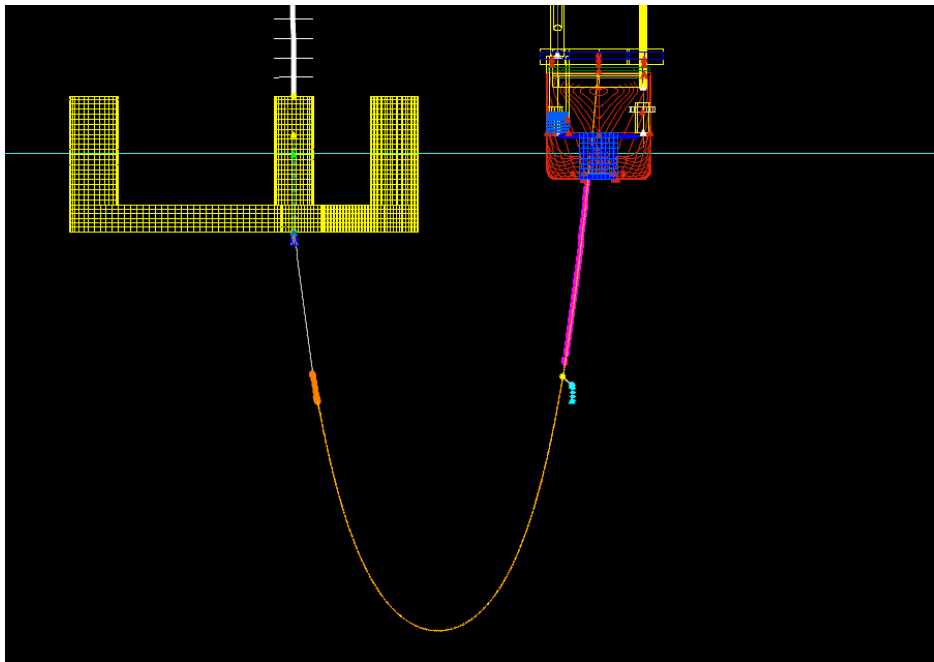


Figure 57: Case 2 - Deployment of DMA and buoyancy modules through the moonpool in progress.

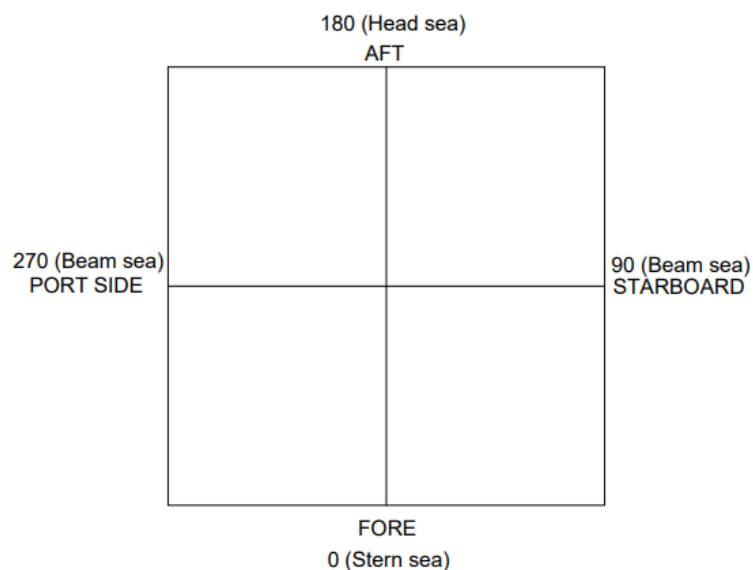


Figure 58: Visual representation of moonpool with dimensions 7.2 m x 7.2 m, made in Bricscad

Moonpool

At no current:

- Upon reviewing the data in table 22, it is observed that there are no instances where the MP clearance is below 0. For all the recorded scenarios, the MP clearance values remain positive, indicating that there is no collision between the moonpool and cable.
- Even though collision between cable and moonpool is not likely with no current speed, it can be observed that increasing wave height at 0° wave direction, drives the IAC cable closer and closer to the moonpool.

Table 22: Moonpool clearance results, no current

No current					
Wave Height [m]	Wave Dir [°]	MP clearance Aft [m]	MP clearance Fore [m]	MP clearance Port side [m]	MP clearance Stbd [m]
2,0	180	2,66	4,34	1,39	4,71
2,0	225	2,12	3,84	1,45	4,83
2,0	270	2,05	3,81	1,66	4,99
2,0	315	2,06	3,83	1,48	4,77
2,0	0	2,65	4,33	0,96	4,63
2,0	45	2,28	3,92	1,43	4,72
2,0	90	2,11	3,77	1,68	5,00
2,0	135	2,33	3,98	1,47	4,78
3,0	180	2,63	4,31	1,30	4,62
3,0	225	1,86	3,65	1,27	4,73
3,0	270	1,77	3,57	1,60	4,94
3,0	315	1,75	3,52	1,42	4,63
3,0	0	2,63	4,31	0,69	4,50
3,0	45	2,09	3,79	1,18	4,57
3,0	90	1,79	3,49	1,64	4,98
3,0	135	2,19	3,82	1,30	4,67
4,0	180	2,62	4,29	1,01	4,56
4,0	225	1,75	3,56	1,14	4,63
4,0	270	1,53	3,41	1,51	4,88
4,0	315	1,61	3,33	1,35	4,54
4,0	0	2,61	4,30	0,43	4,42
4,0	45	1,99	3,69	1,07	4,46
4,0	90	1,61	3,42	1,52	4,93
4,0	135	2,11	3,73	1,19	4,59

At current speed 0.3 m/s:

- By analysing table 23 it can be observed that there are instances where the MP clearance is below 0. In the scenario with a wave height of 4.0 m, wave direction of 180°, and a current speed of 0.3 m/s, the MP clearance value for port side is -0.18 m. The negative values suggest that the cable will clash with the moonpool in these conditions. Additionally, there are instances where the MP clearance values for port side and starboard side are close to 0, indicating a potential risk of collision. These findings indicate a pattern where scenarios with increasing wave heights and wave directions in the range around 180° - 270° appear to have a higher likelihood of the cable clashing with the moonpool.

Table 23: Moonpool clearance results, current: 0.3 m/s

Current 0.3 [m/s]					
Wave Height [m]	Wave Dir [°]	MP clearance Aft [m]	MP clearance Fore [m]	MP clearance Port side [m]	MP clearance Stbd [m]
2,0	180	2,67	4,34	0,64	5,03
2,0	225	1,70	4,15	1,02	5,08
2,0	270	1,35	4,37	1,63	5,02
2,0	315	1,66	4,27	1,81	4,46
2,0	0	2,65	4,34	1,70	4,14
2,0	45	2,65	3,52	1,80	4,42
2,0	90	2,69	3,11	1,68	5,03
2,0	135	2,57	3,57	1,10	5,02
3,0	180	2,64	4,32	0,02	4,93
3,0	225	1,30	4,03	0,70	5,05
3,0	270	1,04	4,33	1,56	4,98
3,0	315	1,29	4,04	1,82	4,24
3,0	0	2,63	4,31	1,70	4,02
3,0	45	2,65	3,40	1,69	4,26
3,0	90	2,62	2,62	1,65	4,99
3,0	135	2,52	3,33	0,90	4,94
4,0	180	2,63	4,29	-0,18	4,77
4,0	225	1,25	3,94	0,46	5,02
4,0	270	0,67	4,24	1,47	4,94
4,0	315	1,36	4,01	1,81	4,29
4,0	0	2,61	4,29	1,68	3,78
4,0	45	2,61	3,33	1,71	4,17
4,0	90	2,52	2,50	1,54	4,94
4,0	135	2,50	3,25	0,79	4,89

At current speed 1.0 m/s:

- Based on the data in table 24 it is clearly shown that the MP clearance values are consistently below 0 for almost all wave directions, indicating collisions. Among the different wave directions, it can be observed that in all instances with wave direction 45°, the MP clearance values remain above 0 with no risk of collision expected. Similarly, for a wave direction of 0°, MP clearance values are above 0 until the wave height reaches 4 m. These findings suggest a potential pattern indicating that wave direction 45° provides a favourable condition with no collision risk.

Table 24: Moonpool clearance results, current: 1.0 m/s

Current 1.0 [m/s]					
Wave Height [m]	Wave Dir [°]	MP clearance Aft [m]	MP clearance Fore [m]	MP clearance Port side [m]	MP clearance Stbd [m]
2,0	180	2,68	4,35	-0,20	5,04
2,0	225	0,08	4,38	-0,20	5,13
2,0	270	-0,15	4,37	1,76	5,06
2,0	315	-0,21	4,35	1,83	2,38
2,0	0	2,66	4,33	1,84	0,97
2,0	45	2,68	1,35	1,84	2,40
2,0	90	2,69	0,00	1,75	5,07
2,0	135	2,69	1,53	-0,19	5,13
3,0	180	2,67	4,34	-0,14	4,97
3,0	225	0,03	4,38	-0,21	5,13
3,0	270	-0,19	4,38	1,71	5,03
3,0	315	-0,21	4,36	1,83	2,23
3,0	0	2,65	4,32	1,84	0,28
3,0	45	2,68	1,19	1,84	2,22
3,0	90	2,69	-0,21	1,71	5,04
3,0	135	2,69	1,43	-0,20	5,13
4,0	180	2,66	4,33	-0,20	4,82
4,0	225	-0,04	4,38	-0,20	5,13
4,0	270	-0,21	4,38	1,67	5,00
4,0	315	-0,21	4,37	1,84	2,00
4,0	0	2,63	4,30	1,84	-0,15
4,0	45	2,68	1,07	1,84	2,09
4,0	90	2,69	-0,21	1,64	5,00
4,0	135	2,69	1,38	-0,21	5,13

Minimum tension on cable

At no current:

- Examining the values in figure 59, it can be observed that two instances fall below this threshold. These occurrences are associated with wave height 4 m and wave directions of 180° and 0°, where tension values of -3.13 kN and -5.91 kN were recorded. However, it should be noted that the majority of the scenarios exhibit tension values well above the minimum allowable tension.

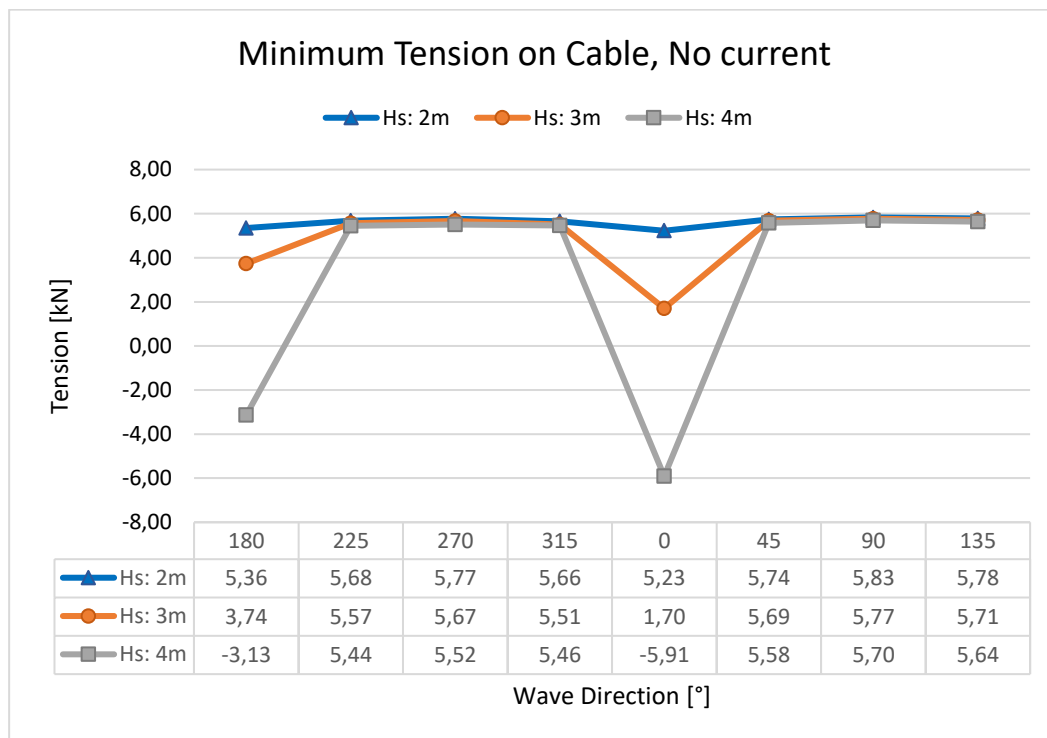


Figure 59: Minimum tension results with no current, note critical compression is below 0 kN

At current 0.3 m/s:

- After examining the values in figure 60, it can be observed that there are instances where the minimum tension falls below the allowed limit. Both of these incidents occurred in the wave direction of 0°, with tensions recorded as -4.89 kN at Hs: 3 m and -16.61 kN at Hs: 4 m. But also, for current speed at 0.3 m/s the majority of the scenarios are well above the minimum limit.
- In the scenarios with current speeds of 0 and 0.3 m/s, a pattern can be observed where tensions below the limit are consistently observed in wave directions around 0°. This observation indicates a potential correlation between the specific wave angle and decreased tension in the cable.

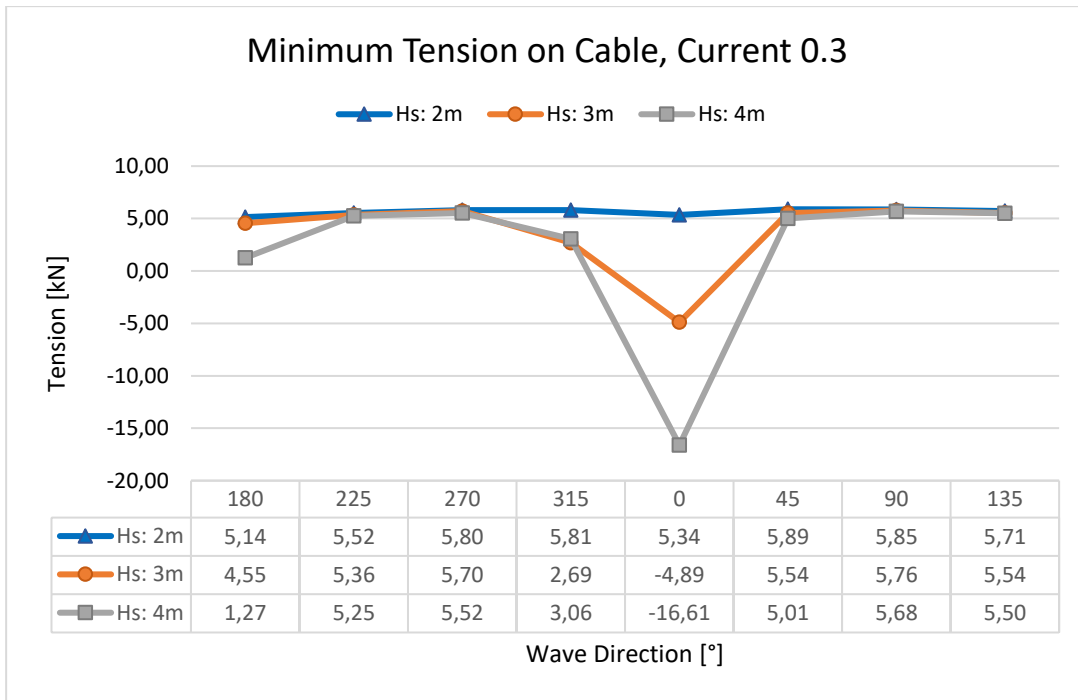


Figure 60: Minimum tension results with current: 0.3 m/s, note critical compression is below 0 kN

At current 1.0 m/s:

- By analysing the data presented in figure 61, it can be observed that there are no instances where the minimum tension in the cable falls below the acceptable 0 kN. The closest scenario recorded reflects a wave direction of 0° and a wave height of 4.0 m, with tension of 0.82 kN.

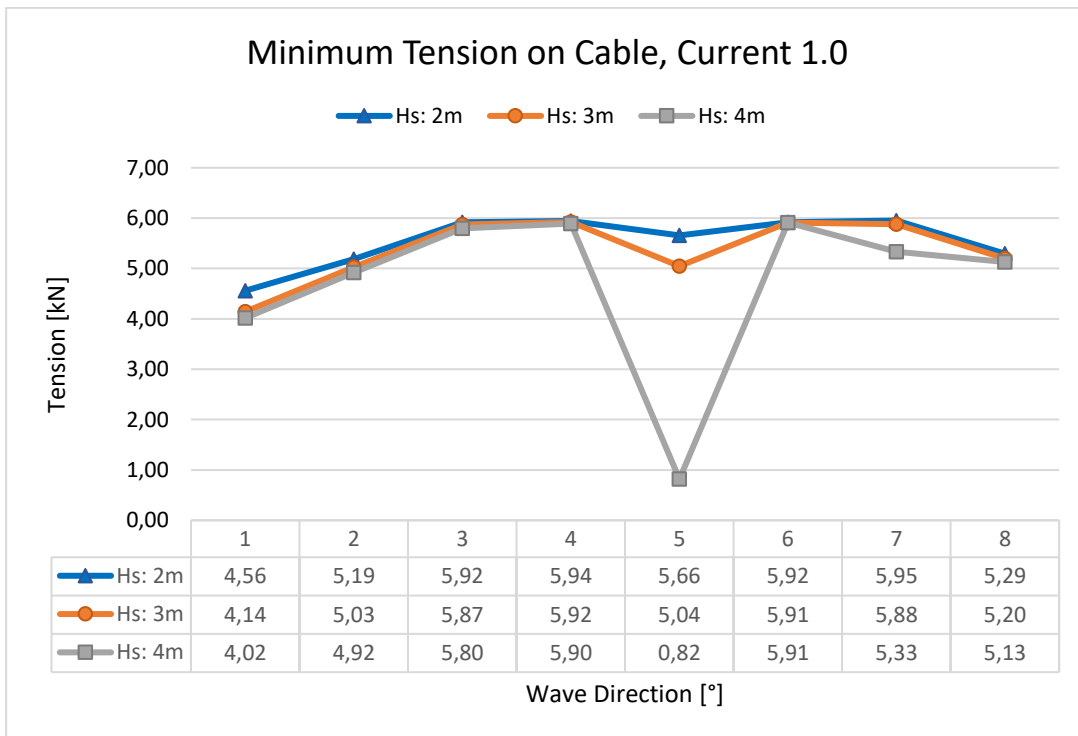


Figure 61: Minimum tension results with current: 1.0 m/s, note critical compression is below 0 kN

7.4 Case 3 - Results

In case 3, both the bending radius and cable tension are of significant importance, especially during the upward movement that occurs after the release of the first DMA. The abrupt shape of the release increases the likelihood of generating additional tension on the IAC and exposes it to low bending radius. Figure 62 illustrates an instance of the procedure after the release. The MBR serves as a critical criterion for assessing the structural integrity and operational bending radius of the cable. A threshold of 3.07 m is set, below which any bending radius is considered critical and can adversely affect the cable's functionality. Variables such as the maximum and minimum cable tension are taken into consideration, with a maximum of 336 kN and a minimum of 0 kN.

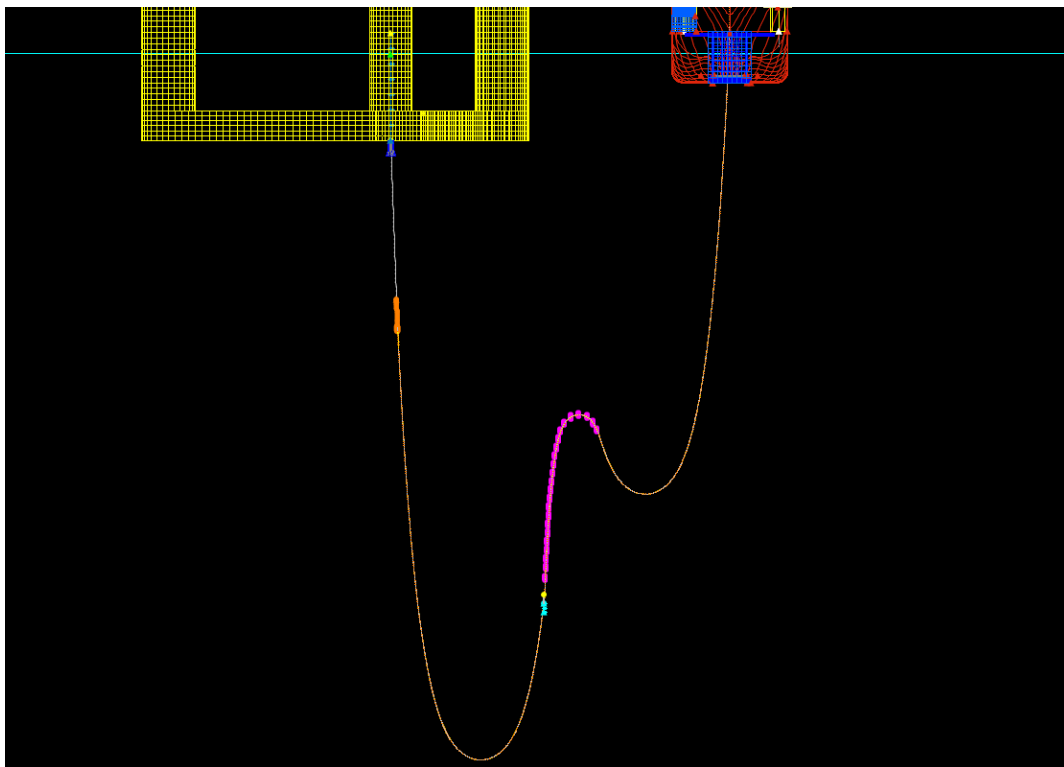


Figure 62: Case 3 - release of DMA

MBR

At no current:

- The findings of analysing figure 63 indicate that almost every scenario with zero current violates the MBR limit, ranging from 2.91 – 3.05 m. Conversely, there are two wave scenarios that falls below the specified threshold for the MBR. Wave direction of 90°, with wave heights of 2 m and 3 m do not exceed the MBR, as these scenarios are just within the acceptable range.

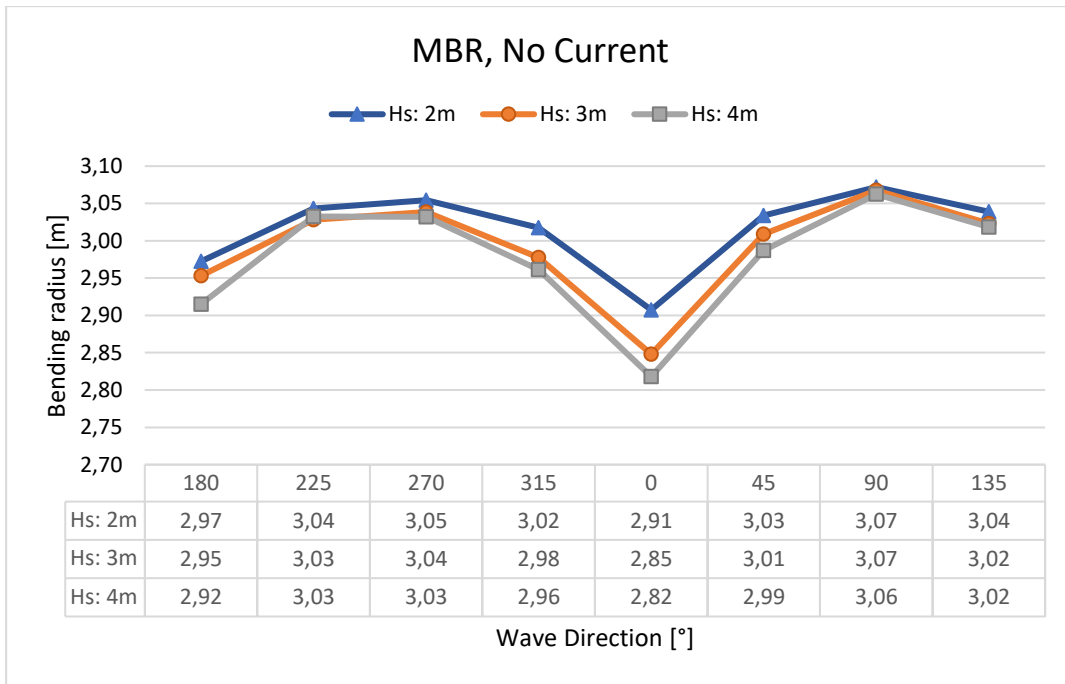


Figure 63: MBR results with no current, note critical MBR is 3.07 m

At current 0.3 m/s:

- From figure 64, the results indicates that wave directions of 315°, 0° and 45° exceed the specified MBR limit, ranging from 2.71 – 2.92 m bend radius, while the rest of wave direction scenarios tend to remain on the acceptable side of the MBR limit. Notably, there is a trend where wave directions ranging from 45° to 315° exhibit lower MBR values, indicating potential directional dependencies.

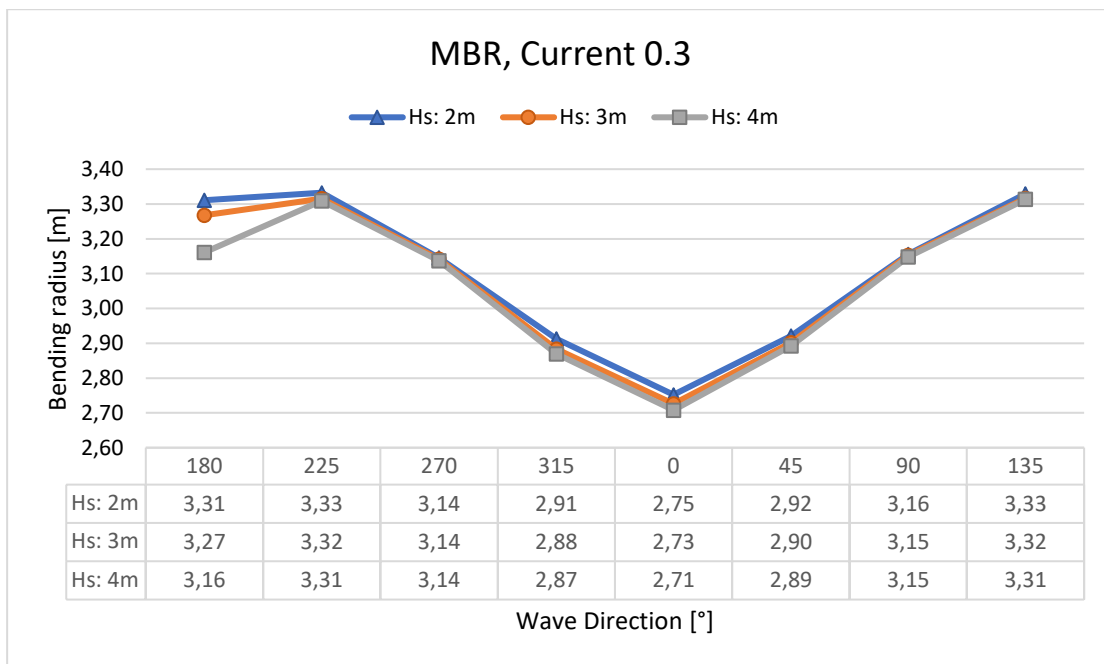


Figure 64: MBR results with current: 0.3 m/s, note critical MBR is 3.07 m

At current 1.0 m/s:

- Figure 65 shows that for 1.0 m/s current, only wave directions of 225-270° and 90-135° are above the specified MBR limit. While wave directions of 45-315° and 180° consistently remain below the MBR limit. These findings suggest a potential pattern where wave directions close to 45-315° and 180° are more likely to exceed the MBR limit (less than 3.07 m), while it is the other way around for the other wave directions.

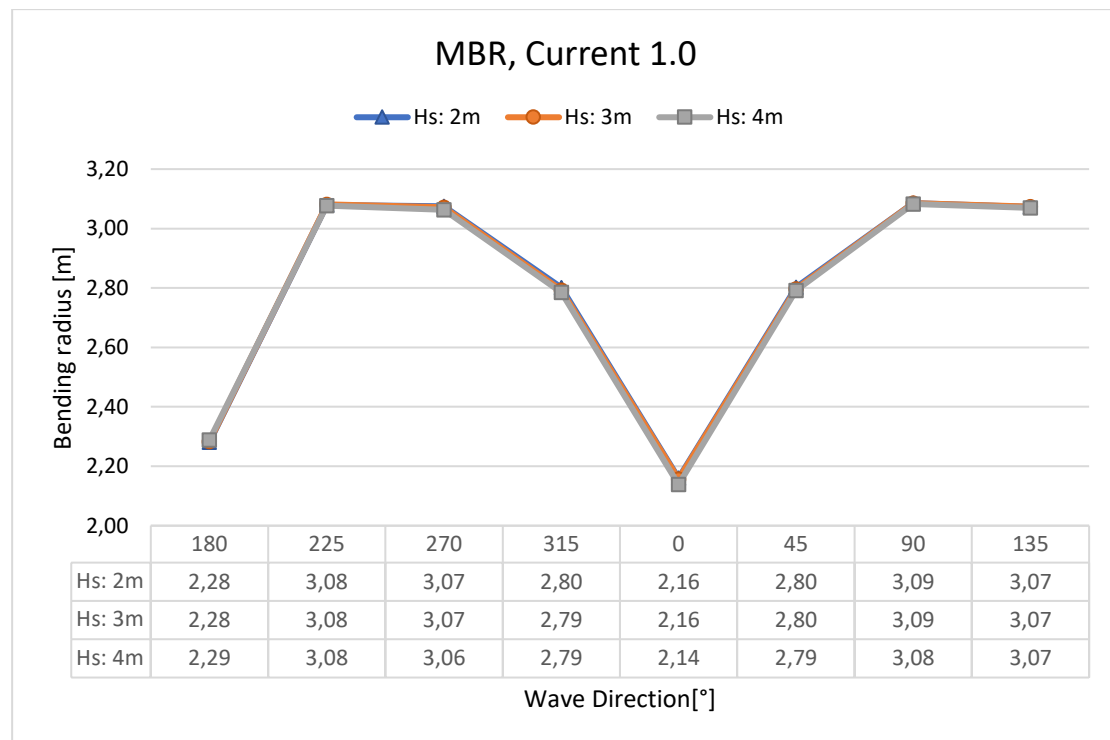


Figure 65: MBR results with current: 1.0 m/s, note critical MBR is 3.07 m

Maximum and minimum tension on Cable

At no current:

- Among the tested wave directions at zero current speed, all scenarios exhibited tensions within the allowed limits. None of the scenarios resulted in tensions exceeding the maximum limit or falling below the minimum requirement. The following maximum and minimum tension was found: 86.48 kN and 1.33 kN.

Therefore, based on the data from figures 66 and 67, and the allowable tension, none of the tested wave directions at zero current speed can be considered as a risk to the cable's integrity. Under these conditions, the cable remains within the acceptable tension range.

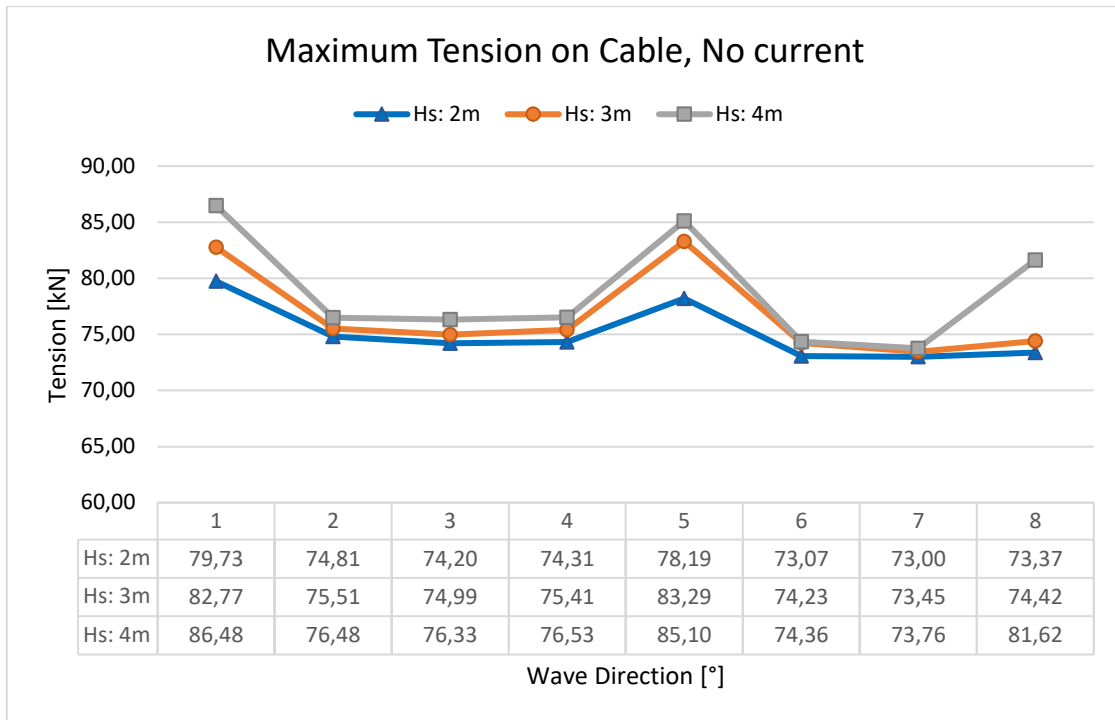


Figure 66: Maximum tension results with no current, note critical limit is 336 kN

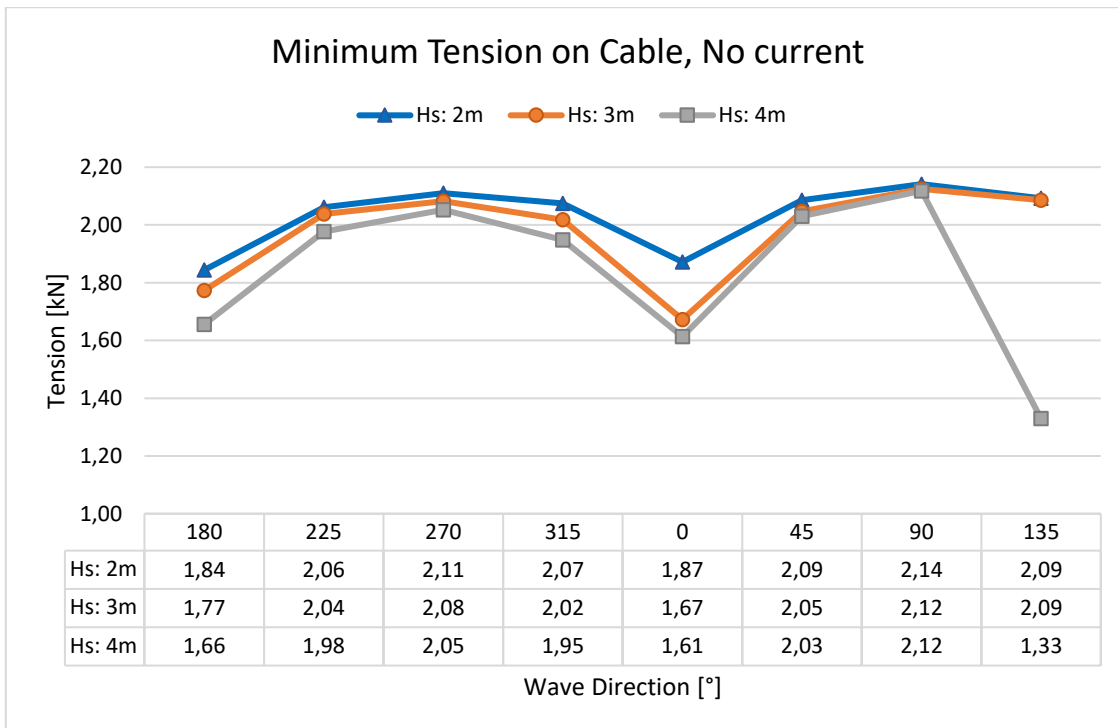


Figure 67: Minimum tension results with no current, note critical compression is below 0 kN

At current 0.3 m/s:

- The most critical scenario found in figure 68 and 69 reflects a wave direction 0° and wave height 4 m. The cable encountered a maximum tension of 344.31 kN and a minimum tension of -133.20 kN, which indicates a significant deviation from the acceptable range. Therefore, the scenario was rerun to identify any measurement errors and validate the accuracy of the results. The subsequent analysis uncovered the presence of measurement errors. The results still showed a deviation at the minimum allowed tension, although the deviation was less pronounced compared to previous results. Additionally, the analysis demonstrated an acceptable value for the maximum allowable tension, with the data indicating a minimum value of -1.09 kN and a maximum value of 83.1 kN.
- The other wave directions and wave heights, at a current speed of 0.30 m/s, showed tensions within the allowed limits. However, another data point in figures 68 and 69 stood out, at wave direction 0° and wave height 2 m, a maximum tension of 185.23 kN and a minimum tension of 0.03 kN were recorded.

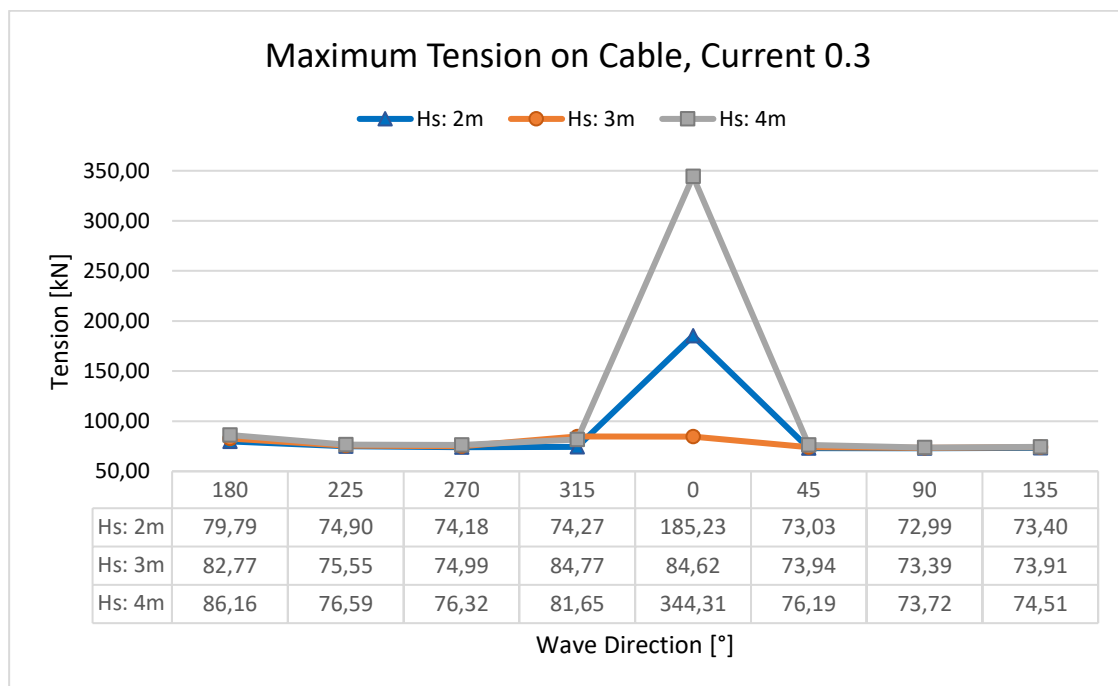


Figure 68: Maximum tension results with current: 0.3 m/s, note critical limit is 336 kN

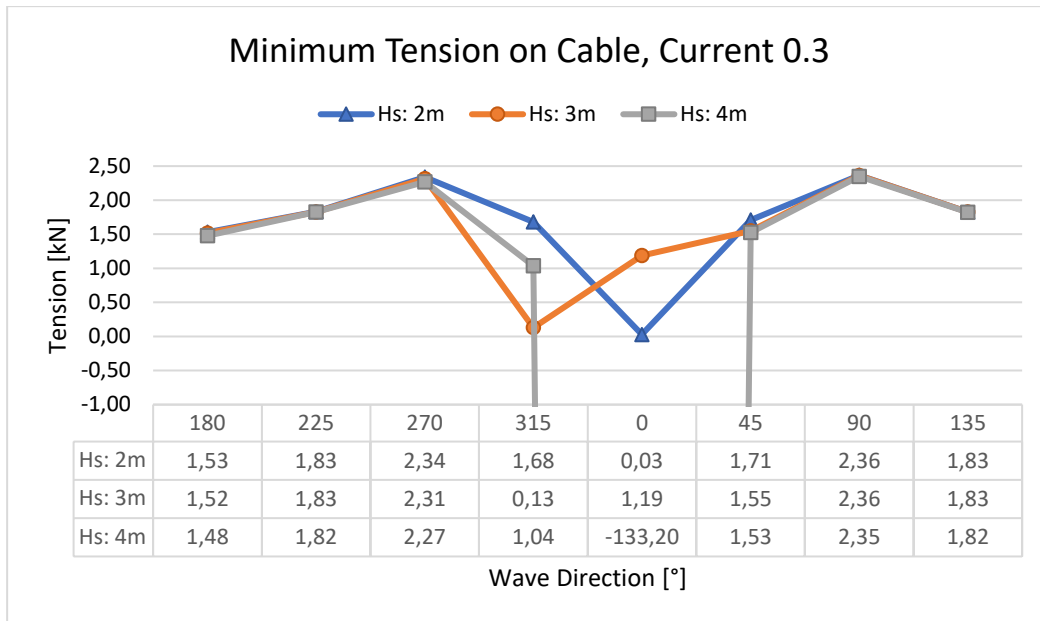


Figure 69: Minimum tension results with current: 0.3 m/s, note critical compression is below 0 kN

At current 1.0 m/s:

- In the scenario with a current speed of 1.0 m/s, it is noteworthy that for each wave height, two cases exceed the minimum tension limit. As shown in figure 70 and 71, these transpire at wave directions 180° and 0°. For a wave height of 2 m, 3 m and 4 m: The most critical wave direction is 180° and 0°, where the cable at 2 m experiences a minimum tension of -0.92 at head sea and -1.09 kN at stern sea. At 3 m, a minimum tension of -0.91 at head sea and -1.08 kN at stern sea. At 4 m, exhibiting a minimum tension of -0.91 kN at head sea and -1.09 kN at stern sea. The maximum tension does not have any scenarios where it exceeds the limit.

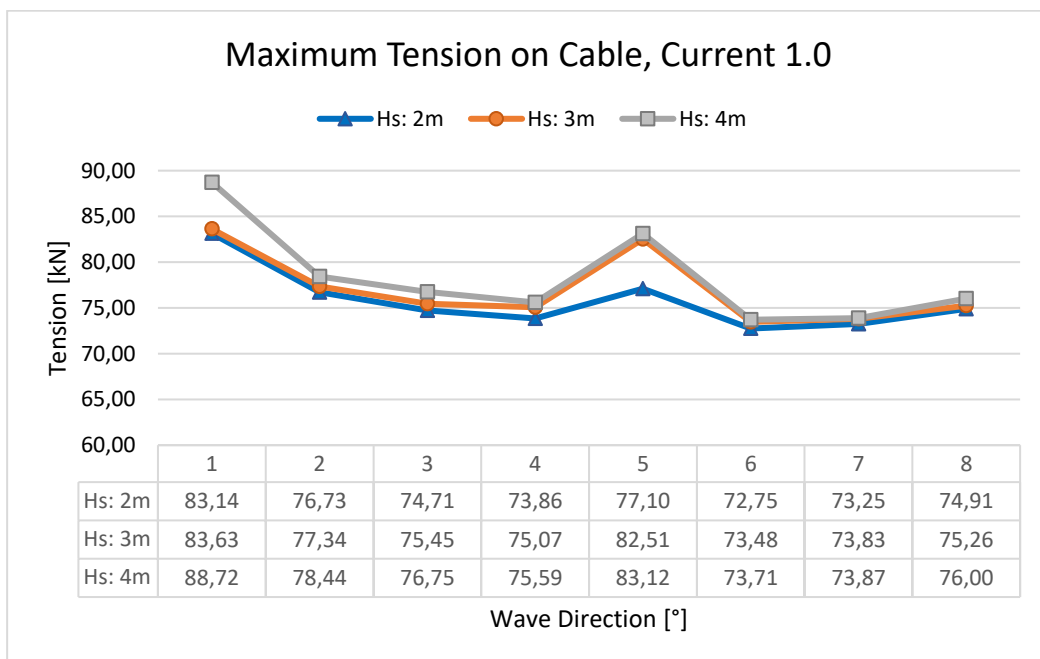


Figure 70: Maximum tension results, current: 1.0 m/s, note critical limit is 336 kN

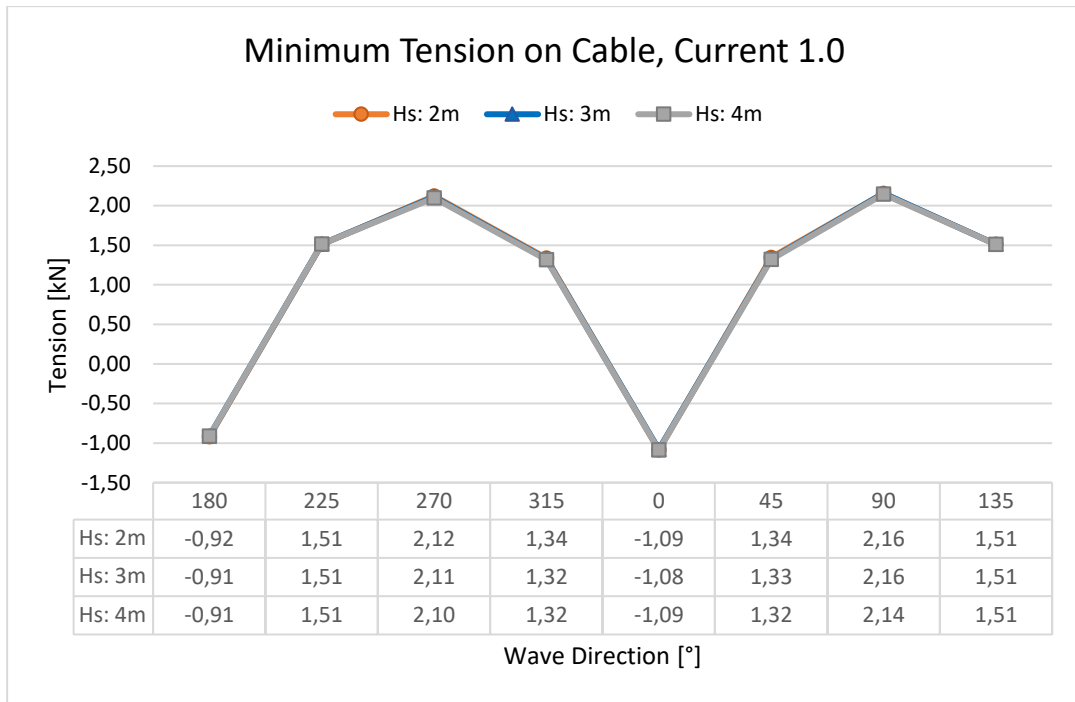


Figure 71: Minimum tension results with current: 1.0 m/s, note critical compression is below 0 kN

8 Discussion

8.1 Study approach and corresponding process

Through the Orcaflex analyses conducted in this thesis, the objective was to examine the limiting parameters for each critical case and their sensitivity to various environmental configurations. The outcome of the research conducted in this master's thesis focuses on outlining an approach for the installation phase of the IAC operations in a floating wind farm. This has been accomplished by illustrating the different scenarios in a cable installation project to understand the effect of the parameters. The study incorporated various parameters, including current, wave height, wave period, and wave direction. The analyses drew inspiration from a model representing the final configuration of an offshore floating wind turbine. In dynamic simulations, there are numerous factors that can influence the accuracy of the simulation results. However, certain simplifications and assumptions were made, in order to provide a feasible and useful study.

The process of conducting a literature search holds great significance in the research process as it provides valuable insights into previous studies and helps establish the existing knowledge base on a particular subject. In the context of this study, the literature search aimed to uncover information regarding the methodology employed for the installation of IAC in floating wind farms. This included identifying the recommended sequence of steps involved in the installation process. By thoroughly reviewing the available literature, the specific steps associated with the installation of the 1st end dynamic section and the 2nd end dynamic section were carefully analysed.

From the steps, it was noted that there was considerable overlap between those found in the "Installation of 1st end dynamic section" and the "Installation of 2nd end dynamic section." As a result, only the steps from the 1st end were selected for further analysis, as they were deemed representative of the overall process. These critical steps were chosen based on insights obtained from previous reports, and a careful study of the main steps of the installation phase and to then identify the critical steps, assessed as steps posing specific risks and hazards. Step 1 and 4 involves steps with abrupt movement and tight angles on the cable, increasing the risk of additional tension and exposing the cable to low bending radius. In step 2, the moonpool area was examined to assess the potential risk of cable clashing, which could result in damage to the cable, during the deployment of DMA and buoyancy modules. To evaluate their execution, the selected steps were incorporated into the Orcaflex analysis program, enabling simulations to be performed.

It is significant to point out that the data availability limits the results and that the sources used may have an influence. Therefore, it may be necessary to further investigate and involve additional sources to gain a broader understanding of the installation phase of IAC. This includes exploring if there are other steps in these two phases that should be considered as critical and be therefore further analysed.

8.2 The effect of environmental parameters and study results

A simple analysis was conducted to assess the impact of various parameters on cable loads during the J-lay method's deployment through the moonpool, considering different sea states. This method is commonly used as offshore wind farms expand into deeper waters. The analysis revealed that the deployment process through the moonpool is sensitive to wave conditions, particularly when waves approach from 0° (stern sea) and 180° (head sea). In sea states characterized by a current velocity of 1.0 m/s, the j-lay method would not be feasible for cable deployment. These findings highlight the importance of carefully considering wave headings and current velocities when planning cable deployment operations using the j-lay method, especially in challenging sea conditions.

For case 1, analyses were conducted on the maximum tension on the pull-in winch, maximum tension on the lower tensioner, minimum tension on the cable, and MBR. The findings for the first three variables indicated that they all remained within the allowable limits for any wave direction, even with varying wave periods and increasing flow velocities from 0 m/s to 0.3 m/s and further to 1 m/s. However, prior to analyzing this scenario, it was known that MBR was the most critical variable due to the abrupt movements during the deployment of the pull-in head, and this proved to be true. The analysis revealed that the MBR fell below the allowable threshold when waves approached from the 0° and 180° directions, posing a risk of damage to the IAC. However, while two wave directions exceeded the limits for all simulated flow velocities, the MBR values for the other wave directions remained within acceptable range. The analysis of case 1 indicates that the installation of IAC can be carried out using Edda Freya in wave directions in the range $45\text{-}135^\circ$ and $225\text{-}315^\circ$.

Unlike case 1, MBR is not a critical factor in case 2, or to put it differently, it is not susceptible to damage. During the deployment of DMA and buoyancy modules, the parameters of moonpool and minimum tension on the cable take center stage and have been subject to closer examination. In this scenario, there are more dynamics at play, and several unfortunate incidents occur, such as collisions with the moonpool and compression leading to instability.

In the analysis with a flow velocity of 0 m/s, the cable experiences only a few instances where the operation cannot be carried out smoothly, mainly when the wave height is 4 m. Furthermore, when the flow velocity is increased to 0.3 m/s, there are still only a few cases where the acceptable cable criteria are not exceeded, again most critical with a wave height of 4 m. It is not until the flow velocity of the waves is increased to 1 m/s that the availability of optimal alternatives for conducting the IAC installation with Edda Freya starts to diminish. Here, encountering problems becomes almost inevitable, regardless of the wave direction, as the cable comes into contact with the moonpool. The only viable option for carrying out this operation for all wave heights is when the waves approach from a 45° direction.

Contact with the moonpool walls is a concern during phases 1 and 2 of the IAC installation. To avoid contact, the CLV must be positioned close to the FWT. For this specific case, the clearance from hull to hull is 33 m. To further minimize the risk of cable collisions with the moonpool, ballast weights are necessary to be attached to the DIACs before each buoyancy section, reducing the chances of DIACs coming into contact with the moonpool doors.

In case 3, once again, MBR was the primary focus due to the movements occurring after the final DMA is released. Maximum tension and minimum tension were also analyzed, and it is observed that they only become highly critical when MBR is exceeded. As seen in the previous cases, with higher flow velocity and wave height, an increasing number of instances arise where either limit are exceeded or values approach critical thresholds, and the same holds true here. The release of DMA clearly affected the cable's MBR under these environmental conditions compared to the other factors. In the scenario where the flow velocity is 0.3 m/s, with wave directions ranging from 30° to 270°, it is most feasible to release DMA using Edda Freya without encountering cable issues.

As mentioned earlier, conducting operations in sea states with wave headings of 0° and 180°, along with a current velocity of 1.0 m/s, is not ideal. It is clear that performing cable operations using the vessel Edda Freya under these sea conditions is not acceptable in these three scenarios as there are high risk of damaging the cable and should be avoided. It is important to consider safer and more favorable sea states to ensure the successful and efficient execution of cable installation activities.

The analysis conducted as part of this thesis revealed valuable insights into identifying the optimal conditions for offshore installation operations. The findings indicate that wave directions ranging from 90-135° and 225-270°, simulated with a current velocity of 0.3 m/s, resulted in the most favourable outcomes. Emerged as the only case where all three analysed scenarios converged to the same result, these scenarios corresponded to peak periods for conducting installation activities. This suggests that offshore installation operations should ideally be scheduled during these wave conditions to minimize complications and ensure efficient execution.

It is important to acknowledge that alternative scenarios exist wherein varying combinations of wave directions, wave heights, and wave periods are also deemed acceptable for offshore installation operations. The simulations conducted with currents of 0 and 0.3 m/s consistently produced the best results with minimal complications. On the other hand, when the current velocity was increased to 1.0 m/s, the feasibility of operations was significantly impacted. This implies that the selection of appropriate current conditions is critical for the success of offshore installation activities.

The success of a cable operation is closely linked to the prevailing sea conditions. While each project may have specific requirements, it is widely acknowledged that the deployment method has a significant impact on the available weather window for conducting operations. This factor could affect

the competition among vessel owners as clients consider costs and operational uptime when selecting a vessel for the operation.

9 Conclusion

The aim of the following master thesis was to optimize marine operations related to IAC installation at Utsira Nord. Thereby investigate the steps involving installation of inter-array cables between the WTGs at the Utsira Nord site. The conclusion will attempt to answer objectives set for this thesis and whether they were achieved or not. The following issues have been guiding the content of the thesis.

- What are the main steps of the installation of inter-array cables, define the critical phases and analyse typical loads acting on the cables to discover the parameters that affect the installation.
- Analysis of the critical steps, to determine the optimal environmental conditions for cable installation.

Several sensitivity analyses were performed concerning if it was feasible to reduce the simulation time period without significantly impacting the accuracy of the results. Here, the objective focused on investigating several parameters that might provide peak tension loads on an IAC under instalment. The cable was investigated for its sensitivity for maximum tension, minimum tension and MBR in varying time durations (5 min, 10 min & 30 min), compared to 1-hour operable sea state. The analyses were all performed by the aid of the software, Orcaflex.

The sensitivity analysis was solely conducted for cases 2 and 3. Case 1, however, did not undergo such analysis. In case 1, a total of 480 wave seeds were employed in the simulations, utilizing the Gumbel method. In contrast, for cases 2 and 3, the Rayleigh method was used with a smaller set of 48 wave seeds. This selection was specifically made to enable a focused sensitivity analysis.

The results from the analysis indicate that conducting operations in sea states with wave directions of 0° and 180° , poses a high risk of cable damage and is not recommended for offshore installation operations. Safer and more favourable sea states should be considered for successful and efficient execution. The analysis conducted in this thesis revealed that wave directions ranging from $90\text{-}135^\circ$ and $225\text{-}270^\circ$, simulated with a current velocity of 0.3 m/s, yielded the most optimal conditions. These scenarios, where all three analysed cases converged, corresponded to peak periods for conducting installation activities. Therefore, scheduling offshore installation operations during these wave conditions is highly recommended to minimize complications and ensure efficient execution.

Different combinations of wave directions, heights, and periods can be considered acceptable for offshore installation operations. The simulations consistently showed that currents of 0 and 0.3 m/s produced the best results with minimal issues, while increasing the current velocity to 1.0 m/s was not ideal.

10 Further work

To further enhance the findings of this master's thesis, it is recommended to analyse the various current velocities further, particularly focusing on currents up to 1.0 m/s, to determine if there are other operable currents for installation that were not extensively explored in this study. Such additional analysis would be valuable to determine if the optimal sea states found in this thesis are the ideal ones for the installation at Utsira Nord.

The analysis employed a non-stationary model; however, due to data limitations, certain assumptions were made, and simplifications were applied. Specifically, the FWT was treated as a fixed structure. Consequently, the analysis was constrained by the assumption that the FWT was in a fixed position, which does not accurately reflect real-world conditions. To address this limitation, future work should consider analysing the system with a moving FWT, provided that sufficient data is available.

References

- [1] WindEurope, "Offshore Wind energy 2022," Windeurope, August 2022. [Online]. Available: <https://windeurope.org/intelligence-platform/product/offshore-wind-energy-2022-mid-year-statistics/>.
- [2] EWEA, "Wind energy scenarios for 2030," August 2015. [Online]. Available: <https://www.ewea.org/fileadmin/files/library/publications/reports/EWEA-Wind-energy-scenarios-2030.pdf>.
- [3] F. F. D. B. C. P. M. Y. C. R. P. & R. V. Dinmohammadi, "IEEEXplore," 2019. [Online]. Available: <https://ieeexplore.ieee.org/document/8704223>.
- [4] N. J. D.-S. & Z. Yang, "Tension Analysis of Submarine Cables During Laying Operations," 2013. [Online]. Available: Tension Analysis of Submarine Cables During Laying Operations.
- [5] DeepOcean, "About us," DeepOcean, 2013. [Online]. Available: <https://www.deeпоceangroup.com/about/about-us>.
- [6] InfoBank, "Havvind, Utsira Nord," InfoBank, November 2022. [Online]. Available: <https://infobank.no/infobank/havvind/>.
- [7] DeepOcean, "Utsira Nord - 2022 (internal report)," DeepOcean, Haugesund, 2022.
- [8] Spinergie, "Utsira Nord (wind farm)," Spinergie, [Online]. Available: <https://spinconstruction.spinergie.com>.
- [9] Integra, "Offshore floating wind... Are we prepared for it?," Integra, August 2022. [Online]. Available: <https://www.integrarechnical.com/articles/offshore-floating-wind-are-we-prepared-for-it/>.
- [10] Aker Solutions, "Subsea Power, Offshore wind days Haugesund," in *Floating wind days*, Haugesund, 2023.
- [11] Corewind, "Review of the state of the art of dynamic cable system design - installation & inspection," Corewind, February 2020. [Online]. Available: <https://corewind.eu/wp-content/uploads/files/publications/COREWIND-D3.1-Review-of-the-state-of-the-art-of-dynamic-cable-system-design.pdf>.
- [12] MDPI, "Analysis of Offshore Wind Turbines: A Review," MDPI, 2022. [Online]. Available: <https://www.mdpi.com/2073-4433/13/3/451>.
- [13] J. M. & A. R. J.F. MANWELL, *Offshore wind turbine engineering*, UiS, 2016.

- [14] Airpes, "What are the main parts of a wind turbine?," Airpes, 2022. [Online]. Available: <https://www.airpes.com/wind-turbine-parts/>.
- [15] Iberdrola, "Offshore wind turbines foundations," Iberdrola, 2019. [Online]. Available: <https://www.iberdrola.com/sustainability/offshore-wind-turbines-foundations>.
- [16] C. L. a. N. D. Kumar, "Foundation Types for Land and Offshore Sustainable Wind," 2020. [Online]. Available: https://www.e3s-conferences.org/articles/e3sconf/pdf/2020/44/e3sconf_icmed2020_01094.pdf.
- [17] F. D. P. T. R. K. G. H. J. Paterson, Offshore wind installation vessels, Ocean Engineering , 2018.
- [18] T. Worzyk, Submarine Power Cables, Springer-Verlag Berlin Heidelberg, 2009.
- [19] DNV, "DNV-RP-0360 Subsea power cables in shallow water," DNV, 2016. [Online]. Available: <https://www.dnv.com/energy/standards-guidelines/dnv-rp-0360-subsea-power-cables-in-shallow-water.html>.
- [20] M. I. H. O. S. M. Y. ., M. F. I. A. F. a. E. K Abdul Razak*, "Relationship between Pipeline Wall Thickness (Gr. X60) and WaterDepth towards Avoiding Failure during Installation," Researchgate, 2018. [Online]. Available: https://www.researchgate.net/publication/325293219_Relationship_between_Pipeline_Wall_Thickness_Gr_X60_and_Water_Depth_towards_Avoiding_Failure_during_Installation.
- [21] D. S. Nikolaos P Ventikos, Submarine power cables: laying procedure, the fleet and reliability analysis, Athens: Journal of Marine Engineering & Technology, 2013, pp. 13-26.
- [22] DeepOcean, "Edda Freya," DeepOcean, March 2022. [Online]. Available: <https://www.deeпоceangroup.com/vessels/edda-freya>.
- [23] European subsea cables association EU, "Submarine Power Cables," escaeu, March 2013. [Online]. Available: <https://www.escaeu.org/articles/submarine-power-cables/>.
- [24] electrical-engineering-portal, "HVDC transmission systems and HVDC submarine power cables in the world," EEP, 2019. [Online]. Available: <https://electrical-engineering-portal.com/download-center/books-and-guides/electricity-generation-t-d/hvdc-transmission-systems>.
- [25] F. A. P. C. K. K. & P. C. V. Manuel U. T. Rentschler, "Parametric study of dynamic inter-array cable systems for floating offshore wind turbines," SpringerLink, 2022. [Online]. Available: <https://link.springer.com/article/10.1007/s40868-020-00071-7>.
- [26] S. Vandenberghe, "Penetrating In The Submarine Power Cable Design," medium, 2022. [Online]. Available: <https://medium.com/ins-and-outs-of-submarine-powercables/penetrating-in-the-submarine-power-cable-design-711ca899caab>.

- [27] Prysmiangroup, "66 kV Submarine Cable Systems," [Online]. Available: https://www.prysmiangroup.com/sites/default/files/business_markets/markets/downloads/datasheets/leaflet_submarine_epr_66%20Kv_%20final.pdf.
- [28] ABB, "Submarine power cables," ABB, 2006. [Online]. Available: [http://library.abb.com/GLOBAL/SCOT/SCOT245.NSF/VerityDisplay/5CC588CA3902AFA6C1257156002C5417/\\$File/Submarine%20Power%20Cables.pdf](http://library.abb.com/GLOBAL/SCOT/SCOT245.NSF/VerityDisplay/5CC588CA3902AFA6C1257156002C5417/$File/Submarine%20Power%20Cables.pdf).
- [29] NKT, "Three-core submarine cable with lead sheath," NKT, [Online]. Available: https://nkt.widen.net/content/v65kevoo21/pdf/A_2X_F_K2YRAA_420_kV_DS_EN_DEHV_HV_DS_DE-EN.pdf?u=gj0n1y.
- [30] SNL, "Kildekritikk," Store Norske Leksikon, May 2021. [Online]. Available: <https://snl.no/kildekritikk>.
- [31] H. Nordvik, Artist, *DeepOcean sitt kontor i Haugesund*. [Art]. E24, 2021.
- [32] Orcina, "Orcaflex - world leading software," Orcina, August 2009. [Online]. Available: <https://www.orcina.com/orcaflex/>.
- [33] Wikipedia, "Microsoft Office Excel," Wikipedia, 2016. [Online]. Available: https://no.wikipedia.org/wiki/Microsoft_Office_Excel..
- [34] Orcina, "Wave theory," Orcina, 2018. [Online]. Available: <https://www.orcina.com/webhelp/OrcaFlex/Content/html/Wavetheory.htm>.
- [35] Orcina, "Theory: Irregular frequencies," Orcina, 2020. [Online]. Available: <https://www.orcina.com/webhelp/OrcaWave/Content/html/Theory,Irregularfrequencies.htm>.
- [36] Orcina, "Environment: setting up a random sea," Orcina, 2018. [Online]. Available: <https://www.orcina.com/webhelp/OrcaFlex/Content/html/Environment,Settinguparandomsea.htm>.
- [37] Orcina, "Waves: Wave spectra," Orcina, 2018. [Online]. Available: <https://www.orcina.com/webhelp/OrcaFlex/Content/html/Waves,Wavespectra.htm>.
- [38] DNV, "Wave loads," DNV, 2018. [Online]. Available: https://home.hvl.no/ansatte/tct/FTP/H2022%20Marinteknisk%20Analyse/Regelverk%20og%20standarder/DnV_documents/DNVGL-CG-0130.pdf.
- [39] Orcina, "Environment: modelling design waves," Orcina, December 2017. [Online]. Available: <https://www.orcina.com/webhelp/OrcaFlex/Content/html/Environment,Modellingdesignwaves.htm>.

- [40] Windstaller alliance, "Dynamic Inter Array Cables Installation study report (internal report)," WA.I.S22.001, Haugesund, 2022.
- [41] BVG associates, "Guide to an Offshore wind farm," The Crown Estate and the Offshore Renewable Energy Catapult, January 2019. [Online]. Available: <https://www.thecrownestate.co.uk/media/2860/guide-to-offshore-wind-farm-2019.pdf>.
- [42] Orcina, "Line theory: Overview," Orcina, 2018. [Online]. Available: <https://www.orcina.com/webhelp/OrcaFlex/Content/html/Linetheory,Overview.htm>.
- [43] JDRcables, "CABLE DATASHEET - SUBSEA POWER CABLE," TFKable group, June 2021. [Online]. Available: <https://www.jdrcables.com/>.
- [44] Oceaneering, "Pull-in and hang off systems," Oceaneering, 2016. [Online]. Available: <https://www.oceaneering.com/datasheets/SDS-Pull-in-and-Hang-Off-Systems-A4.pdf>.
- [45] Trelleborg group, "Protecting offshore power cables," Trelleborg group, 2020. [Online]. Available: <https://www.trelleborg.com/en/media/products-and-solutions-news/protecting-offshore-power-cables>.
- [46] CRP subsea, "Distributed buoyancy module," CRP subsea, 2021. [Online]. Available: <https://www.crpsubsea.com/products/product-families/buoyancy-floats/distributed-buoyancy/distributed-buoyancy-module/>.
- [47] Patentstyret, "Offshore flexible line Installation and removal," Patentstyret, [Online]. Available: <https://search.patentstyret.no/Home/OpenFile?docnr=0901670881361b89&appid=01-04&fileType=pdf>.
- [48] LCETED, "Tension VS Compression," LCETED - Institute for civil engineers, 2021. [Online]. Available: <https://www.lceted.com/2021/04/tension-vs-compression.html>.
- [49] WESCO, "What is minimum bending radius?," Wesco - anixter, January 2016. [Online]. Available: https://www.anixter.com/en_us/resources/literature/wire-wisdom/minimum-bend-radius.html.
- [50] Electrotechnik, "Cable pulling tension calculations," Electrotechnik, 2022. [Online]. Available: <https://elek.com.au/articles/cable-pulling-tension-calculations/>.
- [51] A. G. N. a. C. d. A. Martins, "Structural stability of flexible lines in catenary configuration under torsion," ScienceDirect, December 2013. [Online]. Available: <https://www.sciencedirect.com/science/article/abs/pii/S0951833913000518>.
- [52] Orcina, "Dynamic analysis:Time domain solution," Orcina, 2022. [Online]. Available: <https://www.orcina.com/webhelp/OrcaFlex/Content/html/Dynamicanalysis,Timedomainsolution.htm>.

- [53] Orcina, "Dynamic analysis," ORCINA, 2018. [Online]. Available: <https://www.orcina.com/webhelp/OrcaFlex/Content/html/Dynamicanalysis.htm>.
- [54] Orcina, "Coordinate systems," Orcina, 2018. [Online]. Available: <https://www.orcina.com/webhelp/OrcaFlex/Content/html/Coordinatesystems.htm>.
- [55] O. Gudmestad, Marine Technology and Operations, theory and practice, Southampton: WIT Press, 2015.
- [56] A. Hansen, "The Three Extreme Value Distributions: An Introductory Review," Frontiers, December 2020. [Online]. Available: <https://www.frontiersin.org/articles/10.3389/fphy.2020.604053/full>.
- [57] Orcina, "https://www.orcina.com/webhelp/OrcaFlex/Content/html/Dynamicanalysis,Timehistorysynthesis.htm," Orcina, January 2019. [Online]. Available: <https://www.orcina.com/webhelp/OrcaFlex/Content/html/Dynamicanalysis,Timehistorysynthesis.htm>.
- [58] Orcina, "Results: Extreme value statistics results," Orcina, August 2009. [Online]. Available: <https://www.orcina.com/webhelp/OrcaFlex/Content/html/Results,Extremevaluestatisticsresults.htm>.

Appendix A

- Cable data sheet, subsea power cable (800 mm²)



CABLE DATASHEET

36/60~69(72.5)kV, SUBSEA POWER CABLE

DATE OF ISSUE: June 2021 REVISION NUMBER: 01

SUBSEA POWER CABLE	
MANUFACTURER	JDR CABLE SYSTEMS LTD
MANUFACTURING STANDARDS	IEC 63026
APPLICATION	Dynamic Design
COMPONENTS	3 x Power Cores, 1 x Fibre Optic Cable
RATED OPERATING VOLTAGE (U_r/U_m/U_g)kV	36/60~69(72.5)kV
CONDUCTOR SIZE RANGE	150 - 800 mm ²
SUBSEA CABLE CONSTRUCTION	
LAYUP	Helical, with Polypropylene Rope Fillers
ARMOUR BEDDING	Extruded Polyethylene
STRENGTH MEMBER	Double Layer, Galvanised Steel Wire
OUTER LAYER	Extruded Polyethylene
POWER CORE CONSTRUCTION	
CONDUCTOR	Longitudinally Waterblocked, Stranded Compacted, Plain Copper to IEC 60228 Class II
CONDUCTOR SCREEN	Extruded Semi-conductive Material
INSULATION	Cross Linked Polyethylene
INSULATION SCREEN	Extruded Semi-conductive Material
METALIC SCREEN	Copper Wire Screen with Copper Equalisation Tape
OVERSHEATH	Non-conductive Polyethylene Sheath
FIBRE OPTIC CONSTRUCTION	
OPTICAL FIBRES	Up to 96 Single Mode Fibres to ITU-T G.652D
FIBRE OPTIC TUBING	Gel Filled, Stainless Steel 316L Tube
INNER SHEATH	Non-conductive Polyethylene Sheath
FIBRE OPTIC STRENGTH MEMBER	Single Layer, Galvanised Steel Wire
OVERSHEATH	Non-conductive Polyethylene Sheath



Image for indicative illustration only



CABLE DATASHEET

36/60~69(72.5)kV, SUBSEA POWER CABLE

DATE OF ISSUE: June 2021 REVISION NUMBER: 01

Conductor size (mm ²)	150	185	240	300	400	500	630	800
-----------------------------------	-----	-----	-----	-----	-----	-----	-----	-----

MECHANICAL PARAMETERS

Overall diameter (mm)	141 +/- 3	144 +/- 3	149 +/- 3	152 +/- 3	158 +/- 3	165 +/- 3	178 +/- 3.5	190 +/- 3.5
Weight in air (kg/km)	37,420	39,300	42,350	43,770	48,470	53,260	61,630	72,820
Weight in seawater (kg/km)	22,920	24,110	26,030	26,970	30,130	33,260	38,130	46,120
Specific gravity in seawater	2.34	2.35	2.37	2.35	2.41	2.43	2.41	2.50
Minimum breaking strength (kN)	1,450	1,480	1,535	1,500	1,565	1,635	1,790	2,105
Torsion at recommended working load (N.m)	27.4	21.7	20.7	-35.9	-36.7	-37.7	-18.3	-36.8
Estimated bend stiffness (kN.m ²)	6.91 +/- 2.42	7.51 +/- 2.63	8.85 +/- 3.10	9.60 +/- 3.36	10.85 +/- 3.80	12.96 +/- 4.54	16.34 +/- 5.72	21.19 +/- 7.42
Estimated axial stiffness (MN)	435	456	490	504	557	611	701	845
Estimated torsional stiffness CW (kN.m ² /deg)	2.35	2.53	2.79	2.91	3.33	3.79	4.91	6.58
Estimated torsional stiffness CCW (kN.m ² /deg)	2.3	2.5	2.7	2.8	3.17	3.60	4.73	6.28
Estimated maximum permissible impact energy (kJ/m)	27	27	27	27	27	27	27	27
Maximum permissible crush load (kN/m)	123	125	130	132	137	144	155	165

CABLE HANDLING PARAMETERS (NO JOINTS)

Min. bend radius for drumming, loadout & storage (m)	1.47	1.56	1.73	1.91	2.14	2.04	2.13	2.15
Max. Allowable Tension for drumming, loadout and storage (kN)	24	26	29	32	36	34	36	36

CABLE INSTALLATION / DEPLOYMENT PARAMETERS (NO JOINTS)

Min. Bend Radius (m)	2.10 (up to 100 kN)	2.23 (up to 100 kN)	2.48 (up to 100 kN)	2.72 (up to 100 kN)	3.06 (up to 100 kN)	2.91 (up to 100 kN)	3.04 (up to 100 kN)	3.07 (up to 100 kN)
Max. Allowed Tension (kN)	195	202	214	215	232	250	281	336
Max. Side-Wall Pressure (kN/m)	50	50	50	50	50	50	50	50
Min. Bend Radius at Max. Allowed Tension (m)	3.91	4.05	4.28	4.31	4.66	5.00	5.64	6.74



CABLE DATASHEET

36/60~69(72.5)kV, SUBSEA POWER CABLE

DATE OF ISSUE: June 2021 REVISION NUMBER: 01

Conductor size (mm ²)	150	185	240	300	400	500	630	800
Metallic screen size (mm ²)	42.47	42.47	42.47	42.47	42.47	42.47	42.47	42.47

ELECTRICAL PARAMETERS								
Operating voltage (kV)	66	66	66	66	66	66	66	66
Frequency, f (Hz)	50	50	50	50	50	50	50	50
DC conductor resistance at 20°C (Ω/km)	0.126	0.101	0.0765	0.061	0.0477	0.0371	0.0287	0.0224
AC conductor resistance at 50 Hz at 20°C (Ω/km)	0.127	0.102	0.0782	0.0632	0.0506	0.0408	0.0334	0.0281
AC conductor resistance at 50 Hz at 90°C (Ω/km)	0.161	0.129	0.0989	0.0795	0.0632	0.0504	0.0405	0.0335
Zero sequence resistance at 50 Hz at 20°C (Ω/km)	0.251	0.224	0.197	0.184	0.167	0.153	0.138	0.119
Inductance (mH/km)	0.442	0.428	0.406	0.386	0.368	0.357	0.345	0.335
Zero sequence inductance (mH/km)	0.407	0.393	0.37	0.351	0.333	0.32	0.307	0.298
Capacitance (nF/km)	174	188	214	238	270	288	322	347
Positive/ negative sequence impedance at 50 Hz at 90°C - modulus (Ω/km)	0.213	0.187	0.161	0.145	0.132	0.123	0.116	0.11
Positive/ negative sequence impedance at 50 Hz at 90°C - angle (deg)	40.8	46.2	52.2	56.7	61.3	65.8	69.5	72.3
Zero sequence impedance at 50 Hz at 20°C - modulus (Ω/km)	0.292	0.256	0.229	0.215	0.197	0.183	0.168	0.152
Zero sequence impedance at 50 Hz at 20°C - angle (deg)	27.0	28.8	30.5	31.0	32	33.3	35.0	38.2
Electrical stress at conductor screen (kV/mm)	5.4	5.4	5.4	5.3	5.3	5.2	4.9	4.8
Electrical stress at insulation screen (kV/mm)	2.4	2.5	2.8	3.0	3.2	3.2	3.2	3.2
Maximum allowable conductor temperature (°C)	90	90	90	90	90	90	90	90

SHORT CIRCUIT RATING (NON-ADIABATIC)								
Conductor short circuit at 1s (kA)	21.7	26.8	34.7	43.3	57.7	72.1	90.7	115.1
Screen short circuit at 1s (kA)	5.1	5.1	5.0	5.0	5.0	4.9	4.9	4.9



CABLE DATASHEET

36/60~69(72.5)kV, SUBSEA POWER CABLE

DATE OF ISSUE: June 2021 REVISION NUMBER: 01

Conductor size (mm ²)	150	185	240	300	400	500	630	800
-----------------------------------	-----	-----	-----	-----	-----	-----	-----	-----

ENVIRONMENTAL PARAMETERS (ASSUMED)

Maximum ambient air temperature (°C)	35	35	35	35	35	35	35	35
Air speed (m/s)	10	10	10	10	10	10	10	10
Peak solar radiation (W/m ²)	1,000	1,000	1,000	1,000	1,000	1,000	1,000	1,000
RMS solar radiation (W/m ²)	492	492	492	492	492	492	492	492
Maximum ambient water temperature (°C)	36	36	36	36	36	36	36	36
Water speed (m/s)	0	0	0	0	0	0	0	0
Thermal resistivity of J-tube material (steel) (K.m/W)	0.0625	0.0625	0.0625	0.0625	0.0625	0.0625	0.0625	0.0625
Absorption coefficient	0.5	0.5	0.5	0.5	0.5	0.5	0.5	0.5
J-tube dimensions (mm) (ID = 2.5 x cable OD & 20mm wall thickness)	393 OD 353 ID	400 OD 360 ID	413 OD 373 ID	420 OD 380 ID	435 OD 395 ID	453 OD 413 ID	485 OD 445 ID	515 OD 475 ID

CURRENT RATINGS (BASED ON ASSUMED ENVIRONMENT)

Cable in air (with airflow & no solar radiation) (A)	448	507	591	672	770	870	986	1,094
Cable in air (with peak solar radiation & airflow) (A)	441	499	582	662	759	857	971	1,077
Cable in air (inside monopile - no solar radiation, no airflow) (A)	380	428	496	560	637	717	811	901
Cable in water above seabed (A)	455	515	602	685	786	888	1,007	1,117
Cable in J-tube (no solar radiation) (A)	371	418	484	545	620	697	789	878
Cable in J-tube (RMS solar radiation) (A)	364	410	475	535	508	683	774	861